สารยับยั้งเอชไอวี-1 รีเวอร์สทรานคริปเทสจากพืชวงศ์ขิงZingberaceae

นายเกษม สุขก้องวารี

วิทยานิพนธ์นี้เป็นส่วนหนึ่งของการศึกษาตามหลักสูตรปริญญาวิทยาศาสตรดุษฎีบัณฑิต
สาขาวิชาเคมี ภาควิชาเคมี
คณะวิทยาศาสตร์ จุฬาลงกรณ์มหาวิทยาลัย
ปีการศึกษา 2547

ISBN 974-17-6821-4

HIV-1 REVERSE TRANSCRIPTASE INHIBITORS FROM FAMILY ZINGIBERACEAE

Mr. Kasem Sookkongwaree

A Dissertation Submitted in Partial Fulfillment of the Requirements

for the Degree of Doctor of Philosophy in Chemistry

Department of Chemistry

Faculty of Science

Chulalongkorn University

Academic year 2004

ISBN 974-17-6821-4

Thesis Title	HIV-1 REVERSE TRANSCRIPTASE INHIBITORS FROM FAMILY ZINGIBERACEAE
By	Mr. Kasem Sookkongwaree
Filed of study	Chemistry
Thesis Advisor	Professor Sophon Roengsumran, Ph.D.

Accepted by the Faculty of Science, Chulalongkorn University in Partial Fulfillment of the Requirements for the Doctor's Degree

…….. Dean of Faculty of Science
(Professor Piamsak Menasveta, Ph. D.)

THESIS COMMITTEE

…….. Chairman
(Professor Udom Kokpol, Ph. D.)

…….. Thesis Advisor
(Professor Sophon Roengsumran, Ph. D.)

…….. Member
(Professor Padet Sidisunthorn, Ph. D.)

…….. Member
(Assosiate Professor Amorn Petsom, Ph. D.)

…….. Member
(Assistance Professor Chamnan Pattarapanich, Ph. D.)

เกษม สุขก้องวารี : สารยับยั้งเอชไอวี-1 รีเวอร์สทรานสคริปเทสจากพืชวงศ์ขิง Zingiberaceae (HIV-1 REVERSE TRANSCRIPTASE INHIBITORS FROM FAMILY ZINGIBERACEAE) อ. ที่ปรึกษา : ศ. ดร. โสภณ เริงสำราญ, 197 หน้า. ISBN 974-17-6821-4.

ทำการสกัดพืชสมุนไพรวงศ์ขิง (*Zingiberaceae*) จำนวน 11 ชนิด ด้วยตัวทำละลายน้ำและเมทานอล และนำสารสกัดที่ได้ทดสอบฤทธิ์ยับยั้ง human immunodeficiency virus type 1 reverse transcriptase (HIV-1 rt) และ proteases จาก human immunodeficiency virus type 1 (HIV-1), hepatitis C virus (HCV) และ human cytomegalovirus (HCMV) จากผลการทดลองพบว่า สารสกัดเมทานอลส่วนใหญ่สามารถยับยั้ง protease ทั้งสามชนิดได้ดี โดยเฉพาะสารสกัดเมทานอลของกระชายดำและข่า จึงทำการแยกองค์ประกอบทางเคมีจากกระชายดำและข่าโดยใช้ฤทธิ์ทางชีวภาพเป็นตัวชี้นำการแยก โดยสามารถแยกสารประกอบฟลาโวนอยด์ได้ 8 ชนิด (สารประกอบ **1-8**) จากกระชายดำและสารประกอบ **9-11** จากข่า จากนั้นพิสูจน์สูตรโครงสร้างด้วยเทคนิคทางสเปคโตรสโคปี และได้ทดสอบฤทธิ์ยับยั้ง protease ของไวรัสทั้งสามชนิด พบว่า 5-hydroxy-7-methoxyflavone (**2**) และ 5,7-dimethoxyflavone (**7**) ยับยั้ง HIV-1 protease โดยมี IC_{50} เท่ากับ 19 μM นอกจากนั้น 5-hydroxy-3,7-dimethoxyflavone (**1**) ยังสามารถยับยั้ง HCV protease และ HCMV protease โดยมีค่า IC_{50} เท่ากับ 190 และ 250 μM ตามลำดับ ในขณะที่ 4-hydroxycinnamaldehyde (**10**) ยับยั้ง HIV-1 protease โดยมีค่า IC_{50} เท่ากับ 130 μM และสามารถยับยั้ง HCMV protease โดยมีค่า IC_{50} เท่ากับ 97 μM นอกจากนั้น 4-methoxy cinnamic acid ethyl ester (**13**) และ 4-methoxy cinnamic acid (**14**) ที่แยกได้จากเปราะหอมยับยั้ง α-glucosidase สูงกว่าสารประกอบอนุพันธ์ของ *trans*-cinnamic acid ที่นำมาทดสอบ โดยมีค่า IC_{50} เท่ากับ 0.05 และ 0.04 mM

ภาควิชา.....เคมี..... ลายมือชื่อนิสิต.....
สาขาวิชา.....เคมี..... ลายมือชื่ออาจารย์ที่ปรึกษา.....
ปีการศึกษา..... 2547……

4373805323 : MAJOR CHEMISTRY

KEY WORD: HIV-1 / reverse transcriptase / protease / glucosidase / Zingiberaceae

KASEM SOOKKONGWAREE : HIV-1 REVERSE TRANSCRIPTASE INHIBITORS FROM FAMILY ZINGIBERACEAE. THESIS ADVISOR : PROF. SOPHON ROENGSUMRAN, Ph.D. 197 pp. ISBN 974-17-6821-4.

Eleven medicinal plants in the *Zingiberaceae* family were extracted with water and methanol and then screened for inhibition of human immunodeficiency virus type 1 reverse transcriptase (HIV-1 rt) and proteases from human immunodeficiency virus type 1 (HIV-1), hepatitis C virus (HCV) and human cytomegalovirus (HCMV). The results showed that most of the methanol extracts have strong inhibition of the three different proteases, especially methanol extract of *Kaempferia parviflora* and *Alpinia galanga*. *Kaempferia parviflora* and *Alpinia galanga* were isolated to identify chemical constituents by using bioassay-guided as a navigator of fractionation. Eight flavonoids (**1-8**) were isolated from *Kaempferia parviflora* and compounds **9-11** were isolated from *Alpinia galanga*. The structures of the isolated compounds were determined by spectroscopic techniques. The effects of each compound in inhibiting three different proteases were tested. It was found that 5-hydroxy-7-methoxyflavone (**2**) and 5,7-dimethoxyflavone (**7**) showed a potent inhibitory activity against HIV-1 protease, both with IC_{50} values of 19 μM. Moreover, 5-hydroxy-3,7-dimethoxyflavone (**1**) posses a mild inhibitory activity against HCV protease and HCMV protease with the IC_{50} value of 190 and 250 μM, respectively. While 4-hydroxycinnamaldehyde (**10**) showed HIV-1 protease inhibitory effect with IC_{50} value of 130 μM, and HCMV protease inhibitory effect with IC_{50} value of 97 μM. In addition, 4-methoxy cinnamic acid ethyl ester (**13**) and 4-methoxy cinnamic acid (**14**) which isolated from *Kaempferia galanga* showed the highest activity against α-glucosidase inhibition among the *trans*-cinnamic acid derivatives with IC_{50} value of 0.05 and 0.04 mM, respectively.

Department....Chemistry.....Student's signature.....

Field of study..Chemistry …….....Advisor's signature.....

Academic year…2004….

ACKNOWLEDGEMENTS

The author wishes to express the deepest appreciation to his advisor, Prof. Dr. Sophon Roengsumran, for his kindness, valuable advice, and everything that he gave to the author and Prof. Dr. Helena Danielson for inviting me the opportunity to carry out my research at Uppsala University, and guiding me through the year of my work at BMC, and for many interesting discussions in enzymatic biochemistry and for everything when the author lived in Sweden. The author also wishes to extend his profound thanks to the chairman and members of his thesis committee, Prof. Dr. Udom Kokpol, Prof. Dr. Padet Sidisunthorn, Assoc. Prof. Dr. Amorn Petsom, and Assist. Prof. Dr. Chamnan Pattarapanich.

The author would like to thank Assist Prof. Dr. Warinthorn Chavasiri for providing *trans*-cinnamic acid derivatives. Thanks are also due to Mr. Sophon Kaeotip for assistance with mass spectrometry analyses, Miss Daranee Charoensuk and Miss Jumreang Thammathorn for NMR spectroscopy experiments.

Especially, he would like to express his deepest gratitude to his parents for their love and encouragement throughout the studying.

Moreover, this study was financially supported by RGJ Ph.D. Program, the Thailand Research Fund (TRF), the National Research Council of Thailand and the Swedish Foundation for International Cooperation in Research and Higher Education (STINT).

CONTENTS

Page

Page

Page

Page

Page

Page

LIST OF TABLES

Table Page

Table Page

Table Page

LIST OF FIGURES

Figure Page

Figure Page

Figure Page

LIST OF SCHEMES

ABBREVIATIONS

μg	Microgram
μM	Micromolar
AIDS	Acquire Immunodeficiency Syndrome
br	Broad
$CDCl_3$	Chloroform-d_1
d	Doublet (NMR)
dd	Doublet of doublet (NMR)
DNA	Deoxy nucleic acid
DMSO	Dimethyl sulfoxide
DTT	Dithiothreitol
g	Gram
gp	glycoprotein
HIV	Human Immunodeficiency Virus
HCMV	Human Cytomegalo Virus
HCV	Hepatitis C Virus
Hz	Hertz
Kg	Kilogram
m	Multiplet (NMR)
m	Medium (IR)
M	Molar
m.p.	Melting point
M.W.	Molecular weight
mg	Milligram
ml	Millilitre
Nef	Negative regulatory factor gene
NMR	Nuclear Magnetic Resonance
NS	Non structural
PNP-G	*p*-nitrophenyl-α-D-glucopyranoside
ppm	Part per million

Pr	Protease
Rev	regulator of expression of virion protein gene
RNA	Ribonucleic acid
RT	Reverse transcriptase
s	Singlet (NMR)
s	Strong (IR)
t	Triplet (NMR)
Tat	Transactivator of transcription gene
TLC	Thin layer chromatography
Vif	Viral infectivity factor gene
Vpr	Viral protein R gene
Vpu	Viral protein U gene
w	Weak (IR)
wt.	Weight

CHAPTER I

INTRODUCTION

During the past years HIV-1 infection and acquired immunodeficiency syndrome have become a worldwide pandemic.(1) According to the World Health Organization's assessment, more than 20 years and 20 million deaths since the first AIDS diagnosis in 1981, almost 38 million people (range 34.6 – 42.3 million) are living with HIV. Rates of infection are still on the rise in many countries in sub-Saharan Africa. In 2003 alone, an estimated of 3 million people in the region became newly infected. AIDS is the leading cause of death in Africa and the fourth leading cause of death worldwide.(2)

In most cases, the cause of death is not the virus itself, but infections and cancers that would not have developed in non-HIV-infected individuals with properly functioning immune defense systems.(3) The primary targets of HIV are macrophages and T lymphocytes, both of which are critical for immune defense in humans. In the battle against the virus, the immune system destroys itself.(4)

1.1 HIV background

In 1981 a cluster of unusual diseases was observed in certain groups of people. The two main diseases were pneumonia caused by a yeast, *Pneumocystis carnii*, and unusual tumour called Kaposi's sarcoma.(5,6) These diseases were seen initially in homosexual men but later the same symptoms appeared in intravenous drug users and hemophiliacs who were injecting blood-clotting factors. The observation that individuals with these diseases had low numbers of CD4 T cells was consistent with immunosuppression. This syndrome became known as Acquired Immunodeficiency Syndrome (AIDS).(7)

In 1983 the causative agent of AIDS was identified as a human retrovirus. A few year later a second similar virus, HIV-2, was isolated from patients in West Africa.(8) Both HIV subtypes can lead to AIDS, HIV-1 and HIV-2 differ in their virulence and geographical location, although the pathogenic course with HIV-2 might be longer. The genome homology of HIV-1 and HIV-2 are approximately 40 %.(9) The origin of the two viruses has now been shown to be derived from two African monkeys, the chimpanzee (*Pan troglodytes*) for HIV-1 (10) and the sooty mangabay (*Cercocebus atys*) for HIV-2.(11)

The primary target of HIV seems to be CD4 T lymphocytes which are part of the machinery of our immune system. The primary phase of HIV infection progresses

fairly rapidly and may exhibit a systemic illness including fever, headache, rash, pharyngitis, gastrointestinal disturbance, and lymphadenophathy symptoms within a few week.(12) During this early phase, the extent of infection is high and virion concentration may exceed a million copies per ml blood.(13) Viral replication is still active and cells are rapidly being infected and eliminated during this period.(14,15) In the final phase of infection, the number of CD4 T cells drops more quickly and the viral load increases to produce clinical immunodeficiency. The HIV infection in muscles and the central nervous system results in muscular wastage and AIDS-related dementia.(16) The average life expectancy without therapy from the appearance of AIDS is 1-2 years in developed countries.(17)

1.2 Structure of HIV

HIV-1 and HIV-2 are RNA viruses and belong to the family of retroviruses, *Retroviridae*. The mature HIV virion is an essentially spherical particle with a radius of about 100 nm, shown in figure 1.1.

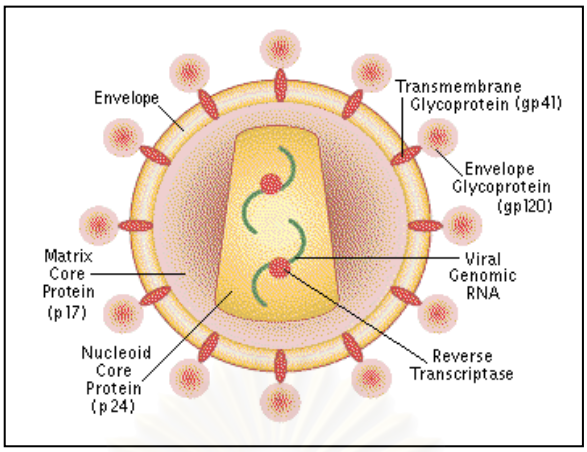

Figure 1.1 Structure of HIV

The virus is surrounded by a lipid bilayer derived from the host cell and contains several cellular membrane proteins.(18) The outer portion of this envelope is spotted with surface glycoprotein gp120 (named for its approximate molecular weight) adhered to transmembrane protein gp41. The inside of the envelope is lined with matrix protein p17. Within this shell is the conical capsid core made up of capsid protein p24. The core holds two copies of the single stranded RNA which makes up the viral genome. HIV is a retrovirus, which means HIV store its genetic information as RNA which needs to reverse transcribed to DNA. Accompanying the genome are multiple copies of nucleocapsid protein p7, auxiliary proteins Nef, Vif and Vpr and the essential enzymes: protease, reverse transcriptase and integrase. (19) Other auxiliary proteins, e.g. Vpu, Tat and Rev, are not thought to be carried in the virion but are synthesized in the host cell. (19, 20)

1.3 Replication cycle of HIV

The attachment of the viral surface protein (gp120) to the CD4 receptor on a human (1) was shown in figure 1.2. The virus subsequently fuses with the cell surface and releases its contents into the cytoplasm of the host cell (2). The viral genome is expressed as single-stranded RNA and is translated to DNA in two steps by the viral enzyme reverse transcriptase (RT) (3, 4).

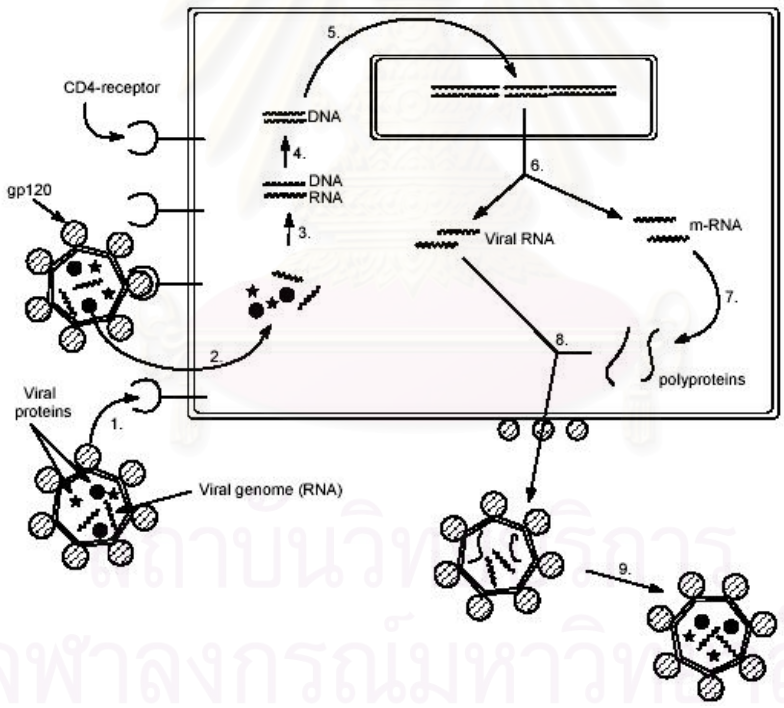

Figure 1.2 Replication cycle of HIV

Under the influence of a second viral enzyme, an integrase, the double-stranded DNA (called the provirus) is incorporated into the DNA of the host cell (5). The cell itself translates the DNA to RNA that can serve either as the genome of newly formed viruses or as messenger RNA (mRNA) (6) to express the viral polyprotein (7). The polyprotein then fuses with newly formed RNA (8) and the cell releases this as a new virus along with hundreds of other new viruses of the same type (9), usually killing the host cell in the process. For a virus to mature, the polyproteins must be cleaved into smaller proteins, which is accomplished by the enzyme protease (PR). (19) They assemble together with the envelope protein to form and immature virus particle that is released from the cell by budding from the cell surface. HIV virion is now ready to infect a new cell and start a new replication cycle.(19, 21)

1.4 Treatment of HIV-infected patients

In principle, every step in the HIV replication cycle can be considered as a potential target for anti-viral chemotherapy. The key in selective anti-viral therapy is therefore to identify any process that is essential for the replication of the virus, but not for the survival of the cell. (22) The gained knowledge about the replication cycle of the HIV has led to the extraction of virus-specific processes. Predominately, scientists have focused their attentions on the following processes: viral binding to target cells,

virus cell fusion, virus uncoating, reverse transcription of RNA by reverse transcriptase, viral integration, gene expression and protease activity.

However, the two strategies, reveres transcriptase and protease have been proven to be the most successful drugs for treatment of AIDS.(23,24) A number of drugs that have been approved for the treatment of HIV infected patients are alternate substrates for RT, can be divided in two categories, the first one is nucleoside reverse transcriptase inhibitors (NRTIs), e.g. AZT or zidovudine. Today, there are six NRTIs approved, shown in figure 1.3

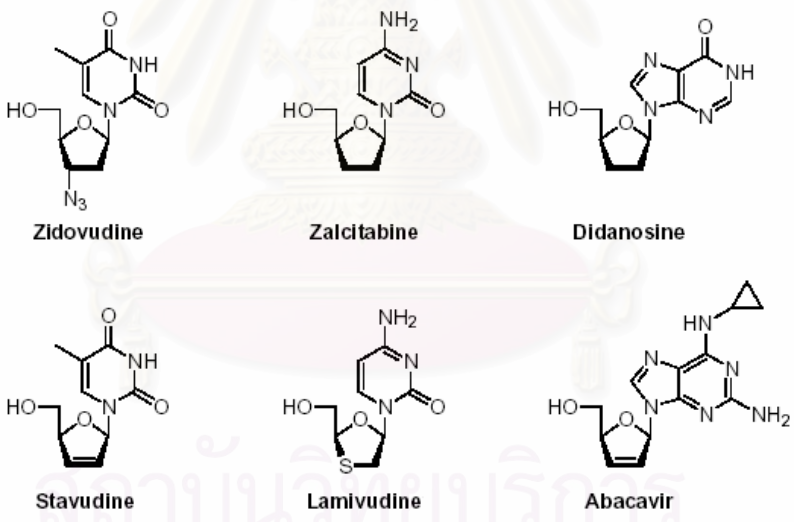

Figure 1.3 Nucleoside reverse transcriptase inhibitors (NRTIs) approved by FDA.

But all of these substances have many side effects, such as bone marrow suppression, peripheral neuropathy and acute pancreatitis.(25,26) And the other one is non-nucleoside reverse transcriptase inhibitors (NNRTIs), currently, three NNRTIs are

used in clinic, shown in figure 1.4. However, rapid eliciting resistance is a major problem with this inhibitor type.(23)

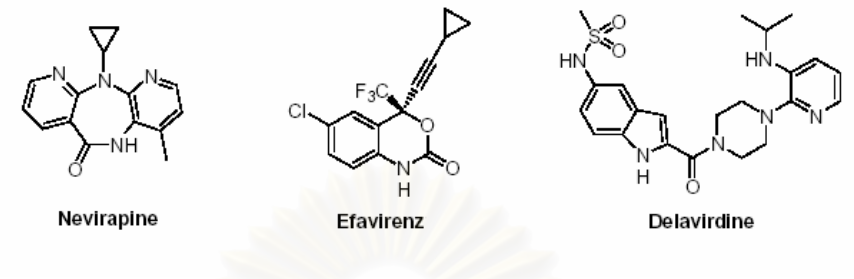

Figure 1.4 Non nucleoside reverse transcriptase inhibitors (NNRTIs) approved by FDA.

The other group of drugs is the HIV-1 protease inhibitors, e.g. amprenavir, that prevent the maturation of the virus particle.(27) Saquinavir was the first approved protease inhibitors and has been in clinical use since 1995.(28) Currently, there are six clinically approved protease inhibitors, shown in figure 1.5.

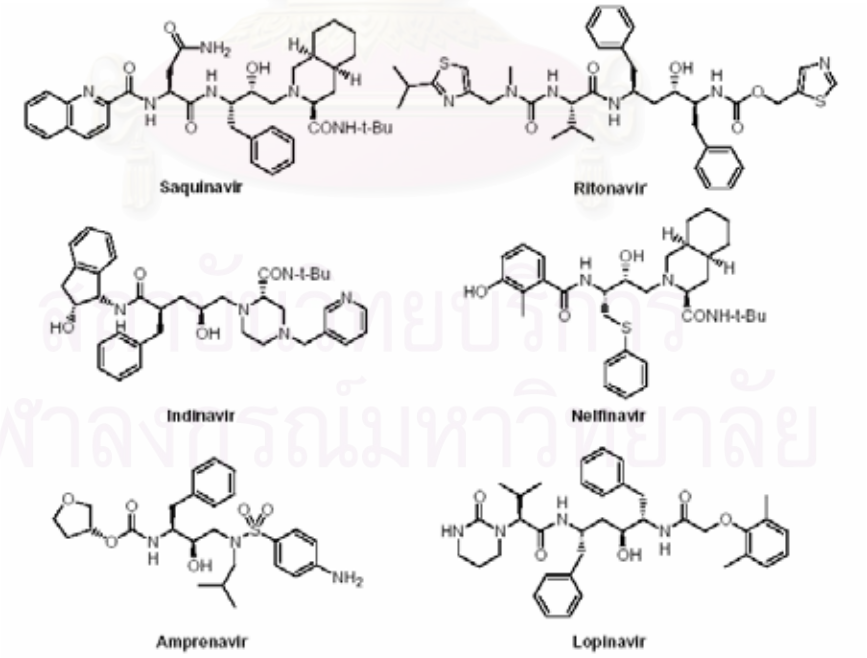

Figure 1.5 Protease inhibitors approved by FDA

Although these inhibitors are highly selective, but they have many side effects such as lipodystophy, hyperlipidaemia, insulin resistance,(29-32) and emergence of resistant mutants upon prolonged use.(33-35)

HIV therapy most often comprises a combination of RT inhibitors and PR inhibitors, called highly active antiretroviral therapy (HAART).(36) Although the dosage of each drug is lower that would be required by a non-combinatorial therapy, this still means several grams a week of each of the individual pharmaceuticals in the combination.(37)

Although HAART is very effective drug for AIDS patients, but the most serious threat though is the development of resistance to the protease inhibitors.(38) Mutation in the protease renders the inhibitors more or less useless. Unfortunately, strong cross-resistance is also encountered, i.e. if the virus becomes resistant to one available protease inhibitor, it becomes resistant to the others as well. So new drugs are need to combat resistant strains of the virus.

1.5 HCV (Hepatitis C virus)

Hepatitis C virus infection represents a major problem of public health with around 350 millions of chronically infected individuals worldwide.(39) Chronic infection with the hepatitis C virus (HCV) is a leading cause of chronic liver disease, cirrhosis

and hepatocellular carcinoma.(39,40) HCV is spread primarily by direct contact with human blood. The major causes of HCV infection worldwide are used of unscreened blood transfusions, and reused of needles and syringes that have not been adequately sterilized. Current therapies for HCV infection include treatment with interferon-α alone and in combination with ribavirin.(41,42) But many patients do not respond to treatment, however there is no preventive vaccine available.(42)

HCV belongs to the genus of *Hepacivirus* and is a member of the *Flaviviridae*, together with the Pestiviruses and Flaviviruses.(39) The diameter of the HCV virus particles is about 500 0A. Its genome is a positive, single strand RNA molecule that contains a single large open reading frame encoding a poly protein.(39,43) The structural proteins, located at the N-terminal end, are released from the polyprotein by cellular proteases (figure 1.6). During replication of HCV, the final stages of polyprotein processing are performed by the viral protease NS3.(43,44) The bifunctional role of NS3 protease makes this protein an attractive target for anti HCV therapy.(43,44)

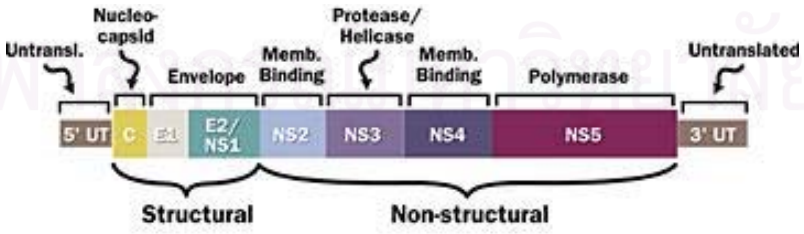

Figure 1.6 HCV genome

1.6 HCMV (Human cytomegalovirus)

Besides the AIDS and the HCV crisis, HCMV is a serious pathogen in immunocompromised individuals, including AIDS patients, neonates and organ transplant recipients.(45) HCMV causes fetal infection in 0.2-3.0% of all newborns, and has been recognized to cause fetal abnormalities of microcephaly, hydrops, intracranial calcification, chorioretinitis, liver dysfunction and thrombocytopenia, known as cytomegalic inclusion disease (CID).(46) HCMV also causes retinitis, especially in AIDS patients.(47)

HCMV is a member of the β-herpes virus family.(45,47,48) As a member of the herpesviridae family, HCMV encodes a serine protease which is involved in capsid assembly and is essential for the production of infectious virions.(45,47) The virion of HCMV consists of a 100 nm diameter icosahedral necleocapsid containing a 230 kbp, double stranded linear DNA genome surrounded by a proteinaceous layer defined as the tegument or matrix, is enclosed by a lipid bilayer containing a large number of viral glycoproteins. HCMV protease represents both an attractive target for the development of new antiviral agents and an excellent candidate for further studies on the catalytic machinery of these serine proteases.(45,48) The drug currently approved for the treatment of HCMV are the nucleoside analogs ganciclovir and cidofovir and the pyrophosphate derivative foscarnet. But the clinical use of these compounds is limited due to their host toxicity and emerging resistance strains of HCMV.(47) Thus the novel

and more effective compounds for antiviral chemotherapy of HCMV infections has to be broadened.

Currently, not only the researches of modern drug and vaccine to anti viral are moving forward, but also the medical plants are interesting too. Because natural products still serve as important sources of novel structures that may be optimized by synthetic procedures and thereby become suitable drugs. Antiviral agents are more commonly synthetic than derived from natural sources, perhaps a reflection of the simultaneous development of the fields of antiviral drugs and rational drug discovery.

The development and therapeutic use of viral reverse transcriptase inhibitors and viral protease inhibitors has contributed to improved treatment of patients, and has increased our knowledge of the targets and ligands involved. However, the need for improved inhibitors is great. For these reasons, viral enzymes targets were chosen for the present investigation.

From the preliminary screening of the methanol and aqueous extracts of eleven plants in *Zingiberaceae* family on the HIV-1 reverse transcriptase and HIV-1 protease (Table A1 and A2), the result showed that the methanol and aqueous extracts of all examined plants have no inhibitory activity on HIV-1 reverse transcriptase. For the HIV-1 protease, most of the methanol extracts of the examined plants exhibited the potent inhibition on HIV-1 protease.

1.7 The objectives of this research

1. To screen eleven medicinal plants in *Zingiberaceae* on HIV reverse transcriptase and HIV protease

2. To isolate the active compounds from the selected active crude extracts

3. To determine the structure of the active and isolated compounds

4. To determine the IC_{50} value and kinetic inhibition of the active compounds

1.8 The scope of this research

This research will explore the inhibitory activity on HIV-1 reverse transcriptase, HIV-1 protease, HCV protease and HCMV protease from eleven medicinal plants in *Zingiberaceae* family. The plant which had the highest activity will be selected for further study. That plant will be extracted with suitable solvents, and then the crude extracts will be separated by chromatographic techniques following bioassay guided as a navigator. Structural elucidation of the isolated compounds was deduced from spectroscopic evidences. Finally, the isolated compounds were conducted for inhibitory activity on viral proteases.

1.9 The advantage of the research

1. To obtain the inhibitory activity of HIV-1 reverse transcriptase, HIV-1 protease, HCV protease and HCMV protease from aqueous and methanol crude extract of eleven medicinal plants in *Zingiberaceae* family.

2. To obtain the structure and activity relationship information of isolated compounds.

3. To obtain the information on antiviral agents which may lead to the development of antiviral drug.

CHAPTER II

LITERATURE REVIEWS

HIV, HCV and HMCV have been extensively studied, and several specific processes in the viral life cycle identified that can serve as anti viral drug target. The unique steps in the replication of viral are fusion, transcription and protease activity.

2.1 Anti-HIV

Anti HIV research has been focused on compounds that interfere with various parts of the HIV life cycle following stages: viral binding and fusion, reverse transcription of RNA and cleavage event of long polypeptide chain by protease enzyme.(49,50) Many natural products have been shown to be active as a fusion inhibitor (α-glucosidase inhibitors), reverse transcriptase inhibitors and protease inhibitors. These compounds belong to a wide range of different structural classes, coumarins, flavonoids, tannins, alkaloid, lignins, terpenes, naphtho- and anthraquinones, and polysaccharides.

2.1.1 α-glucosidase inhibitors

For HIV, in attachment step of HIV to CD4 cell, infection of cells by HIV is initiated by binding of the viral surface glycoprotein gp120 to the cellular viral receptor

CD4. This binding is dependent on the state of glycosylation of gp120; a non glycosylated product of recombinant gp120 gene if enzymatically deglycosylated gp120 was not able to bind to the receptor, nor does the more highly glycosylated precursor protein gp160. Thus compounds that interfere with accurate carbohydrate processing of this viral glycoprotein may prevent viral binding to cellular receptors and hence may be useful anti-HIV agents.(23,51,52)

Tetsuo Nishioka et al. isolated the methanol extracts of *Scutellaria baicalensis*., *Rheum officinale* and *Paeonia suffruticosa*. From the chromatographic separation of the extracts of *R. officinale* Baill. and *P. suffruticosa* Andr. resulted in the isolation of methyl gallate, whereas the *S. baicalensis* Georgi. extract gave baicalein (5,6,7-trihydroxyflavone). Baicalein showed distinct inhibitory activity with IC_{50} value of 3.5×10^{-5} M.(53)

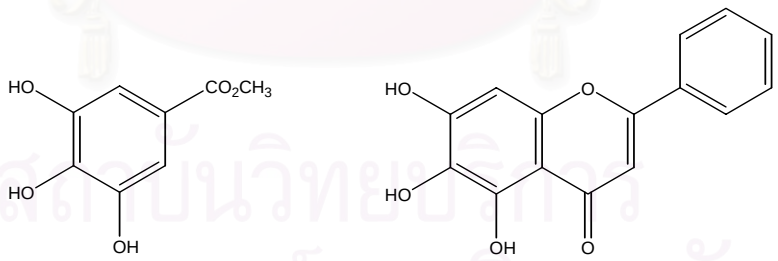

methyl gallate baicalein

Figure 2.1 Structures of methyl gallate and baicalein

Yoichi Nakao et al. screened for α-glucosidase inhibitory activity from Japanese marine invertebrates. And the hydrophilic extract of *Penares sp*. was highly

active. From bioassay-guided fractionation led to the isolation of two active compounds, penarolide sulfates A_1 and A_2, and these active compounds inhibit α-glucosidase with IC_{50} value of 1.2 and 1.5 μg/mL, respectively.(54)

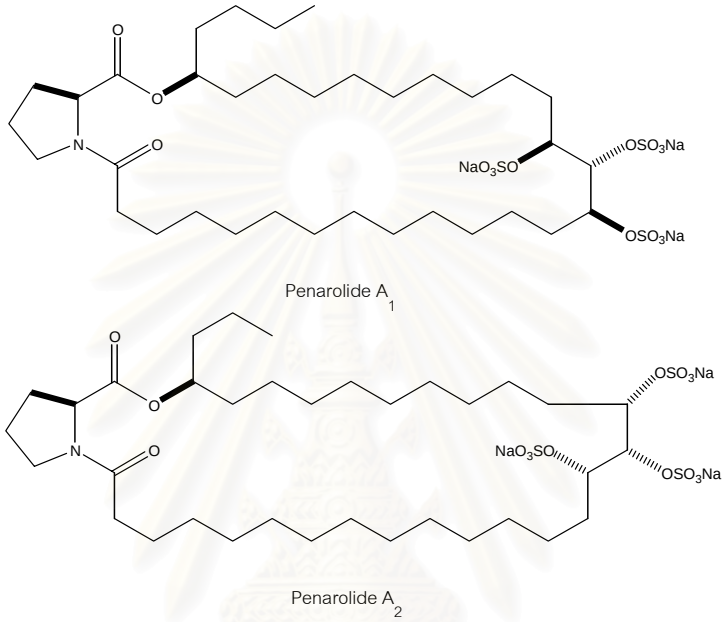

Figure 2.2 Structures of Penarolide A_1 and Penarolide A_2

Dong-Sun Lee and Sang-Han Lee isolated *Streptomyces sp*. to obtain genistein as a potent α-glucosidase inhibitor with IC_{50} value of 50 nM. Genistin was shown to be a reversible, slow binding, non-competitive inhibitor with a K_i value of 5.7 x 10^{-8} M.(55)

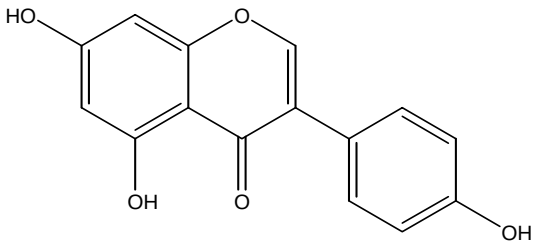

Genistein

Figure 2.3 Structure of genistein

Kentaro Takada et al. found potent α-glucosidase inhibitory activity on the hydrophilic extract of the marine sponge *Penares schulzei*, and bioassay guided isolation afforded three new tetrahydroisoquinoline alkaloids named schulzeines A-C, and found that schulzeines A-C inhibit α-glucosidase with IC_{50} values of 48-170 nM.(56)

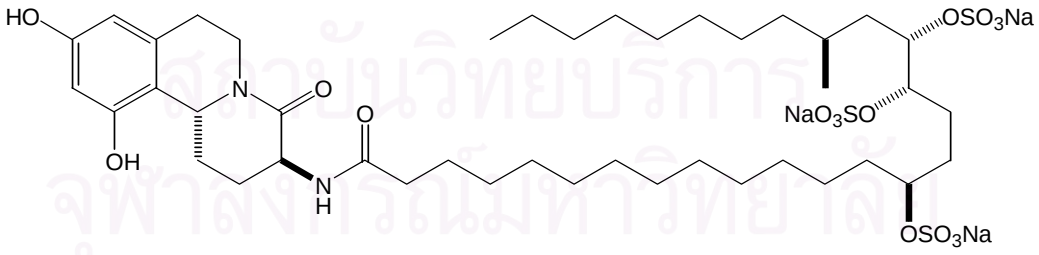

Schulzeines A

Figure 2.4 Structures of Schulzeines A, B and C

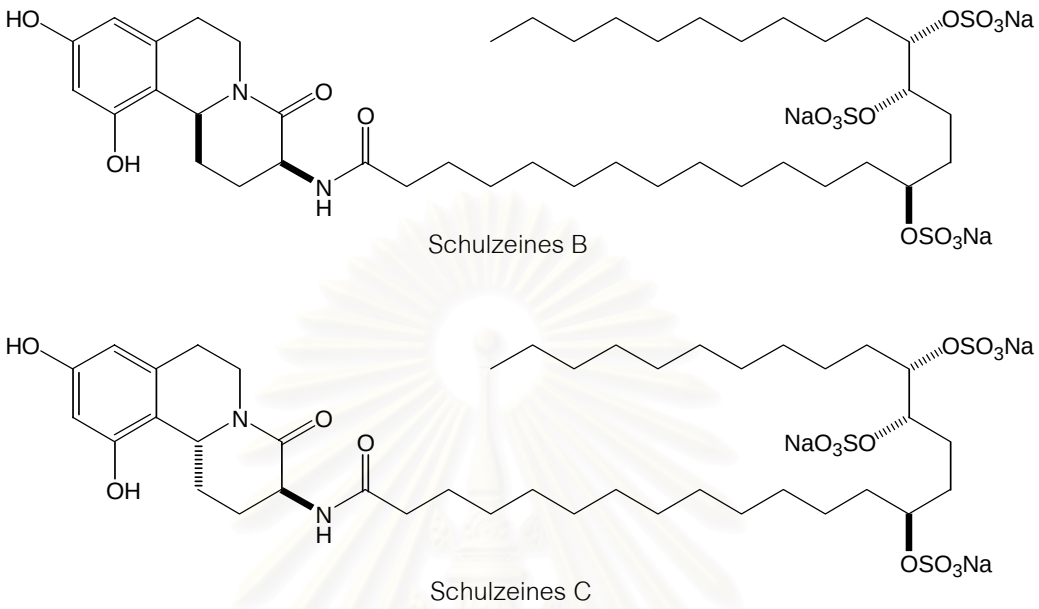

Figure 2.4 Structures of Schulzeines A, B and C (continue)

2.1.2 HIV-1 Reverse transcriptase inhibitors

After virus fuses with the cell surface and releases its contents into the cytoplasm of the host cell, the viral genome is expressed as single-stranded RNA and is translated to DNA in two steps by the viral enzyme reverse transcriptase (RT). In principle, HIV reverse transcriptase is a DNA polymerase that synthesizes double stranded DNA using a single stranded RNA as template. Currently, there are two type of reverse transcriptase inhibitors; nucleoside reverse transcriptase inhibitors and non-nucleoside reverse transcriptase inhibitors. Unfortunately, these substances have many side effects, such as bone morrow suppression, peripheral neuropathy and

acute pancreatitis and the high mutation rate of HIV frequently results in the rapid development of resistance towards the employed drugs. For these reasons, the new compounds with reverse transcriptase inhibitory activity were synthesized or isolated from natural products.

Yoel Kashman et al. isolated eight coumarin compounds by anti HIV bioassay-guided fractionation of an extract of *Calophyllum lanigerum*. The structures of calanolide A, 12-acetoxycalanolide A, 12-methoxycalanolide A, calanolide B, 12-methoxycalanolide B, calanolide C and related derivatives were solved by extensive NMR experiments. Calanolides A and B were completely protective against HIV-1 reverse transcriptase with an IC_{50} value of 20 and 15 μM, respectively, but were inactive against HIV-2.(57)

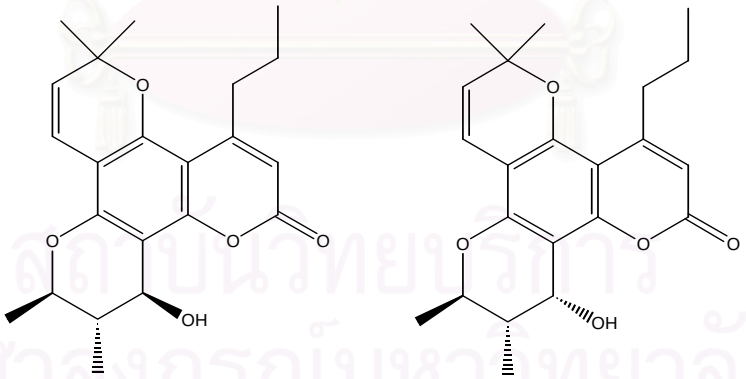

Calanolide A Calanolide B

Figure 2.5 Structures of calanolide A and B

Fang-Rong Chang et al. isolated two kaurane diterpenoids, annoglabasin A (methyl-16β-acetoxy-19-al-*ent*-kauran-17-oate) and annoglabasin B (16α-hydro-19-acetoxy-*ent*-kauran-17-oic acid), along with 11 kaurane derivatives from the fruits of *Annona glabra*. Among these, methyl-16β-acetoxy-19-al-ent-kauran-17-oate, 16α-hydro-19-acetoxy-ent-kauran-17-oic acid, 16β-hydroxy-17-acetoxy-ent-kauran-19-oic acid, 16β-hydro-ent-kauran-17-oic acid, 16α-hydro-ent-kauran-17-oic acid and methyl-16α-hydro-19-al-ent-kauran-17-oate showed significant inhibition of HIV-reverse transcriptase with IC_{50} value of 15, 40, 65, 32, 40 and 20 μg/ml, respectively.(58)

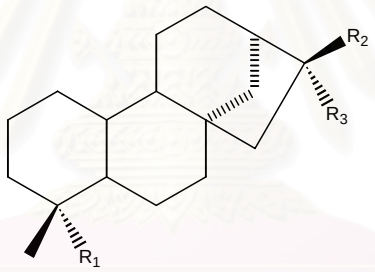

	R1	R2	R3
Methyl-16β-acetoxy-19-al-*ent*-kauran-17-oate	CHO	OAc	$COOCH_3$
16α-hydro-19-acetoxy-*ent*-kauran-17-oic acid	CH_2OAc	COOH	H
16β-hydroxy-17-acetoxy-*ent*-kauran-19-oic acid	COOH	OH	CH_2OAc
16β-hydro-*ent*-kauran-17-oic acid	CH_3	H	COOH
16α-hydro-*ent*-kauran-17-oic acid	CH_3	COOH	H
methyl-16α-hydro-19-al-*ent*-kauran-17-oate	CHO	$COOCH_3$	H

Figure 2.6 Structures of isolated active compounds from the fruits of *Annona glabra*

Jeffrey W. Corbett et al. synthesized benzothiadiazine derivatives as non nucleoside reverse transcriptase inhibitors of HIV. Because the benzothiadiazine ring system was chosen since it has been demonstrated that structurally similar compounds containing the quinazolin-2(*1H*)-one ring system are potent NNRTIs. 2,2-dioxide-*1H*-2,1,3-benzothiadiazines are synthesized by nucleophilic addition to an anthranilinitrile followed by hydrolysis of the resulting imine anion to afford the *o*-amino ketone. Treatment of the resulting amino ketones with sulfamide at elevated temperatures delivers the desired benzothiadiazines. One of these synthesized benzothiadiazines exhibited good inhibitory activity on HIV-1 reverse transcriptase with an IC_{50} value of 4627 nM.(59)

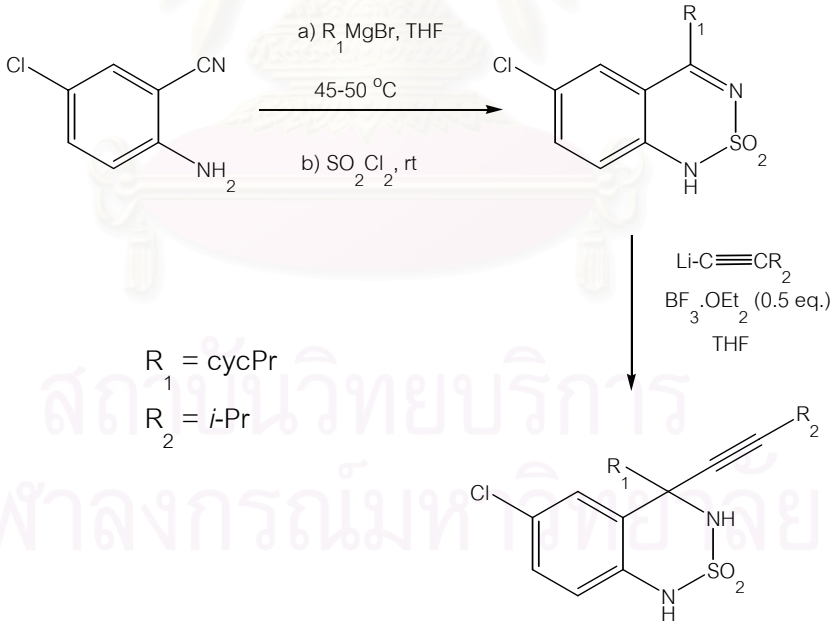

Figure 2.7 Synthesis of benzothiadiazines

One year later, Jeffrey W. Corbett et al. synthesized a series of unique 3,3a-dihydropyrano[4,3,2-*de*]quinazolin-2(1H)-ones and a 2a,5-dihydro-2H-thieno[4,3,2-*de*]quinazoline-4(3H)-thione. These compounds were found to be HIV-1 reverse transcriptase inhibitors. One of these compounds, DPC 961, possessed an IC_{50} value of 31 nM against HIV-1 reverse transcriptase.(60)

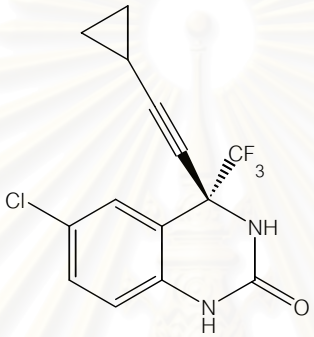

Figure 2.8 Structure of DPC 961

2.1.3 HIV-1 Protease inhibitors

Replication of human immunodeficiency virus (HIV) entails expression of several viral polyproteins which require the presence of a virus-specific protease for their maturation. Inhibition of this enzyme results in immature viral particles and inhibition of viral replication *in vitro*. HIV protease is an attractive target for mechanism-based natural product screening in order to identify candidates for development of chemotherapeutics for AIDS.

Barbara C.M. Potts and John D. Faulkner collected the magenta ascidian Didemnum sp. at Auluptagel Island, Paulu. Using bioassay-guided fractionation, the

hexane soluble material from a 1:1 methanol-dichloromethane extract was chromatographed on Sephadex LH-10 to obtain two active fractions, which were further purified by reverse phase HPLC to obtain didemnaketals A and B. The IC_{50} value of HIV-1 protease by didemnaketals A and B were 2 and 10 μM, respectively.(61)

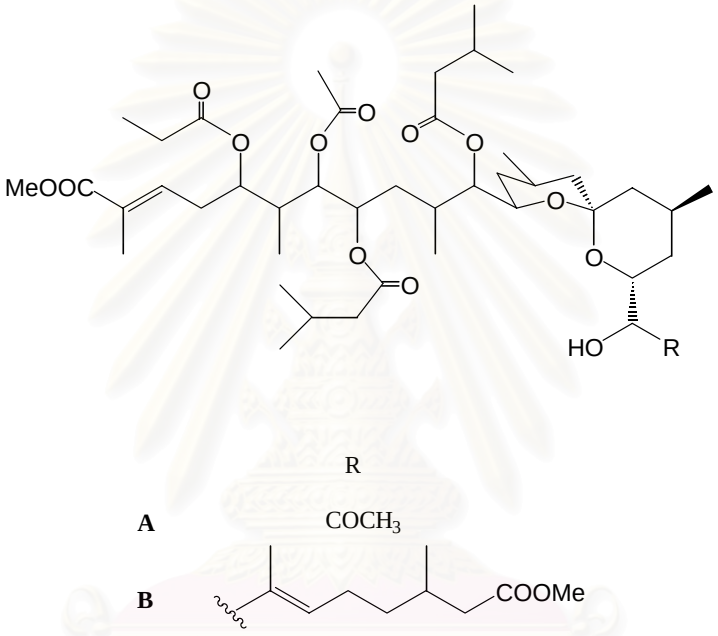

Figure 2.9 Structures of didemnaketals A and B

Abhijit Mazumder et al. found the compound which contains four 4-hydroxycoumarin residues exhibit antiviral, anti protease and anti integrase activity. NSC 158393 and NSC 117027, not only showed the potent integrase inhibitory activity with the IC_{50} value of 0.8±0.3 and 2.7±0.9 μM, respectively, but also exhibit the best protease inhibitory activity with the IC_{50} value of 1.7 and 0.75 μM, respectively. Hydroxycoumarins may provide lead compounds for development of novel antiviral

agents based on the concurrent inhibition of two viral targets, HIV-1 integrase and protease.(62)

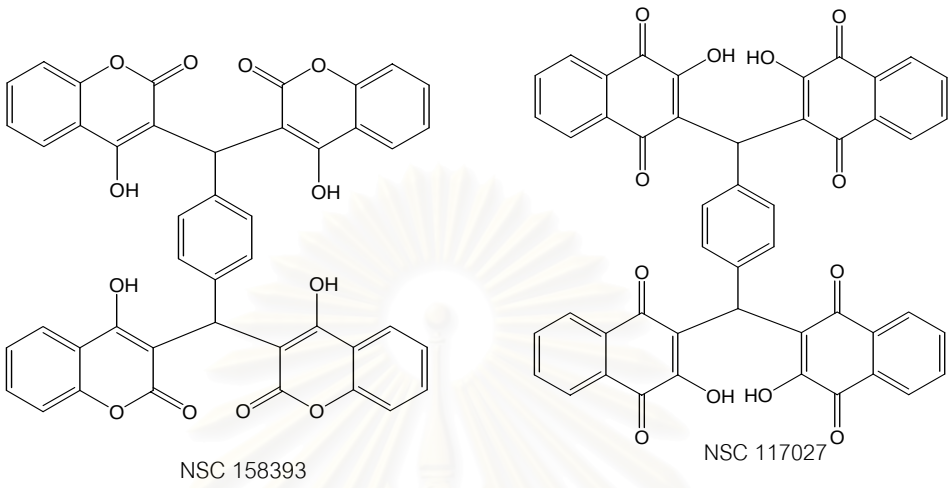

Figure 2.10 Structures of NSC 158393 and NSC 117027

Sahar El-Mekkawy et al. isolated thirteen compounds from the methanol extract of the fruiting bodies of *Ganoderma lucidum*. The structures of isolated compounds were determined by spectroscopic method. Ganoderiol F and ganodermanontriol were found to be active as anti-HIV-1 agents with an inhibitory concentration of 7.8 μg/ml for both, and ganoderic acid C1, 3β-5α-dihydroxy-6β-methoxy-ergosta-7,22-diene, ganoderic acid α, ganoderic acid H and ganoderiol A were moderately active inhibitors against HIV-1 protease with a IC_{50} value of 0.17-0.23 mM.(63)

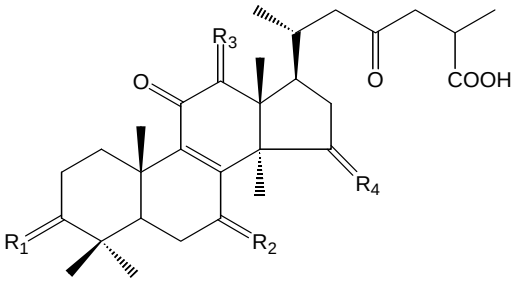

	R_1	R_2	R_3	R_4
Ganoderic acid a	OH H	O	OAc H	OH H
Ganoderic acid B	OAc H	O	OAc H	OAc H
Ganoderic Cl	OH H	OH H	H_2	O
Ganoderic acid H	OH H	O	OAc H	O

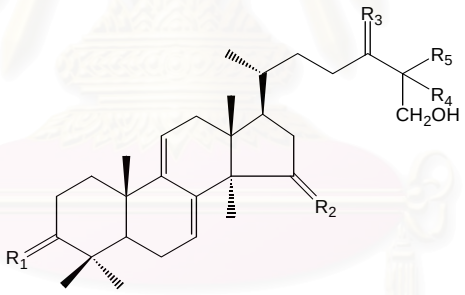

.

	R_1	R_2	R_3	R_4	R_5
Ganoderiol A	OH H	H_2	OH H	OH	CH_3
Ganoderiol B	O	OH H	$D^{24(25)}$		CH_2OH
Ganoderiol F	O	H_2	$D^{24(25)}$		CH_2OH
Ganodermanontriol	O	H_2	OH H	OH	CH_3

Figure 2.11 Structure of isolated compounds from *Ganoderma Lucidum*

Hong-Xi Xu et al. studied twenty-nine flavonoids and six hydrolysable tannins for their inhibitory activity against HIV-1 protease using fluorescence assay. Among these examined compounds, flavonols were the most active category while flavanones and catechols showed low activity. Quercetin was the most potent inhibitor with an IC_{50} value of 58.8 μM, while butein and luteolin showed moderate activity. For hydrolysable tannin, three ellagitannins which contain a hexahydroxydiphenoyl unit linked to the O-3 and O-6 positions of the sugar were found to be strongly inhibit HIV-1 protease. The IC_{50} value of corilagin and repandusinic acid on the target enzyme were 20.7 and 12.5 μM, respectively.(64)

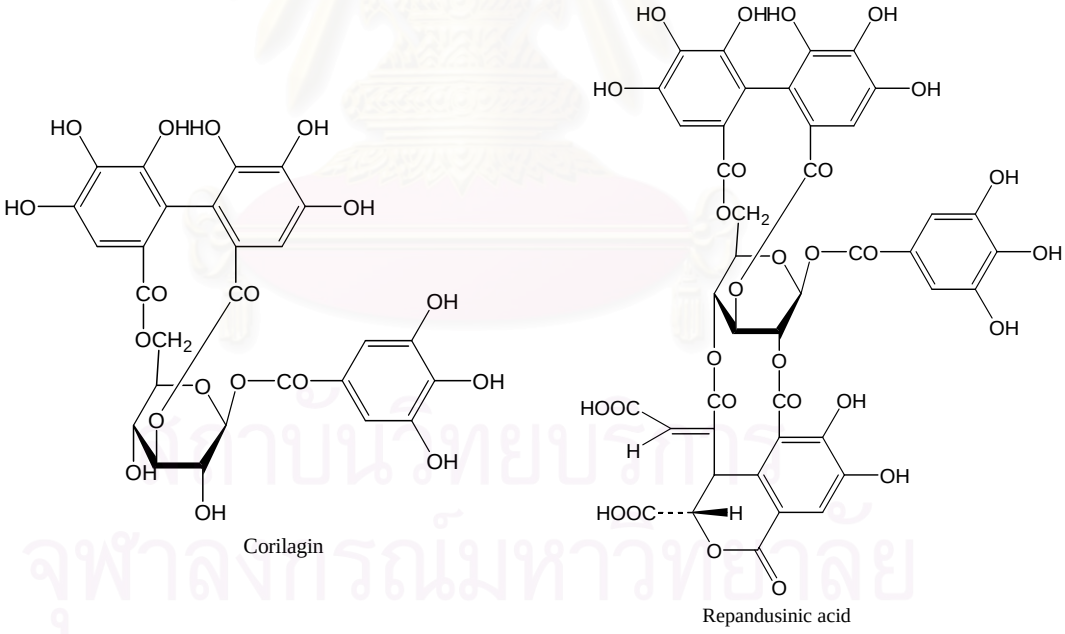

Figure 2.12 Structures of coliragin and repandusinic acid

2.2 Anti HCV

The hepatitis C virus is the principle etiologic agent if both parenterally transmitted and sporadic non-A non-B hepatitis. HCV infection most commonly results in chronic hepatitis that eventually develops into cirrhosis, hepatocellular carcinoma or liver failure. Current therapies for HCV infection have limited efficacy and frequently are accompanied by side effects.(41) So the need for improving inhibitors for anti HCV protease is greater. And the final stages of polyprotein processing are performed by the viral protease NS3. These reasons, HCV protease was chosen for investigation.

Jin-Rui Dai et al. found the crude extract of the broth of *Aspergillus ochraceus* can inhibit the final stage of polyprotein processing during HCV replication. And bioassay-guided fractionation led to the isolation of mellein as a active compound.(43)

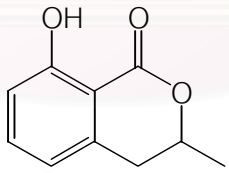

Figure 2.13 Structure of mellein

Vinod R. Hegde et al. screened several semi-purified fractions of aqueous methanolic extracts of many plants. One of these fractions, which was derived from a plant identified as *Stylogne cauliflora* sp., was active in NS3/4A protease assay. Two

novel oligophenolic compounds SCH 644343 and SCH 644342 were isolated from the 70% aq methanolic extract. Compound SCH 644343 and SCH 644342 showed an IC_{50} value of 0.3 and 0.8 μM, respectively. (42)

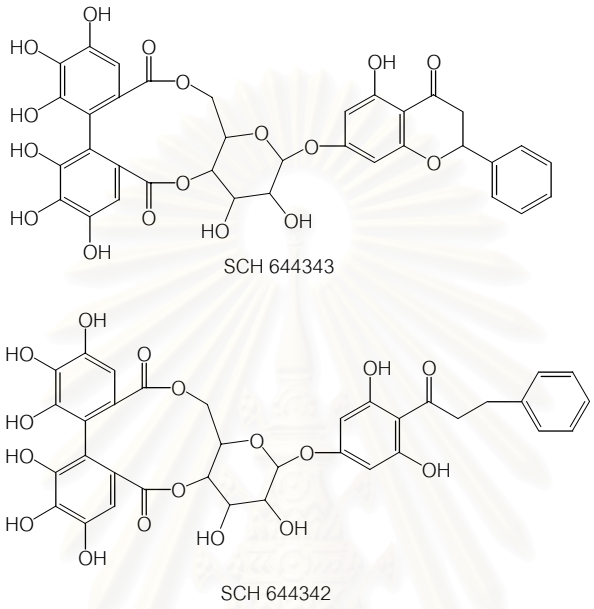

Figure 2.14 Structures of oligophenolic compounds SCH 644343 and SCH 644342

Min Chu et al. isolated SCH 351633, A new hepatitis C virus (HCV) protease inhibitor from the fungus, *Penicillium griseofulvum.* Structure elucidation of SCH 351633 was accomplished by analysis of spectroscopic data, which determined SCH 351633 to be a bicyclic hemiketal lactone. SCH 351633 exhibited inhibitory activity in the HCV protease assay with an IC_{50} value of 3.8 μg/mL.(65)

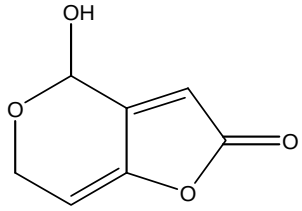

Figure 2.15 Structure of SCH 351633

Wei Han et al. used the α-ketoamides as templates for HCV protease inhibitors. The glycine carboxylic acid was found to be the most effective prime group. An IC_{50} of the optimized glycine α-ketoamide was 0.060 μM.(41)

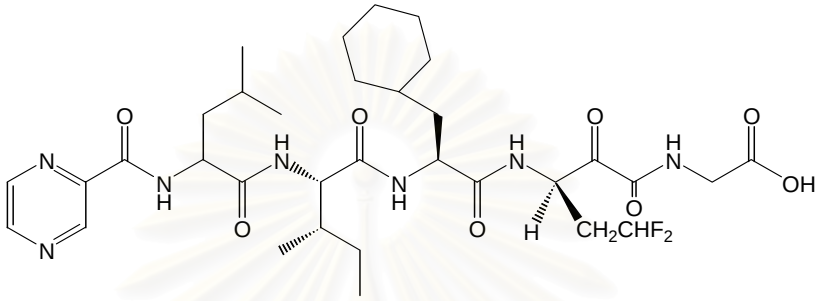

Figure 2.16 Structure of glycine α-ketoamide

2.3 Anti HCMV

Human cytomegalovirus (HCMV) is an opportunistic pathogen in immunocompromised individuals such as AIDS patients and organ transplant recipients.(66) For example, HCMV infection of the central nervous system is a probable cause of major learning disabilities.(47) Thus the need for effective and safe therapeutic agents for HCMV infection has to be broadened by investigating new targets that are essential for HCMV replication. HCMV protease has become a viable target for antiviral chemotherapy because of its critical role in capsid assembly and viral maturation.(67)

Jingfang Qian-Cutrone et al. isolated two new naphthacenequinone glycosides, quanolirones I and II together with the known compound galtamycin from the fermentation broth of *Streptomyces* sp. WC76535. Quanolirones I and II and galtamycin showed inhibitory activity against HCMV protease with IC_{50} values of 14, 35, and 52 μM, respectively.(68)

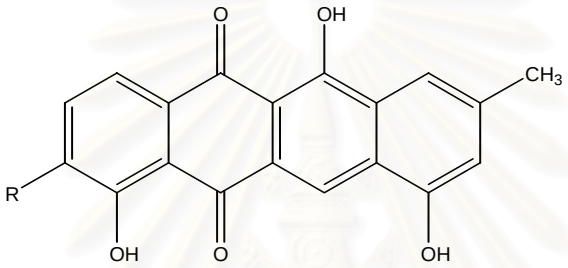

Quanolirone I : R =

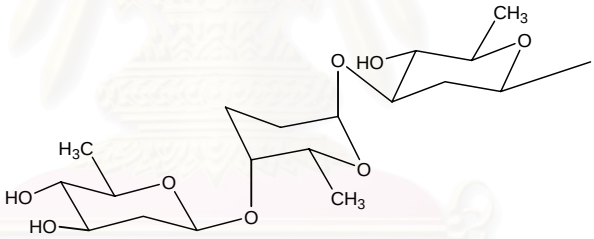

Quanolirone II : R =

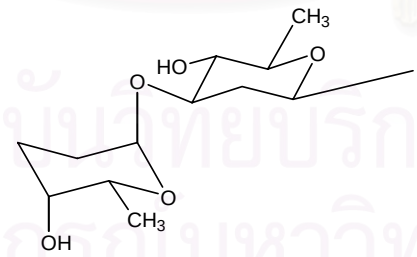

Figure 2.17 Structures of quanolirone I and II

Yue-Zhong Shu et al. isolated bripiodionen from Streptomyces sp. WC76599 during the screening of microbial fermentation extracts for their ability to inhibit human cytomegalovirus protease. Bripiodionen exhibited inhibitory activity against HCMV protease with an IC_{50} value of 30 μM.(47)

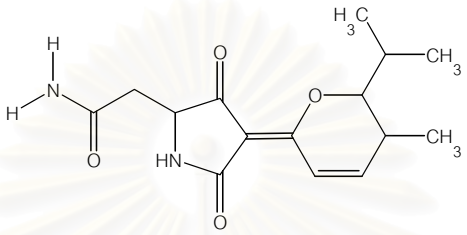

Figure 2.18 Structure of bripiodionen

Bingying Guo et al. found a solid state fermentation extract of the fungus Cytonaema sp. showed the inhibitory activity against HCMV protease with an IC_{50} value 31 μg/ml. Using bioassay-guided fractionation, cytonic acid A and B were isolated from the active crude extract. Cytogenic A and B showed inhibitory activity against HCMV protease with IC_{50} values of 43 and 11 μM, respectively.(69)

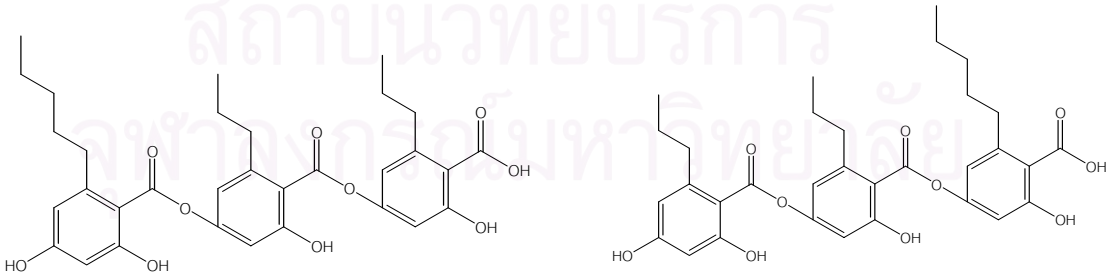

Cytogenic A

Cytogenic B

Figure 2.19 Structures of cytogenic A and B

Martin J. Di Grandi et al. searched for novel small molecule heterocycles with HCMV protease inhibitory activity, and dihydrotetrazine was identified as a potent inhibitor of HCMV protease. But dihydrotetrazine was oxidized by air oxidation to obtain tetrazine as a minor impurity. So this study became interested in developing an analogue of this compound and their inhibitory activity on HCMV protease. From the SAR data as well as synthetic considerations suggested the modification of C-3 substituent of tetrazine is a useful starting point.(70)

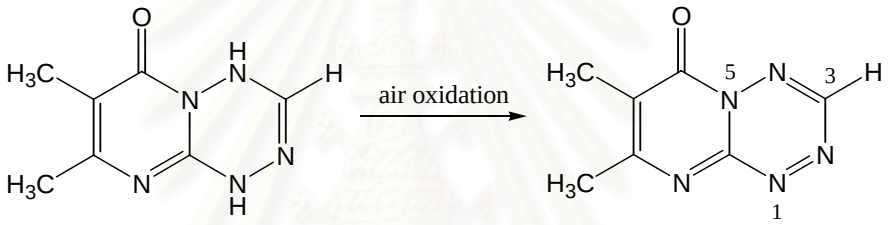

Figure 2.20 Air oxidation of dihydrotetrazine to tetrazine

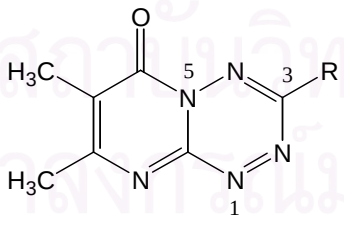

R	IC_{50} (μM)
H	0.1
CH_3	0.3
*n*Bu	0.4
*t*Bu	0.6
$CH(Ph)_2$	1.7
Ph	0.4
4-MePh	0.3
4-MeOPh	0.5
4-NO_2Ph	1.7

Figure 2.21 Summary of the HCMV protease inhibitory activity of tetrazines

CHAPTER III

EXPERIMENT

3.1 Plant materials

All medicinal plants in family *Zingiberaceae* were purchased from a local herbal shop in Bangkok, Thailand; *Curcuma aromatica*, *Curcuma sp.* (En leung), *Kaempferia galanga*, *Curcuma zedoaria*, *Curcuma longa*, *Kaempferia parviflora* (black rhizome), *Boesenbergia pandurata* (yellow rhizome), *Curcuma sp.* (Kamin Dum), *Zingiber zerumbet*, *Zingiber officinale* and *Alpinia galanga*.

3.2 Chemical reagents

3.2.1 All solvents used in this research such as hexane, chloroform, ethyl acetate and methanol, were purified by distillation prior to use, except reagent grade and HPLC grade solvents.

3.2.2 Merck's silica gel 60 G Art. 7734 (70-230 mesh ASTM) and 9385 (230-400 mesh ASTM) were used as adsorbents for column chromatography and flash column chromatography.

3.3.3 Merck's TLC aluminum sheets, siliga gel $^{60}F_{254}$ precoated 25 sheets, 20x20 cm^2, layer thickness 0.2 mm were used for TLC analysis.

3.3.4 HIV-1 RT was purchased from Cavidi Tech, Uppsala Science Park, Uppsala Sweden

3.3.5 HIV-1 protease obtained from Omar Gutierrez Arenas

3.3.6 α-glucosidase was purchased from Fluka

3.3.7 HCV protease obtained from Anton Poliakov

3.3.8 HCMV protease obtained from Matthis Geitmann

3.3.9 *trans*-cinnamic acid derivatives, compounds **15**, **19-28** obtained from Assist Prof. Warinthorn Chavasiri and compounds **16-18** were purchased from Fluka, and were used for the structure and activity relationship study on α-glucosidase.

3.3 Instruments and equipments

3.3.1 Melting point apparatus

The melting points were recorded on a Fisher - Johns melting point apparatus.

3.3.2 Rotary Evaporator

The Buchi rotary evaporator was used for the rapid removal of large amounts of volatile solvents.

3.3.3 Optical Rotation

The optical rotation values were measured by a Perkin - Elmer 341 polarimeter.

3.3.4 **Ultraviolet - visible Spectrophotometer (UV-VIS)**

The UV - VIS spectra were recorded on a Hewlett Packard 8452A diode array spectrophotometer in chloroform and methanol.

3.3.5 **Fourier Transform - Infrared Spectrophotometer (FT- IR)**

The FT-IR spectra were recorded on a Nicolet Impact 410 spectrophotometer. Spectra of solid samples were recorded as KBr pellets.

3.3.6 **Nuclear Magnetic Resonance Spectrometer (NMR)**

The ^{1}H and ^{13}C Nuclear Magnetic Resonance Spectra were recorded at 400 and 100 MHz, respectively, on a Varian Model Mercury 400 MHz in deuterated chloroform ($CDCl_3$), dimethylsulfoxide (DMSO) and water (D_2O).

3.3.7 **Mass Spectrometer (MS)**

The mass spectra were acquired by a Bruker MALDI-TOF Mass Spectrometer Model Trio 2000.

3.3.8 **Fluoroscan**

The fluoroscan which used to follow the changing of the enzyme activity is at the Department of Biochemistry, BMC, Faculty of Science and Technology, Uppsala University, Sweden.

3.4 Preparation of crude medicinal plants for testing against HIV-1 reverse transcriptase, HIV-1 protease, HCV protease and HCMV protease

Eleven medicinal plants in family *Zingiberaceae* analyzed in this study were purchased from a local herbal shop. The rhizome (2g) was extracted with 10 ml of methanol overnight or with 10 ml boiling distilled water under reflux for 2 hours. After filtration to remove insoluble debris, the water extract was lyophilized and the methanol extract was dried by evaporation.(71, 72) The dried extracts were stored at -20^{o}C until assay.

3.5 Reverse Transcriptase activity assay

The RT assay included in the ExaVir Load kit was used for the determination of the level of RT activity in the lysates. Briefly, poly(rA) covalently bound to the wells of a 96-well microtiter plate serves as template for the incorporation of 5-bromodeoxyuridine 5'-triphosphate (BrdUTP) during reverse transcription, which is allowed to proceed overnight (16-24 hours) at 33^{o}C. The amount of bromodeoxyuridine monophosphate (BrdUMP) incorporated into DNA is detected with an alkaline phosphate (Ap) conjugated anti-BrdU monoclonal antibody. The Ap substrate 4-methylumbelliferyl phosphate, was finally used for fluorometric detection. A serially diluted recombinant HIV-1 RT standard was included on each plate. The detection sensitivity of the assay depends on the duration of the enzyme reactions.(73)

3.6 HIV-1 protease activity assay

Enzymatic assays were performed in 100 mM sodium acetate, 1mM EDTA, 1 M NaCl, pH 4.7, 3% DMSO (v/v). Inhibitors and the fluorogenic substrate Dabcyl-γ-Abu-Ser-Gln-Asn-Tyr-Pro-Ile-Val-Gln-Edans were dissolved in DMSO before being used (final concentration: 3% DMSO v/v). For the determination of the IC_{50} values, 0.52 μl of a 3 mM substrate solution (final concentration 5.2 μM) was added to 5 μl of 4-7 different concentrations of inhibitor (final volume 300 μl). The enzymatic reaction was initiated by adding of enzyme (prediluted in buffer). The final enzyme concentration was 7.5 nM. The increase in fluorescence at 500 nm (λ_{exc} = 350 nm) was monitored over a period of 5 min at 30°C.(74,75)

3.7 HCV protease assay

The activity of the protease was measured at 30°C by a fluorescent assay, using Ac-DED(Edans)EEAbuψ[COO]ASK(Dabcyl)-NH_2 as a substrate and the peptide KKGSVVIVGRIVLSGK as a cofactor. The enzyme was incubated in 50 mM HEPES pH 7.5, 10 mM DTT, 40% glycerol, 0.1% n-octyl-β-D-glucoside, 3.3% DMSO with 25 μM cofactor and inhibitor at 30°C for 10 min, the reaction was initiated by addition of substrate. Any modifications of the standard assay buffer are indicated in

the text. Kinetic constants were determined with substrate concentration from 0.25-4 μM and enzyme concentrations from 0.5-1 nM, inhibition measurements were performed with 1nM enzyme, 0.5 μM substrate, and a final concentration of 3.3 %DMSO. Inhibitors were dissolved in DMSO, a mixture of DMSO and assay buffer, or assay buffer alone, sonicated for 30 s and vortexed. The solutions were stored at -20 ^{o}C between measurements. (76,77)

3.8 HCMV protease assay

Enzymatic assays were performed in 50 mM Tris-HCl, pH 8.5, 1mM EDTA, 14 mM NaCl, 9.3% glycerol and 3.3%DMSO (v/v). Inhibitors and the fluorogenic substrate Dabcyl-Arg-Gly-Val-Val-Asn-Ala-Ser-Ser-Arg-Leu-Ala-Edans were dissolved in DMSO before using. For determination of %inhibition, 3.16 μM of a fluorescent substrate solution was added to 5 μl of inhibitor (final volume 300 μl). The enzymatic reaction was initiated by adding of enzyme (prediluted in buffer). The final concentration of substrate and enzyme were 3 μM and 120 nM, respectively. The increase in fluorescence at 500 nm (λ_{exc} = 355 nm) was monitored over a period of 5 min at 30^{o}C in assay buffer.(78,79)

3.9 α-glucosidase assay

α-glucosidase from baker's yeast was assayed using 0.1 M phosphate buffer at pH 6.9, and 1 mM *p*-nitrophenyl-α-D-glucopyranoside (PNP-G) was used as a substrate. The concentration of the enzymes was 1 U/ml in each experiment. α-Glucosidase (40 μl) was incubated in the absence or presence of various concentrations of trans-cinnamic acid derivatives (10 μl) at 37°C. The preincubation time was specified at 10 min and PNP-G solution (950 μl) was added to the mixture. The reaction was carried out at 37 °C for 20 min, and then 1 ml of 1 M Na_2CO_3 was added to terminate the reaction. Enzyme activity was quantified by measuring the absorbance at 405 nm. 1-Deoxynorjirimycin was used as the positive control in this study.(80)

From the preliminary screening results on the HIV-1 protease enzyme inhibitory activity, the methanol extracts of *Kaempferia parviflora* and *Alpinia galanga* showed the potent inhibitory activity on the HIV-1 protease. Therefore, *Kaempferia parviflora* and *Alpinia galanga* were selected to extract and isolate to obtain the active compounds.

3.10 The extraction of *Kaempferia parviflora*

Fresh black rhizomes of *Kaempferia parviflora* (5 kg) were cut and crushed. After extraction with methanol (5 litres, 2 times) at room temperature, the filtrate was dried by evaporation under reduced pressure. The methanolic extract was extracted with hexane. The filtrate hexane solution was evaporated to afford the hexane extract as yellow viscous oil (0.50 g). The residue of the previous was extracted with ethyl acetate repeatedly. The combined ethyl acetate solution was concentrated under reduced pressure to give the ethyl acetate extract as a mixer of white solid and yellow oil 5.15 g) and the final insoluble residue was evaporated to obtain a brown - violet liquid (49.23 g). The extraction procedure of the black rhizomes of *Kaempferia parviflora* with various solvents is shown in scheme 3.1.

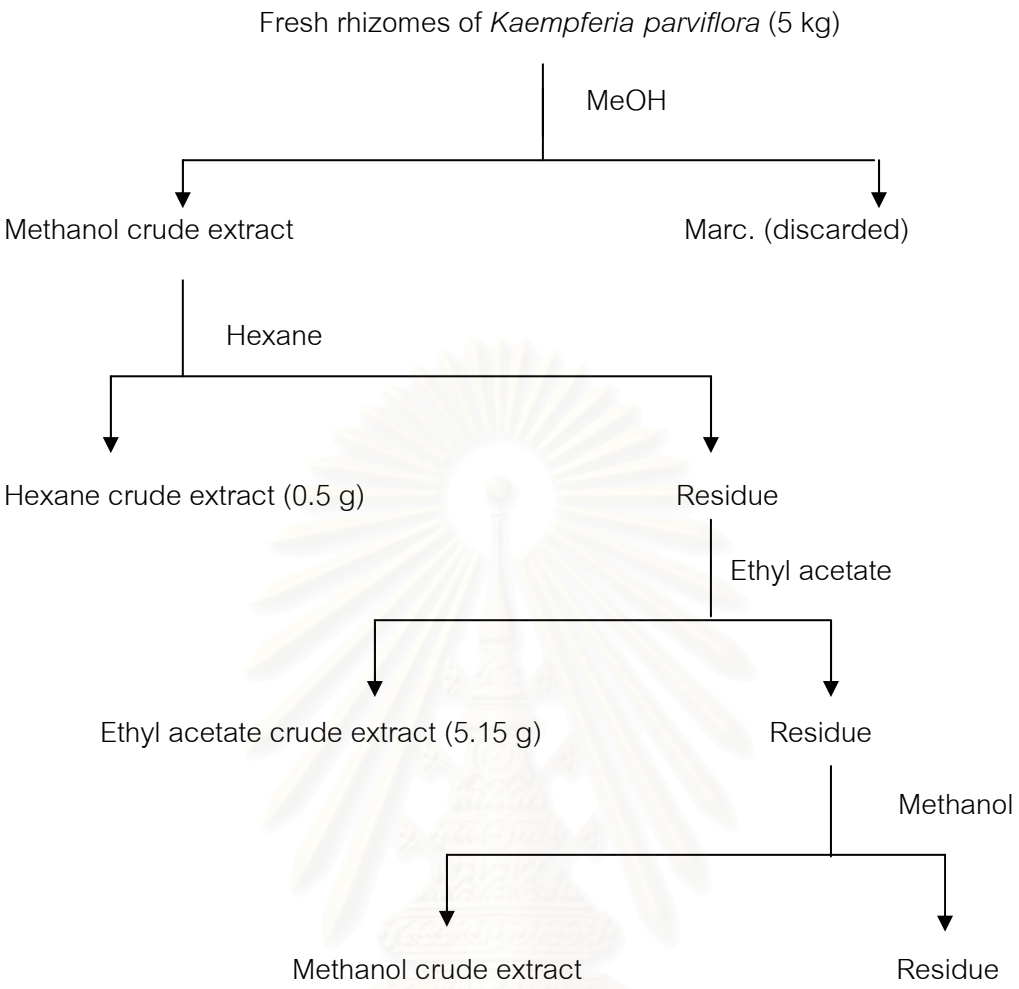

Scheme 3.1 The diagram showed procedure of *Kaempferia parviflora*

3.11 The isolation of crude extract from *Kaempferia parviflora*

After checking the chemical composition of the hexane, ethyl acetate and methanol crude extracts by TLC analysis, the result showed that hexane and ethyl acetate crude extracts has the same chemical composition. So the hexane and ethyl acetate crude extracts were combined. And the combined crude extract showed the inhibitory activity against HIV-1 protease more than methanol crude extract.

The combined hexane and ethyl acetate crude (5.2 g) was subjected to the silica gel column. The column was eluted with 100% hexane, then increased the concentration of ethyl acetate to 100% ethyl acetate and then after that increased the concentration of methanol to 10% methanol in ethyl acetate. Each fraction were monitored by TLC, the similar fractions were combined, the solvent was removed by evaporation, and then recrystallized to give compounds **1**, **2**, **3**, **4**, **5**, **6**, **7** and **8**, respectively. The isolation of compounds **1-8** from the combined hexane and ethyl acetate crude extract is briefly summarized in scheme 3.2.

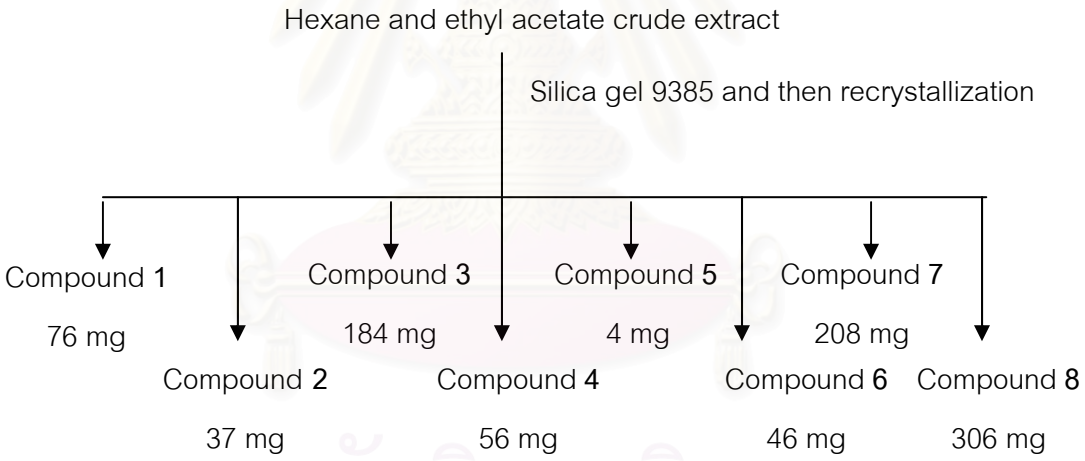

Scheme 3.2 The diagram showed isolation procedures and quantities of isolated compounds from hexane and ethyl acetate crude extract of fresh rhizomes *Kaempferia parviflora*

3.12 Purification and physical properties of isolated compounds from *Kaempferia parviflora*

3.12.1 Purification and physical properties of compound 1

Compound **1** was isolated from the combined hexane and ethyl acetate crude extract by the elution of silica gel column chromatography with 10% EtOAc/Hex. Compound **1** is yellow needle crystals (76 mg, 1.4% wt. by wt. of combined crude extract). Compound **1** had m.p. 129-130 °C and showed the R_f value of 0.58 on TLC plate using 20% ethyl acetate in hexane as the mobile phase.

3.12.2 Purification and physical properties of compound 2

Compound **2** is yellow plate crystals (37 mg, 0.71% wt. by wt. of combined crude extract). Compound **2** was obtained by elution of silica gel column chromatography with 10% ethyl acetate in hexane. Compound **2** had m.p. 170-171 °C and showed a single spot at the R_f value 0.45 on TLC plate using 20% ethyl acetate in hexane as the mobile phase.

3.12.3 Purification and physical properties of compound 3

Compound **3** was obtained from the combined hexane and ethyl acetate crude extract as a yellow needles crystal (184 mg, 3.54% wt. by wt. of combined crude extract) by the elution of silica gel column chromatography with 10% ethyl acetate in

hexane. Compound **3** had m.p. 146-148°C and showed a single spot at the R_f value 0.35 on TLC plate using 20% ethyl acetate in hexane as the mobile phase.

3.12.4 Purification and physical properties of compound 4

Compound **4** was obtained from the combined hexane and ethyl acetate crude extract by the elution of silica gel column chromatography with 15 % ethyl acetate in hexane. Compound 9 was a greenish – yellow solid (56 mg, 1.08% wt. by wt. of combined crude extract) with m.p. 175-176 °C and showed a single spot at the R_f value 0.35 on TLC plate using 20% ethyl acetate in hexane as the mobile phase.

3.12.5 Purification and physical properties of compound 5

Compound **5** was obtained from the combined hexane and ethyl acetate crude extract as a white powder (4 mg, 0.08% wt. by wt. of combined crude extract). Compound **5** was eluted from silica gel column chromatography with 30% EtOAc / Hex. Compound **5** had m.p. 148-150 °C and showed a single spot at the R_f value 0.4 on TLC plate using 50% EtOAc / Hex as the mobile phase.

3.12.6 Purification and physical properties of compound 6

Compound **6** from the combined hexane and ethyl acetate crude extract is a colorless needle crystal (total 46 mg, 0.88% wt. by wt. of combined crude extract). Compound **6** was obtained from the elution of silica gel column chromatography with 40% ethyl acetate in hexane and washed the crystals with 25% ethyl acetate in hexane. Compound **6** had m.p. 200-202 °C and showed a single spot at the R_f value of 0.41 on TLC plate using 70 % ethyl acetate in hexane as the mobile phase.

3.12.7 Purification and physical properties of compound 7

Compound **7** from the combined hexane and ethyl acetate crude extract as white solid (total 208 mg, 4.00% wt. by wt. of the combined crude extract), was obtained by the elution of silica gel column chromatography with 60% ethyl acetate in hexane. It was re-crystallized with 50% ethyl acetate in hexane to obtain colorless needle crystals and was washed with 30% ethyl acetate in hexane. Compound **7** had m.p.149-151°C and showed a single spot at the R_f value of 0.21 on TLC plate using 70 % ethyl acetate in hexane as the mobile phase.

3.12.8 Purification and physical properties of compound 8

Compound **8** was obtained from the combined hexane and ethyl acetate crude extract by the elution of silica gel column chromatography with 75% EtOAc / Hex, as a white powder (total 306 mg, 5.88% wt. by wt. of combined crude extract). Compound **8** had m.p.160-162°C and showed a single spot at the R_f value 0.23 on TLC plate using 80% EtOAc / Hex as the mobile phase.

3.13 Extraction of *Alpinia galanga*

The fresh rhizomes of *Alpinia galanga* (5 kg) were cut and extracted with methanol at room temperature. The filtrate was evaporated under reduced pressure. The crude methanolic extract was extracted with hexane (3 litres). The filtrate hexane solution was evaporated to afford the hexane extract as yellow oil (1 g). The residue of this step was extracted with ethyl acetate (4 litres). The combined ethyl acetate solution was concentrated by rotary evaporator under reduced pressure to give the ethyl acetate extract as yellow oil (29 g) and the final insoluble residue was evaporated to obtain a dark yellow gummy (20 g). The extraction procedure of the fresh rhizomes of *Alpinia galanga* with various solvents is shown in scheme 3.3.

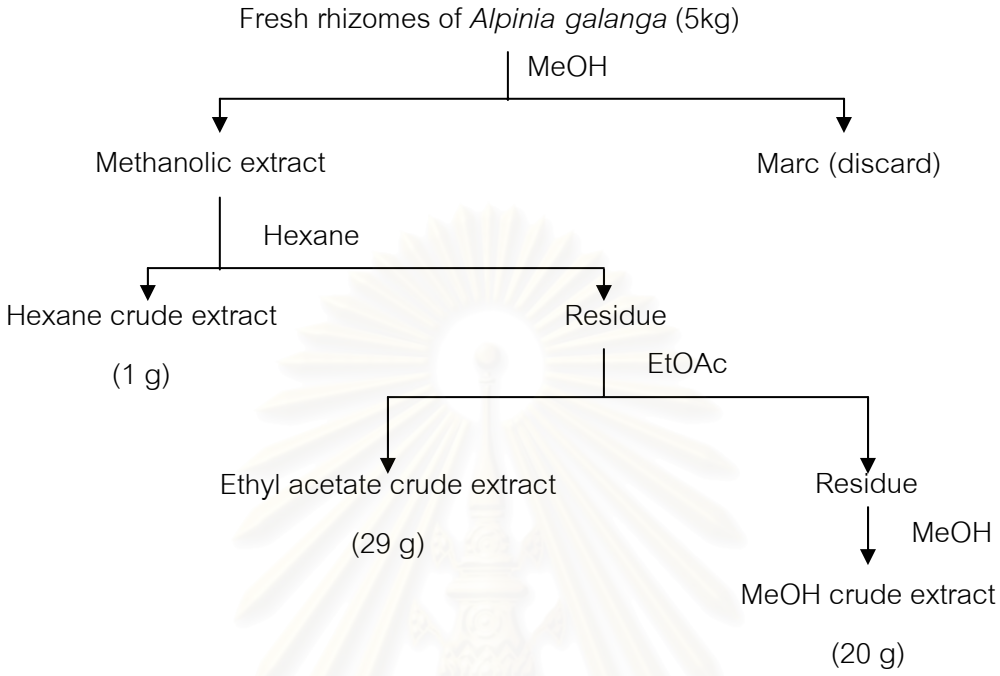

Scheme 3.3 The diagram showed extraction procedure of *Alpinia galanga*

3.14 Isolation of crude extract from *Alpinia galanga*

Because of the chemical composition of the hexane and ethyl acetate crude extracts has the same chemical composition, so the hexane and ethyl acetate crude extracts were combined. And the combined crude extract showed the inhibitory activity against viral protease enzyme more than methanol crude extract.

The combined hexane and ethyl acetate crude (20 g) was subjected to the silica gel column. The column was eluted with 100% hexane, then increased the concentration of ethyl acetate to 100% ethyl acetate and then after that increased the

concentration of methanol to 100% methanol. Each fraction was monitored by TLC, the similar fractions were combined, and the solvent was removed by evaporation to give compound **9** and **10**, respectively. Compound **11** was recrystallized from the fraction which eluted by 100% methanol. The isolation of compounds **9-11** from the combined hexane and ethyl acetate crude extract is briefly summarized in scheme 3.4.

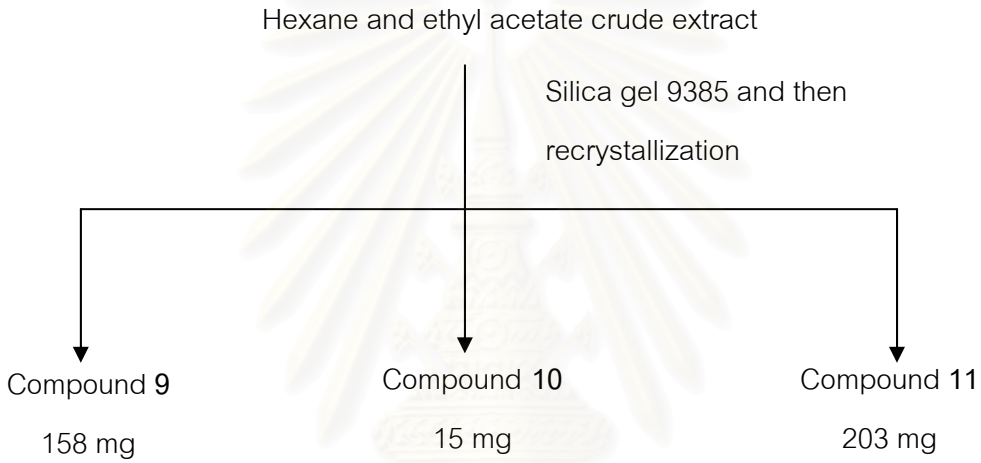

Scheme 3.4 The diagram showed isolation procedures and quantities of isolated compounds from hexane and ethyl acetate crude extract of fresh rhizomes *Alpinia galanga*

3.15 Purification and physical properties of isolated compounds from *Alpinia galanga*

3.15.1 Purification and physical properties of compound 9

Compound **9** was obtained from the methanol extract as yellow oil (total 158 mg, 0.79% wt. by wt. of the combined crude extract). Compound **9** was eluted from

silica gel column chromatography with 20% ethyl acetate in hexane. Compound **9** had the R_f value 0.47 on TLC plate using 20% EtOAc / Hex as the mobile phase.

3.15.2 Purification and physical properties of compound 10

Compound **10** was obtained from combined hexane and ethyl acetate crude extract as a colorless needle crystal (total 15 mg, 0.075% wt. by wt. of the combined crude extract). Compound **10** was eluted from silica gel column chromatography with 40% EtOAc / Hex. Compound **10** showed a single spot at the R_f value 0.11 on TLC plate using 20% EtOAc / Hex as the mobile phase.

3.15.3 Purification and physical properties of compound 11

Compound **11** was obtained from combined hexane and ethyl acetate crude extract as a white solid (total 203 mg, 1.01% wt. by wt. of the combined crude extract). Compound **11** was eluted from silica gel column chromatography with 100% MeOH. Compound **11** had m.p. 136-138°C and showed a single spot at the R_f value 0.24 on TLC plate using 100% MeOH as the mobile phase.

3.16 Extraction of *Kaempferia galanga*

The dried rhizomes of *Kaempferia galanga* (3 kg) were crushed and refluxed with methanol (6 litres) overnight, the filtrate was evaporated under reduced pressure.

The methanolic extract was reextracted with hexane (4 litres). The filtrate hexane solution was evaporated to afford the hexane extract as yellow oil (80 g). And then after that the residue of previous step was repeatedly reextracted with ethyl acetate (3 litres). The ethyl acetate solution was concentrated by rotary evaporator under reduced pressure to give the ethyl acetate extract as a mixer of white needle crystal and yellow oil (15 g) and the final insoluble residue was evaporated to obtain a dark-brown (32 g) gummy methanol crude extract. The extraction procedure of the dried rhizomes of *Kaempferia galanga* with various solvents is shown in scheme 3.5.

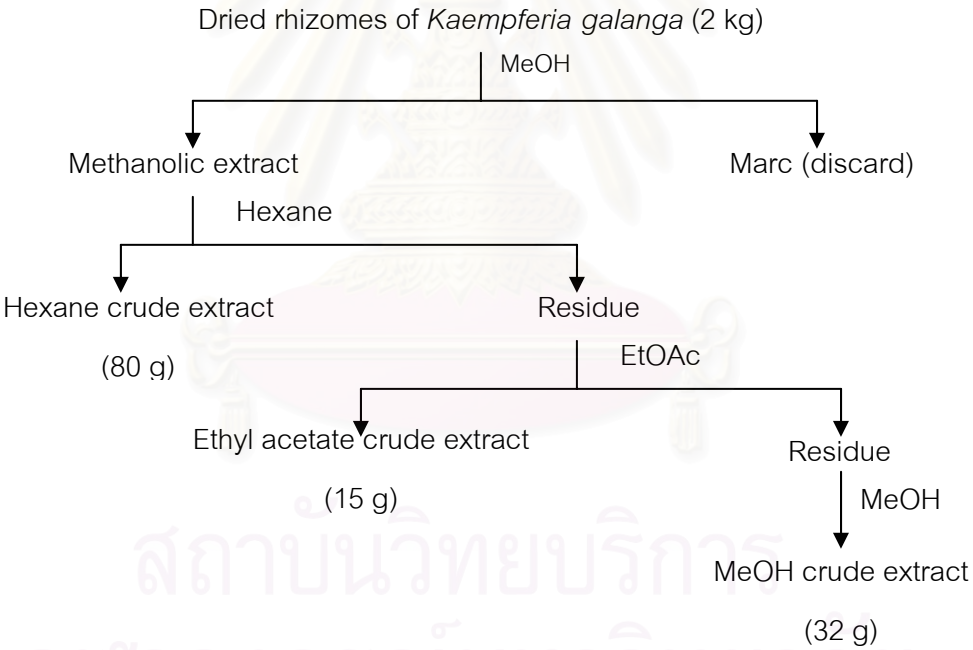

Scheme 3.5 The diagram showed extraction procedure from *Kaempferia galanga*

3.17 Isolation of crude extract from *Kaempferia galanga*

From TLC analysis, the hexane and ethyl acetate crude extracts has the same chemical composition, so the hexane and ethyl acetate crude extracts were combined. And the combined crude extract also showed the inhibitory activity against HIV-1 protease more than methanol crude extract.

The combined hexane and ethyl acetate crude (50 g) was subjected to the silica gel column. The column was eluted with 100% hexane, then increased the concentration of ethyl acetate to 100% ethyl acetate and then after that increased the concentration of methanol to 10% methanol in ethyl acetate. Each fraction was monitored by TLC, the similar fractions were combined, and the solvent was removed by evaporation to give compound **12**, **13** and **14**, respectively. The isolation of compounds **12-14** from the combined hexane and ethyl acetate crude extract is briefly summarized in scheme 3.4.

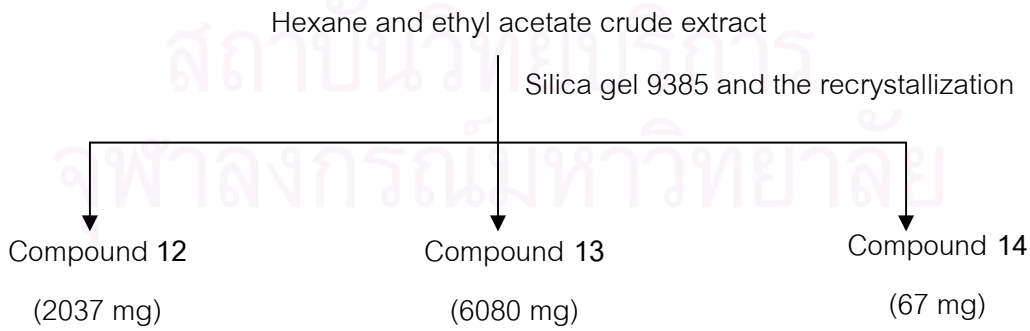

Scheme 3.6 The diagram showed isolation procedures and quantities of isolated compounds from hexane and ethyl acetate crude extract of *Kaempferia galanga*

3.18 Purification and physical properties of isolated compounds from *Kaempferia galanga*

3.18.1 Purification and physical properties of compound 12

Compound **12** was obtained from ethyl acetate crude extract as yellow oil (total 2037 mg, 4.07% wt. by wt. of the combined hexane and ethyl acetate crude extract). Compound **12** was eluted from silica gel column chromatography with 100% Hexane. Compound **12** had the R_f value 0.69 on TLC plate using 20% EtOAc / Hex as the mobile phase.

3.18.2 Purification and physical properties of compound 13

Compound **13** was obtained from ethyl acetate crude extract as a colorless crystal (total 6080 mg, 12.16% wt. by wt. of the combined crude extract). Compound **13** was eluted from silica gel column chromatography with 10% EtOAc/Hexane. Compound **13** had m.p. 48-50°C and showed the R_f value of 0.52 on TLC plate using 20% EtOAc / Hex as the mobile phase.

3.18.3 Purification and physical properties of compound 14

Compound **14** was obtained from ethyl acetate crude extract as a white needle crystal (total 67 mg, 0.13% wt. by wt. of the combined crude extract). Compound **14** was eluted from silica gel column chromatography with 25% EtOAc /

Hexane. Compound **14** had m.p.173-175 °C and showed the R_f value of 0.12 on TLC plate using 40% EtOAc / Hex as the mobile phase.

3.19 Structure and activity relationship study of trans-cinnamic acid and its derivative on inhibitory activity of α-glucosidase

Three isolated compounds from the rhizomes of *Kaempferia galanga* (**12**, **13**, and **14**), *trans*-cinnamic acid derivatives (**15**, **19-28**) which synthesized by the Perkin reaction between aromatic aldehydes and aliphatic carboxylic acids following the procedure of Chiriac et al, and compounds **16-18** were purchased from Fluka Co. Ltd. were tested against α-glucosidase to study the structure and activity relationship.

CHAPTER IV

RESULTS AND DISCUSSION

4.1 Screening of methanol and aqueous crude extracts for inhibition of HIV-1 reverse transcriptase, HIV-1 protease, HCV protease and HCMV protease activity

Methanol and aqueous crude extracts were prepared from 11 medicinal plants in the *Zingiberaceae* family. The inhibitory effect of each extract was tested at a concentration of 20 μg/ml and 200 μg/ml with HIV-1 reverse transcriptase, HIV-1 protease HCV protease and HCMV protease. For HIV-1 reverse transcriptase, the methanol extracts had no inhibitory activity and most of the aqueous extracts also had no inhibitory activity at high concentration (Table A1). But for viral proteases, the methanol extracts were overall more inhibitory activity than the aqueous extracts (Table A2-4). Only three aqueous extracts resulted in more than 90% inhibition, while ten methanol extracts exhibited at least 90% inhibition of the proteases studied. Furthermore, none of the aqueous extracts were inhibitory to this degree at the lower concentration tested, while two of the methanol extracts were. Of the three aqueous extracts that showed at least 90% inhibition, two of the corresponding methanol extracts were also inhibitory to this degree.

4.1.1 Inhibition of HIV-1 reverse transcriptase

The methanol crude extracts of examined plants were found to inhibit HIV-1 reverse transcriptase less than 50% at a concentration of 200 μg/ml. On studying inhibition of reverse transcriptase by plant extracts an IC_{50} of 200 μg/ml or greater was considered to be inactive.(71,81) But the aqueous extracts of *Curcuma zedoaria*, *Curcuma longa* and *Zingiber officinale* showed an inhibitory activity more than 50% at high concentration. (Table A1)

4.1.2 Inhibition of HIV-1 protease

The methanol crude extracts of *Curcuma zedoaria, Curcuma longa, Kaempferia parviflora* and *Alpinia galanga* were found to inhibit HIV-1 protease activity by more than 90% at a concentration of 200 μg/ml (Table A2). The *Alpinia galanga* extract retained more than 90% inhibition of HIV-1 protease activity at a ten-fold lower concentration. The aqueous extracts of *Curcuma zedoaria, Curcuma longa* showed an inhibitory effect (80% inhibition) at high concentration (Table A2).

4.1.3 Inhibition of HCV protease

The methanol crude extracts of *Curcuma sp.* (En leung), *Curcuma zedoaria*, *Curcuma longa*, *Kaempferia parviflora, Boesenbergia pandurata Zingiber zerumbet*, *Zingiber officinale* and *Alpinia galanga* were found to inhibit HCV protease activity by

more than 70% at a concentration of 200 μg/ml (Table A3). At a low concentration (20 μg/ml), the methanol crude extracts of *Curcuma sp.* (En leung), *Curcuma zedoaria*, *Zingiber officinale* and *Alpinia galanga* elicited inhibition over 50%. For the aqueous extracts, most of examined herbal aqueous extracts except *Kaempferia galanga* showed more than 70% inhibition of HCV protease at a concentration of 200 μg/ml (Table A3). At a concentration of 20 μg/ml, the aqueous extracts of *Curcuma aromatica*, *Curcuma zedoaria*, *Curcuma longa*, *Kaempferia parviflora* and *Boesenbergia pandurata* showed more than 50% inhibition.

4.1.4 Inhibition of HCMV protease

The methanol crude extract of *Curcuma aromatica*, *Curcuma sp.* (En leung), *Curcuma zedoaria*, *Curcuma longa*, *Kaempferia parviflora, Boesenbergia pandurata* and *Alpinia galanga* showed to inhibit HCMV protease activity by more than 70% at high concentration (200 μg/ml) (Table A4). At low concentration (20 μg/ml), the methanol crude extracts of *Curcuma longa* and *Alpinia galanga* were inhibitory by more than 60%. The aqueous extracts of *Curcuma aromatica*, *Curcuma longa* were found to inhibit HCMV protease by more than 50% at high concentration (Table A4).

Because of the methanol extracts of *Kaempferia parviflora* and *Alpinia galanga* exhibited more than 80% inhibition of HIV-1 protease at high concentration and more than 70% inhibition of HCV protease and HCMV protease, so methanol

extracts of *Kaempferia parviflora* and *Alpinia galanga* were selected to extract and purify to obtain the active compounds.

4.2 Structure elucidation of the isolated compounds from *Kaempferia parviflora*

4.2.1 Structure elucidation of compound 1

Compound **1** is a yellow needle crystal (76 mg) which obtained from the combined crude extract. The UV spectrum of compound **1** exhibited absorption maxima at 268 and 330 nm.

The IR spectrum (figure A1) of compound **1** showed a broad absorption band between 3600-3300 cm^{-1} of OH stretching vibration and a strong absorption band at 1661 cm^{-1} which indicated the presence of a carbonyl group. The IR spectrum of compound **1** is summarized in table 4.1.

Table 4.1 The IR absorption band assignment of compound **1**

Wave number (cm^{-1})	Intensity	Vibration
3600 - 3000	Broad	O-H stretching vibration of hydroxy group
2930, 2820	Weak, Weak	C - H stretching vibration of $-CH_3$
1661	Strong	C=O stretching vibration of carbonyl Conjugated ketone
1594, 1496	Strong, Weak	C=C stretching vibration of aromatic
1180, 1127	Medium, Medium	C-O symmetry stretching Vibration of C-O-C

The ^{1}H-NMR spectrum pattern (Figure A2, A6, A10, A14, A18, A22, A26 and A30) of compounds **1-8** exhibited the flavonoid nucleus identity (C_6-C_3-C_6) that showed in figure 4.1. As previously observed the C-6 and C-8 protons of the A-ring of flavonoids give rise to two signals usually between 6-6.5 ppm when, as is often the case, the other positions of ring A are substituted. The signals from the B-ring protons normally absorb downfield around 6.7-7.5 ppm.(82, 83)

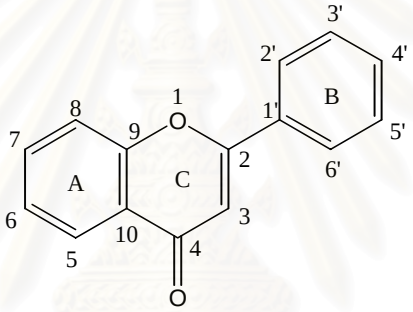

Figure 4.1 Flavonoid nucleus

The ^{1}H-NMR spectrum ($CDCl_3$, 400 MHz) (figure A2) was integrated for 14 protons, two singlets at δ 3.91 and 3.92 which exhibited methoxy protons at H-7 and H-3, respectively. Two singlets at δ 6.41 and 6.50 were due to the protons at H-6 and H-8. The hydroxyl group at C-5 appeared at δ 12.56. The ^{1}H-NMR spectrum indicated the presence of three protons and two protons signals at δ 7.56 and 8.11, respectively, which are typical of a flavonoid nucleus with an unsubstituted B ring. (Table 4.2)

The ^{13}C-NMR spectrum ($CDCl_3$, 100 MHz) (figure A3) showed that compound **1** has 17 carbons in which 15 carbons of flavonoid nucleus and two methoxy groups which appeared at δ 55.8 and 60.4 ppm. One carbonyl carbon appeared at δ 178.9 ppm (C-4). At A-ring, there were six aromatic carbons, δ 156.9 (C-5), δ 98.0 (C-6), δ 165.6 (C-7), δ 92.2 (C-8), δ 155.9 (C-9) and δ 106.2 (C-10). At B-ring, there were four signals for six aromatic carbons, δ 130.4 (C-1'), δ 128.4 (C-2', 6'), δ 128.6 (C-3', 5') and δ 130.9 (C-4'). The remaining two signals were at δ 162.0 and δ 139.7 which assigned to C-2 and C-3 respectively. (Table 4.2)

The MALDI-TOF mass spectrum (Figure A4) of compound **1** was exhibited $[M+H]^+$ at m/z 299.21, so the molecular weight of compound **1** was 298.

The molecular formula of compound **1** was determined as $C_{17}H_{14}O_5$ by MALDI-TOF, ^{1}H and ^{13}C-NMR spectral data.

Table 4.2 ^{1}H and ^{13}C-NMR spectral data of compound **1** (ppm)

Position	δ_H Compound **1**	δ_H 5-hydroxy-3,7-dimethoxyflavone (84)	δ_C Compound **1**
2	-	-	162.0
3	-	-	139.7
4	-	-	178.9
5	-	-	156.9
6	6.41 (1H, s)	6.37 (1H, d, *J* = 2.5 Hz)	98.0
7	-	-	165.6
8	6.50 (1H, s)	6.47 (1H, d, *J* = 2.5 Hz)	92.2
9	-	-	155.9
10	-	-	106.2
1’	-	-	130.4
2'	8.11 (2H, s)	8.08 (2H, m)	128.4
3'	7.56 (3H, s)	7.50 (3H, m)	128.6
4'	7.56 (3H, s)	7.50 (3H, m)	130.9
5'	7.56 (3H, s)	7.50 (3H, m)	128.6
6'	8.11 (2H, s)	8.08 (2H, m)	128.4
3-OCH_3	3.91 (3H, s)	3.87 (6H, s)	60.4
7-OCH_3	3.92 (3H, s)	3.87 (6H, s)	55.8
5-OH	12.63 (1H, s)	12.53 (1H, s)	-

According to all spectroscopic data and comparison of ^{1}H-NMR spectral data between compound **1** and 5-hydroxy-3,7-dimethoxyflavone (84) was carried out in

order to confirm compound **1** was assigned as 5-hydroxy-3,7-dimethoxyflavone. The structure of 5-hydroxy-3,7-dimethoxyflavone is shown in figure 4.2.

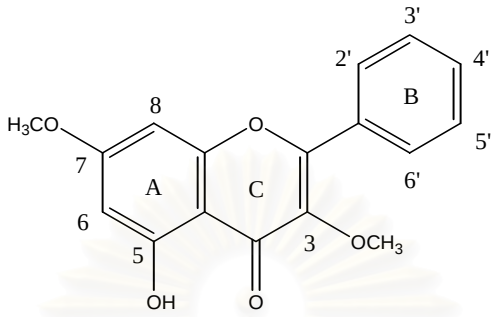

Figure 4.2 The structure of compound **1**

4.2.2 Structure elucidation of compound 2

Compound **2** is a yellow plate crystal (37 mg) which obtained from the combined crude extract. The UV spectrum of compound **2** exhibited absorption maxima at 270 nm.

The IR spectrum (Figure A5) of compound **2** showed a broad absorption band between 3600-3200 cm^{-1} of OH stretching vibration and a strong absorption band at 1665 cm^{-1} which consistent with a carbonyl group. The IR spectrum of compound **2** is summarized in table 4.3.

Table 4.3 The IR absorption band assignment of compound **2**

Wave number (cm-1)	Intensity	Vibration
3600 - 3200	Broad	O-H stretching vibration of hydroxy group
1665	Strong	C=O stretching vibration of carbonyl Conjugated ketone
1606, 1496	Strong, medium	C=C stretching vibration of aromatic
1157, 1100, 1020	Medium, weak, weak	C-O symmetry stretching vibration of C-O-C
880, 820, 780	Weak	= C-H out of plane bending vibration of aromatic

From the ^{1}H-NMR spectrum (Figure A6) and ^{13}C-NMR (Figure A7) spectrum of compound **2** exhibited the flavonoid nucleus identity (C_6-C_3-C_6) like compound **1** that showed in figure 4.1.

The ^{1}H-NMR spectrum of compound **2** ($CDCl_3$, 400 MHz) (Figure A6) was integrated for twelve protons, a singlet at δ 3.92 which assigned as a methoxy group. Both protons on H-6 and H-8 appeared as two doublets at δ 6.42 (J = 2 Hz) and 6.54 (J = 2 Hz). The singlet at δ 6.71 was assigned to the H-3 proton and the hydroxyl proton appeared at δ 12.77. A monosubstituted B-ring appeared as two multiplets at δ 7.57 and 7.92 with integration for 3*H and 2*H, respectively.

The ^{13}C-NMR spectrum ($CDCl_3$, 100 MHz) (Figure A7) showed that compound **2** has 16 carbons in which a methoxy group appeared at δ 55.8 ppm and 15 carbons of flavonoid moiety. One carbonyl carbon appeared at δ 182.5 ppm (C-4). At A-ring, there were six aromatic carbons, δ 162.1 (C-5), δ 98.2 (C-6), δ 165.6 (C-7), δ 92.6 (C-8), δ 157.7 (C-9) and δ 105.7 (C-10). At B-ring, there were four signals for six aromatic carbons, δ 131.2 (C-1'), δ 126.3 (C-2', 6'), δ 129.1 (C-3', 5') and δ 131.9 (C-4'). The remaining two signals were at δ 163.9 and δ 105.8 which assigned to C-2 and C-3 respectively. (Table 4.4)

The MALDI-TOF mass spectrum (Figure A8) of compound **2** was exhibited the $[M+H]^+$ at m/z 269.45, so the molecular weight of compound **2** is 268.

Compound **2** was assigned molecular formula $C_{16}H_{12}O_4$ based on MALDI-TOF and NMR spectral data.

Table 4.4 ^{1}H and ^{13}C-NMR spectral data of compound **2** (ppm)

Position	δ_H Compound **2**	δ_H 5-hydroxy-7-methoxyflavone (85)	δ_C Compound **2**	δ_C 5-hydroxy-7-methoxyflavone (85)
2	-	-	163.9	163.98
3	6.71 (1H, s)	6.65 (1H, s)	105.8	105.86
4	-	-	182.5	182.50
5	-	-	162.1	162.18
6	6.42 (1H, d, *J* = 2 Hz)	6.37 (1H, d, *J* = 1.5 Hz)	98.2	98.21
7	-	-	165.6	165.62
8	6.54 (1H, d, *J* = 2 Hz)	6.47 (1H, d, *J* = 1.5 Hz)	92.6	92.68
9	-	-	157.7	157.80
10	-	-	105.7	105.71
1’	-	-	131.2	131.31
2'	7.92 (2H, m)	7.89 (2H, m)	126.3	126.29
3'	7.57 (3H, m)	7.54 (3H, m)	129.1	128.76
4'	7.57 (3H, m)	7.54 (3H, m)	131.9	131.85
5'	7.57 (3H, m)	7.54 (3H, m)	129.1	128.76
6'	7.92 (2H, m)	7.89 (2H, m)	126.3	126.29
7-OCH_3	3.92 (3H, s)	3.87 (3H, s)	55.8	55.83
5-OH	12.77 (1H, s)	12.73 (1H, s)	-	-

The result of ^{13}C-NMR spectra correlated to result of ^{1}H-NMR spectrum which agreed with the literature(85), compound **2** was assigned as 5-hydroxy-7-methoxyflavone and the structure of 5-hydroxy-7-methoxyflavone showed in figure 4.3.

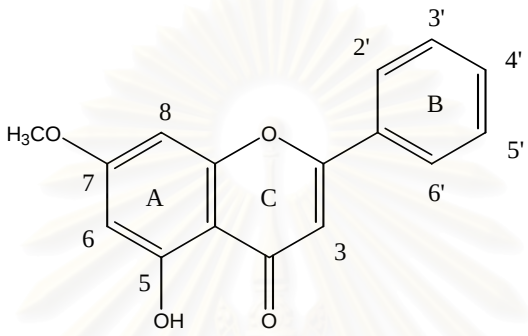

Figure 4.3 The structure of compound **2**

4.2.3 Structure elucidation of compound 3

Compound **3** is a yellow needles crystal (184 mg) which obtained from the combined crude extract. The UV spectrum of compound **3** exhibited absorption maxima at 270 and 346 nm.

The IR spectrum (Figure A5) of compound **2** showed a broad absorption band between 3600-3200 cm^{-1} of OH stretching vibration and a strong absorption band at 1665 cm^{-1} which consistent with a carbonyl group. The IR spectrum of compound **2** is summarized in table 4.5.

Table 4.5 The IR absorption band assignment of compound **3**

Wave number (cm^{-1})	Intensity	Vibration
3500 - 3100	Broad	O-H stretching vibration of hydroxy group
3050, 3000, 2850	weak	C - H stretching vibration of aromatic
1661	Medium	C=O stretching vibration of carbonyl Conjugated ketone
1587, 1500	Strong, Medium	C=C stretching vibration of aromatic
1172, 1090	Strong, Medium,	C-O symmetry stretching vibration of C-O-C
939, 880, 828	Medium, Medium, Medium	= C-H out of plane bending vibration of aromatic

As same as the compound **1** and **2**, ^{1}H-NMR and ^{13}C-NMR spectra showed that compound **3** has the flavonoid nucleus identity. The ^{1}H-NMR spectrum ($CDCl_3$, 400 MHz) (Figure A10) of compound **3** showed two singlets at δ 6.40 (*J* = 2 Hz) and 6.49 (*J* = 2 Hz) and each was integrated for one proton, suggesting a 5,7-disubstitued at A ring. Signals at δ 3.89, 3.91 and 3.94 (all singlets, each 3*H) were attributable to three methoxy groups. The pattern of two doublets appeared at δ 7.06 (*J* = 9 Hz) and 8.12 (*J* = 9 Hz), indicating the *para*-substituted at B ring. The singlet at δ 12.70 was assigned to the hydroxyl proton at A ring which had hydrogen bond with 4-C=O.

The ^{13}C-NMR spectrum ($CDCl_3$, 100 MHz) (Figure A11) showed that compound **3** has 18 carbons in which the methoxy groups appeared at δ 55.4, 55.8,

60.1 ppm and 15 carbons of flavonoid nucleus. One carbonyl carbon appeared at δ 178.8 (C-4). The aromatic region contained a total of 12 resonances. At A-ring, there were six aromatic carbons, δ 155.9 (C-5), δ 92.1 (C-6), δ 165.4 (C-7), δ 97.8 (C-8), δ 162.0 (C-9) and δ 106.0 (C-10). At B-ring, there were four signals for six aromatic carbons, δ 122.8 (C-1'), δ 130.2 (C-2', 6'), δ 114.1 (C-3', 5') and δ 161.7 (C-4'). At δ 156.7 and δ 138.8 were assigned to C-2 and C-3 respectively. (Table 4.6)

The MALDI-TOF mass spectrum (Figure A12) of compound **3** was exhibited the $[M+H]^+$ at m/z 329.48, so the molecular weight of compound **3** is 328.

Compound **3** was assigned molecular formula $C_{18}H_{16}O_6$ based on MALDI-TOF and NMR spectral data.

Table 4.6 ^{1}H and ^{13}C-NMR spectral data of compound **3** (ppm)

Position	δ_H Compound **3**	δ_H 5-hydroxy-3,7,4'-trimethoxyflavone (86)	δ_C Compound **3**
2	-	-	156.7
3	-	-	138.8
4	-	-	178.8
5	-	-	155.9
6	6.40 (1H, s)	6.35 (1H, d, *J* = 2.5 Hz)	92.1
7	-	-	165.4
8	6.49 (1H, s)	6.45 (1H, d, *J* = 2.5 Hz)	97.8
9	-	-	162.0
10	-	-	106.0
1’			122.8
2'	8.12 (2H, d, *J* = 9 Hz)	8.07 (2H, d, *J* = 9 Hz)	130.2
3'	7.06 (2H, d, *J* = 9 Hz)	7.02 (2H, d, *J* = 9 Hz)	114.1
4'	-	-	161.7
5'	7.06 (2H, d, *J* = 9 Hz)	7.02 (2H, d, *J* = 9 Hz)	114.1
6'	8.12 (2H, d, *J* = 9 Hz)	8.07 (2H, d, *J* = 9 Hz)	130.2
3-OCH_3	3.89 (3H, s)	3.87 (6H, s)	60.1
7-OCH_3	3.94 (3H, s)	3.89 (6H, s)	55.8
4'-OCH_3	3.91 (3H, s)	3.87 (6H, s)	55.4
5-OH	12.70 (1H, s)	12.70 (1H, s)	-

According to the literature (86) and all spectroscopic data compound **3** was interpreted for 5-hydroxy-3,7,4'-trimethoxyflavone and the structure was shown in figure 4.4. The molecular formula is $C_{18}H_{16}O_6$ and molecular weight is 328.

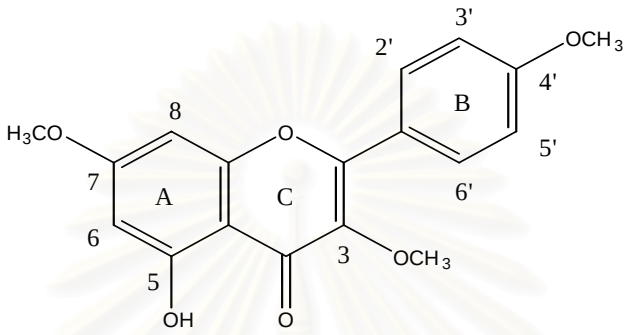

Figure 4.4 The structure of compound **3**

4.2.4 Structure elucidation of compound 4

Compound **4** is a greenish - yellow solid (56 mg) which obtained from the combined crude extract. The UV spectrum of compound **4** exhibited absorption maxima at 250 and 322 nm.

The IR spectrum (Figure A13) of compound **4** showed a broad absorption band between 3500-3200 cm^{-1} of OH stretching vibration and a strong absorption band at 1665 cm^{-1} which consistent with a carbonyl group. The IR spectrum of compound **4** is summarized in table 4.7.

Table 4.7 The IR absorption band assignment of compound **4**

Wave number (cm^{-1})	Intensity	Vibration
3500 - 3200	Broad	O-H stretching vibration of hydroxy group
1665	Medium	C=O stretching vibration of carbonyl Conjugated ketone
1602, 1508	Strong, Medium	C=C stretching vibration of aromatic
1188, 1165, 1026	Weak, Medium, Weak	C-O symmetry stretching Vibration of C-O-C
883	Medium	= C-H out of plane bending vibration of aromatic

From ^{1}H-NMR and ^{13}C-NMR spectrum of compound **4** showed that compound **4** has the flavonoid nucleus identity. The ^{1}H-NMR spectrum ($CDCl_3$, 400 MHz) (Figure A14) of compound **4** showed two singlets at δ 3.92 and 3.93 which were assigned to the two methoxy groups. Two singlets at δ 6.40 and 6.52 were due to the protons on H-6 and H-8. The singlet at δ 6.62 was assigned to the H-3 proton. The hydroxyl group appeared at δ 12.86 (5-OH). Two doublets at δ 7.05 (J = 8 Hz) and 7.88 (J = 8 Hz) indicated the *para*-disubstitution of the ring-B and were assigned to the protons of H-3', H-5' and H-2', H-6', respectively.

The ^{13}C-NMR spectrum ($CDCl_3$, 100 MHz) (Figure A15) showed that compound **4** has 17 carbons in which the methoxy groups appeared at δ 55.5, 55.8 ppm and 15 carbons of flavonoid nucleus. One carbonyl carbon appeared at δ 182.4

(C-4). The aromatic region contained a total of 12 resonances. For A-ring, there were six aromatic carbons, δ 162.1 (C-5), δ 92.6 (C-6), δ 165.4 (C-7), δ 98.0 (C-8), δ 157.7 (C-9) and δ 105.5 (C-10). At B-ring, there were four signals for six aromatic carbons, δ 123.5 (C-1'), δ 128.0 (C-2', 6'), δ 114.5 (C-3', 5') and δ 164.0 (C-4'). At δ 162.6 and δ 104.3 were assigned to C-2 and C-3 respectively. (Table 4.8)

The MALDI-TOF mass spectrum (Figure A16) of compound **4** was exhibited the $[M+H]^+$ at m/z 299.61, so the molecular weight of compound **4** is 298.

Compound **4** was assigned molecular formula $C_{17}H_{14}O_5$ based on MALDI-TOF and NMR spectral data.

Table 4.8 ^{1}H and ^{13}C-NMR spectral data of compound **4** (ppm)

Position	δ_H Compound **4**	δ_H 5-hydroxy-7,4'-dimethoxyflavone (87)	δ_C Compound **4**
2	-	-	162.6
3	6.62 (1H, s)	6.54 (1H, s)	104.3
4	-	-	182.4
5	-	-	162.1
6	6.40 (1H, s)	6.35 (1H, d, *J* = 3 Hz)	92.6
7	-	-	165.4
8	6.52 (1H, s)	6.47 (1H, d, *J* = 3 Hz)	98.0
9	-	-	157.7
10	-	-	105.5
1'	-	-	123.5
2'	7.88 (2H, d, *J* = 8 Hz)	7.82 (2H)	128.0
3'	7.05 (2H, d, *J* = 8 Hz)	7.00 (2H)	114.5
4'	-	-	164.0
5'	7.05 (2H, d, *J* = 8 Hz)	7.00 (2H)	114.5
6'	7.88 (2H, d, *J* = 8 Hz)	7.82 (2H)	128.0
7-OCH_3	3.93 (3H, s)	3.88 (6H,s)	55.8
4'-OCH_3	3.92 (3H, s)	3.88 (6H,s)	55.5
5-OH	12.86 (1H, s)	12.80 (1H, s)	-

The above evidence and the literature (87) strongly suggested that compound **4** was 5-hydroxy-7,4'-dimethoxyflavone and the structure of 5-hydroxy-7,4'-dimethoxyflavone was shown in figure 4.5. The molecular formula is $C_{17}H_{14}O_5$ and molecular weight is 298.

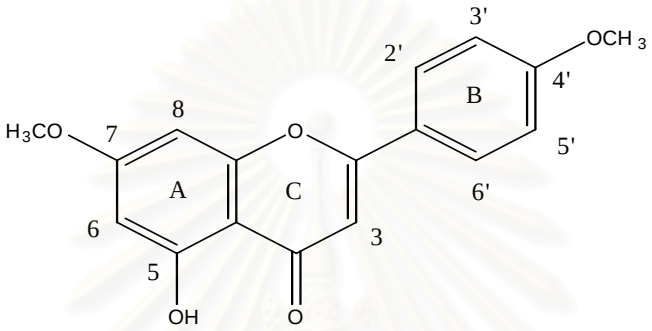

Figure 4.5 The structure of compound **4**

4.2.5 Structure elucidation of compound 5

Compound **5** is a yellow powder (4 mg) which obtained from the combined crude extract. The UV spectrum of compound **5** exhibited absorption maxima at 260 and 322 nm.

The IR spectrum (Figure A17) of compound **5** showed a broad absorption band between 3500-3100 cm^{-1} of OH stretching vibration and a strong absorption band at 1649 cm^{-1} which consistent with a carbonyl group. The IR spectrum of compound **5** is summarized in table 4.9.

Table 4.9 The IR absorption band assignment of compound **5**

Wave number (cm^{-1})	Intensity	Vibration
3500-3100	Broad	O-H stretching vibration of hydroxy group
2993, 2931, 2839	weak	C - H stretching vibration of aromatic
1649	Strong	C=O stretching vibration of carbonyl conjugated ketone
1587, 1497	Strong, medium,	C=C stretching vibration of aromatic
1165, 1111, 1010	Medium, medium, weak	C-O symmetry stretching vibration of C-O-C
818, 787, 709	All weak	= C-H out of plane bending vibration of aromatic

The ^{1}H-NMR spectrum ($CDCl_3$, 400 MHz) (figure A18) of compound **5** had four doublets at δ 7.73, 7.03, 6.49 and 6.40, signals δ 6.39 and 6.49 showed a 5,7-disubstituted in ring A with *meta* coupling (*J*=2 Hz), and was integrated for protons at H-6 and H-8 in ring A (respectively). Signals at δ 7.03 and 7.77 showed *meta* coupling (*J* = 2 Hz) and was assigned for protons at H-5' and H-6' in ring B, respectively. Doublet of doublet at δ 7.77 coupled with δ 7.73 with *J* = 2 Hz, so doublet at δ 7.73 was assigned for a proton at H-1' in ring B. Singlets at δ 3.90, 3.92, 4.00 and 4.01 were attributable to four methoxy groups at C-3, 7, 3' and 4' , respectively. And the signal at δ 12.68 was integrated for –O<u>H</u> at C-5. The ^{1}H-NMR chemical shifts of

compound **5** and 5-hydroxy-3,7,3',4'-tetramethoxyflavone were compared as shown in table 4.4.

The ^{13}C-NMR spectrum ($CDCl_3$, 100 MHz) (figure A19) showed that compound **5** consists of 19 carbons in which four methoxy groups at 60.2, 56.1, 56.0 and 55.9 ppm and 15 carbons of flavonoid nucleus. One signal of the carbonyl carbon appeared at 178.8 ppm (C-4). The aromatic region contained a total of 12 resonances. For A-ring, there were six aromatic carbons, δ 156.7 (C-5), δ 97.9 (C-6), δ 165.5 (C-7), δ 92.2 (C-8), δ 162.0 (C-9) and δ 106.1 (C-10). At B-ring, there were six signals for aromatic carbons, δ 122.9 (C-1'), δ 111.2 (C-2'), δ 148.7 (C-3'), δ 155.9 (C-4'), δ 110.8 (C-5') and δ 122.1 (C-6'). At δ 151.4 and δ 139.0 were assigned to C-2 and C-3 respectively. (Table 4.10)

The MALDI-TOF mass spectrum (Figure A20) of compound **5** showed the $[M+H]^+$ as follow, *m/z* 359.59. Therefore the molecular weight of compound **5** is 358.

Table 4.10 ^{1}H and ^{13}C-NMR spectral data of compound **5** (ppm)

Position	δ_H Compound **5**	δ_H 5-hydroxy-3,7,3',4'-tetramethoxyflavone (88)	δ_C Compound **5**	δ_C 5-hydroxy-3,7,3',4'-tetramethoxyflavone (88)
2	-	-	151.4	151.2
3	-	-	139.0	138.8
4	-	-	178.8	178.5
5	-	-	156.7	156.5
6	6.39 (1H, d, *J* = 2 Hz)	6.35 (1H, br s)	97.9	97.7
7	-	-	165.5	165.2
8	6.49 (1H, d, *J* = 2 Hz)	6.44 (1H, br s)	92.2	92.1
9	-	-	162.0	161.8
10	-	-	106.1	105.9
1'	-	-	122.9	122.8
2'	7.73 (1H, d, *J* = 2 Hz)	7.69 (1H, br s)	111.2	111.1
3'	-	-	148.7	148.6
4'	-	-	155.9	155.6
5'	7.03 (1H, s, *J* = 8 Hz)	6.99 (1H, d, *J* = 8.4 Hz)	110.8	110.7
6'	7.77 (1H, dd, *J* = 2, 8 Hz)	7.71 (1H, dd like)	122.1	120.0
3-OCH_3	4.00 (1H, s)	3.97 (3H, s)	60.2	60.2
7-OCH_3	3.92 (1H, s)	3.87 (3H, s)	55.9	55.8
3'-OCH_3	4.01 (1H, s)	3.97 (3H, s)	56.1	56.0
4'-OCH_3	3.89 (1H, s)	3.86 (3H, s)	56.0	56.0
5-OH	12.68 (1H, br s)	12.63 (1H, br s)	-	-

According to the literature (88) and above evidences strongly suggested that compound **5** is 5-hydroxy-3,7,3',4'-tetramethoxyflavone and the structure was shown in figure 4.6. The molecular formula is $C_{19}H_{18}O_7$ and molecular weight is 358.

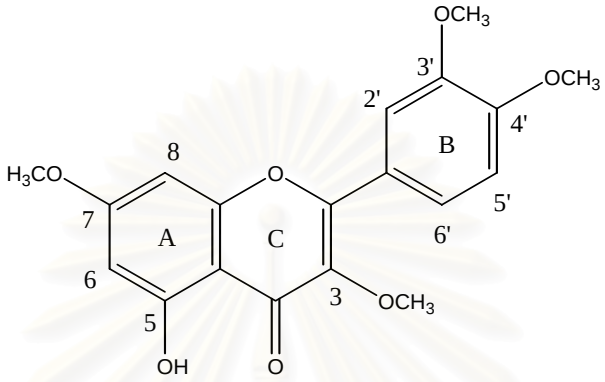

Figure 4.6 Structure of compound **5**

4.2.6 Structure elucidation of compound 6

Compound **6** is a colorless needle crystal (46 mg) which obtained from the combined crude extract. The UV spectrum of compound **6** exhibited absorption maxima at 262 and 322 nm.

The IR spectrum (Figure A21) of compound **6** showed a strong absorption band at 1649 cm^{-1} which consistent with a carbonyl group. The IR spectrum of compound **6** is summarized in table 4.11.

Table 4.11 The IR absorption band assignment of compound **6**

Wave number (cm^{-1})	Intensity	Vibration
2993, 2931, 2839	All weak	C - H stretching vibration of aromatic
1637	Strong	C=O stretching vibration of carbonyl conjugated ketone
1618, 1461, 1427	Strong, medium, medium	C=C stretching vibration of aromatic
1165, 1111, 1010	Medium, medium, weak	C-O symmetry stretching vibration of C-O-C
818, 787, 709	All weak	.= C-H out of plane bending vibration of aromatic

As same as the above isolated compounds, from ^{1}H-NMR and ^{13}C-NMR of compound **6** showed that compound **6** was the flavonoid identity also. The ^{1}H-NMR spectrum ($CDCl_3$, 400 MHz) (Figure A22) of compound **6** had two doublets at δ 6.38 and 6.55, each showed a 5,7-disubstituted in ring A with *meta* coupling (J = 2 Hz), and was integrated for proton at C-6 and C-8 in ring A, respectively. Signals at δ 3.92, 3.93 and 4.00 (all singlets) were attributable to three methoxy groups at C-3, 5 and 7, respectively. The aromatic protons of B-ring appeared as two multiplets at δ 7.52 (3*H) and δ 8.10 (2*H).

The ^{13}C-NMR spectrum ($CDCl_3$, 100 MHz) (figure A23) showed that compound **6** consists of 18 carbons in which three methoxy groups at 55.8 (7-OCH_3), 56.4 (5-OCH_3) and 60.1 (3-OCH_3) ppm and 15 carbons of flavonoid nucleus. One signal of the carbonyl carbon appeared at 174.2 ppm (C-4). The aromatic region contained a total of 12 resonances. For A-ring, there were six aromatic carbons, δ 158.9 (C-5), δ 95.8 (C-6), δ 163.9 (C-7), δ 92.4 (C-8), δ 152.6 (C-9) and δ 109.5 (C-10). At B-ring, there were four signals for six aromatic carbons, δ 141.8 (C-1'), δ 128.1 (C-2', 6'), δ 128.5 (C-3', 5'), δ 130.3 (C-4'). At δ 161.0 and δ 130.8 were assigned to C-2 and C-3 respectively. (Table 4.12)

The MALDI-TOF mass spectrum (Figure A24) of compound **6** showed the $[M+H]^+$ as follow, *m/z* 313.23. Therefore the molecular weight of compound **6** is 312.

Table 4.12 ^{1}H and ^{13}C-NMR spectral data of compound **6** (ppm)

Position	δ_H Compound **6**	δ_H 3,5,7-trimethoxyflavone (89)	δ_C Compound **6**
2	-	-	161.0
3	-	-	130.8
4	-	-	174.1
5	-	-	158.9
6	6.38 (1H, d, *J* = 2 Hz)	6.26 (1H, d, *J* = 2 Hz)	95.8
7	-	-	163.9
8	6.55 (1H, d, *J* = 2 Hz)	6.43 (1H, d, *J* = 2 Hz)	92.4
9	-	-	152.6
10	-	-	109.5
1’	-	-	141.8
2'	8.10 (2H, m)	8.00 (2H, m)	128.1
3'	7.52 (3H, m)	7.42 (3H, m)	128.5
4'	7.52 (3H, m)	7.42 (3H, m)	130.3
5'	7.52 (3H, m)	7.42 (3H, m)	128.5
6'	8.10 (2H, m)	8.00 (2H, m)	128.1
3-OCH_3	3.93 (3H, s)	3.88 (3H, s)	60.1
5-OCH_3	4.00 (3H, s)	3.91 (3H, s)	56.4
7-OCH_3	3.92 (3H, s)	3.83 (3H, s)	55.8

According to the literature (89) and the above evidences strongly suggested that compound **6** is 3,5,7-trimethoxyflavone. This compound was crystallized from ethyl acetate/hexane. The molecular formula is $C_{18}H_{16}O_5$ and molecular weight is 312. The structure of 3,5,7-trimethoxyflavone showed in figure 4.7.

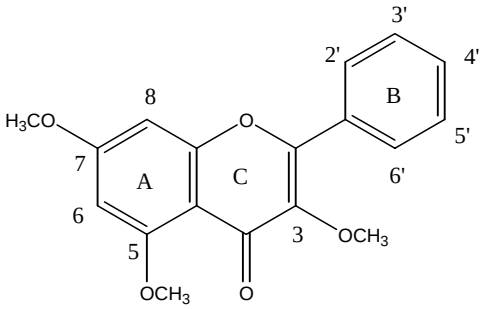

Figure 4.7 Structure of compound **6**

4.2.7 Structure elucidation of compound 7

Compound **7** is a colorless needle crystal (208 mg) which obtained from the combined crude extract. The UV spectrum of compound **7** exhibited absorption maxima at 262 and 302 nm.

The IR spectrum (Figure A25) of compound **7** showed a strong absorption band at 1645 cm^{-1} which consistent with a carbonyl group. The IR spectrum of compound **6** is summarized in table 4.13.

Table 4.13 The IR absorption band assignment of compound **7**

Wave number (cm^{-1})	Intensity	Vibration
3070, 2931, 2862	All weak	C - H stretching vibration of aromatic
1645	Strong	C=O stretching vibration of carbonyl conjugated ketone
1604, 1457	Strong, medium	C=C stretching vibration of aromatic
1157, 1118	Medium, medium	C-O symmetry stretching vibration of C-O-C
949, 818, 764	All weak	= C-H out of plane bending vibration of aromatic

The ^{1}H-NMR spectrum ($CDCl_3$, 400 MHz) (Figure A26) of compound **7** was integrated for fourteen carbons that showed two singets at δ 6.41 and 6.60 with *meta* coupling and each singlet were integrated for one proton at C-6 and C-8. Two singlets at 3.95 and 3.99 were integrated for two methoxy groups at C-7 and C-5, respectively. A singlet at δ 6.72 represented the C-3 aromatic proton. The aromatic protons appeared as two multiplets at δ 7.53 (3*H) and 7.91 (2*H).

The ^{13}C-NMR spectrum ($CDCl_3$, 100 MHz) (Figure A27) showed that compound **7** has 17 carbons. Moreover, the data revealed two signals of methoxy groups at δ 55.8 and 56.4, and one signal of ketone at 177.7 ppm. For A-ring, there were six aromatic carbons, δ 160.7 (C-5), δ 96.2 (C-6), δ 164.1 (C-7), δ 92.8 (C-8), δ 159.9 (C-9) and δ 108.9 (C-10). At B-ring, there were four signals for six aromatic

carbons, δ 131.4 (C-1'), δ 125.9 (C-2', 6'), δ 128.9 (C-3', 5'), δ 131.2 (C-4'). At δ 160.9 and δ 109.2 were assigned to C-2 and C-3 respectively. The ^{13}C-NMR chemical shifts of compound **7** were shown in table 4.14.

Table 4.14 ^{1}H and ^{13}C-NMR spectral data of compound **7** (ppm)

Position	δ_H Compound **7**	δ_H 5,7-dimethoxyflavone (84)	δ_C Compound **7**
2	-	-	160.9
3	6.72 (1H, s)	6.65 (1H, s)	109.2
4	-	-	177.7
5	-	-	160.7
6	6.41 (1H, s)	6.38 (1H, d, *J* = 2.5 Hz)	96.2
7	-	-	164.1
8	6.60 (1H, s)	6.57 (1H, d, *J* = 2.5 Hz)	92.8
9	-	-	159.9
10	-	-	108.9
1'	-	-	131.4
2'	7.91 (2H, m)	7.88 (2H, m)	125.9
3'	7.53 (3H, m)	7.48 (3H, m)	128.9
4'	7.53 (3H, m)	7.48 (3H, m)	131.2
5'	7.53 (3H, m)	7.48 (3H, m)	128.9
6'	7.91 (2H, m)	7.88 (2H, m)	125.9
5-OCH_3	3.99 (3H, s)	3.97 (3H, s)	56.4
7-OCH_3	3.95 (3H, s)	3.92 (3H, s)	55.8

The MALDI-TOF mass spectrum (Figure A28) of compound **7** showed the $[M+H]^+$ as follow, *m/z* 283.06.

According to the literature (84) agreed with the above evidences strongly suggested that compound **7** was 5,7–dimethoxyflavone and structure of 5,7-dimethoxyflavone was shown in figure 4.8. The molecular formula and molecular weight were $C_{17}H_{14}O_4$ and 282, respectively.

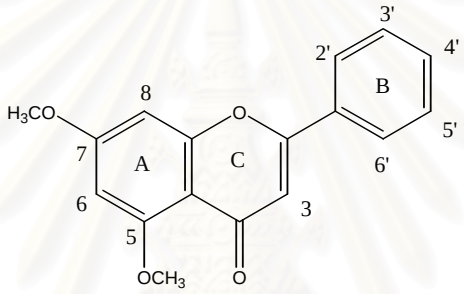

Figure 4.8 Structure of compound **7**

4.2.8 Structure elucidation of compound 8

Compound **8** is a white powder (306 mg) which obtained from the combined crude extract. The UV spectrum of compound **8** exhibited absorption maxima at 266 and 318 nm.

The IR spectrum (Figure A29) of compound **8** showed a strong absorption band at 1645 cm^{-1} which consistent with a carbonyl group. The IR spectrum of compound **8** is summarized in table 4.15.

Table 4.15 The IR absorption band assignment of compound **8**

Wave number (cm^{-1})	Intensity	Vibration
3070, 2939	Weak, weak	C - H stretching vibration of aromatic
1658	Medium	C=O stretching vibration of carbonyl conjugated ketone
1596, 1504, 1435	Strong, medium, medium	C=C stretching vibration of aromatic
1165	Medium	C-O symmetry stretching vibration of C-O-C
995, 833, 702	All weak	= C-H out of plane bending vibration of aromatic

The ^{1}H-NMR spectrum ($CDCl_3$, 400 MHz) (Figure A30) of compound **8** showed three singlets at δ 3.85, 3.88, and 3.92 due to nine methoxy protons. Two doublets at δ 6.40 (J = 2 Hz) and 6.59 (J = 2 Hz) were assigned to the protons at C-6 and C-8. The singlet at δ 6.63 was due to the C-3 proton. Two doublets at δ 7.85 (J = 9 Hz) and 7.03 (J = 9 Hz) were assigned to the aromatic protons at C-2', C-6' and C-3', 5', respectively.

From the ^{13}C-NMR spectrum (Figure A31), the signals at δ 55.5, 55.8, 56.4 ppm were signals of the three methoxy groups and δ 177.7 was the signal of ketone. For A-ring, there were six aromatic carbons, δ 160.8 (C-5), δ 96.1 (C-6), δ 164.0 (C-7), δ 92.8 (C-8), δ 159.8 (C-9) and δ 109.0 (C-10). At B-ring, there were four signals for

six aromatic carbons, δ 123.7 (C-1'), δ 127.6 (C-2', 6'), δ 114.3 (C-3', 5'), δ 160.8 (C-4'). At δ 162.1 and δ 107.5 were assigned to C-2 and C-3 respectively. The ^{13}C-NMR chemical shifts of compound **7** were shown in table 4.16.

Table 4.16 ^{1}H and ^{13}C-NMR spectral data of compound **8** (ppm)

Position	δ_H Compound **8**	δ_H 5,7,4'-trimethoxyflavone (84)	δ_C Compound **8**
2	-	-	162.1
3	6.63 (1H, s)	6.55 (1H, s)	107.5
4	-	-	177.7
5	-	-	160.8
6	6.40 (1H, d, *J* = 2 Hz)	6.35 (1H, d, *J* = 2.5 Hz)	96.1
7	-	-	164.0
8	6.59 (1H, d, *J* = 2 Hz)	6.55 (1H, d, *J* = 2.5 Hz)	92.8
9	-	-	159.8
10	-	-	109.0
1'	-	-	123.7
2'	7.85 (2H, d, *J* = 9 Hz)	7.81 (2H, d, *J* = 9 Hz)	127.6
3'	7.03 (2H, d, *J* = 9 Hz)	6.98 (2H, d, *J* = 9 Hz)	114.3
4'	-	-	160.8
5'	7.03 (2H, d, *J* = 9 Hz)	6.98 (2H, d, *J* = 9 Hz)	114.3
6'	7.85 (2H, d, *J* = 9 Hz)	7.81 (2H, d, *J* = 9 Hz)	127.6
5-OCH_3	3.99 (3H, s)	3.93 (3H, s)	56.4
7-OCH_3	3.94 (3H, s)	3.88 (3H, s)	55.8
4'-OCH_3	3.92 (3H, s)	3.85 (3H, s)	55.5

The MALDI-TOF mass spectrum (Figure A32) of compound **8** showed the $[M+H]^+$ as follow, *m/z* 313.21.

According to the literature (84) and the above evidence suggested that compound **8** is 5,7,4'-trimethoxyflavone and the structure of this compound was shown in figure 4.9. The molecular formula and molecular weight of compound **8** are $C_{18}H_{16}O_5$ and 312, respectively.

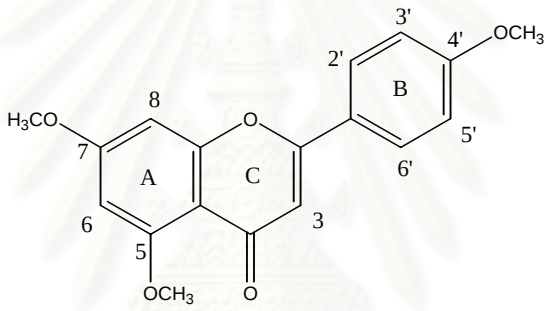

Figure 4.9 Structure of compound **8**

4.3 Structure elucidation of the isolated compounds from *Alpinia galanga*

4.3.1 Structure elucidation of compound 9

Compound **9** is yellow oil (158 mg) which obtained from the combined crude extract. The UV spectrum of compound **9** exhibited absorption maxima at 217 nm. $[\alpha]_D^{20}$ -60° (MeOH, c 0.5).

The IR spectrum (Figure A33) of compound **9** showed a strong absorption band at 1758 cm^{-1} which consistent with a carbonyl group. The IR spectrum of compound **9** is summarized in table 4.17.

Table 4.17 The IR absorption band assignment of compound **9**

Wave number (cm^{-1})	Intensity	Vibration
3069, 2976	Weak, weak	C - H stretching vibration of aromatic
1758	Strong	C=O stretching vibration of carbonyl conjugated ketone
1637, 1606	medium, medium	C=C stretching vibration of aromatic
1423, 1369	All medium	C-H stretching vibration of $-CH_3$
1093	Medium	C-O symmetry stretching vibration of C-O-C
906, 843	All weak	= C-H out of plane bending vibration of aromatic

The ^{1}H-NMR spectrum ($CDCl_3$, 400 MHz) (Figure A34) of compound **9** was integrated for fourteen protons. Signals at δ 7.10 and 7.40 (all doublets with J = 8 Hz) were attributable to four protons in aromatic ring (δ 7.10 (H-2, H-6); δ 7.40 (H-3, H-5)) with *para* disubstituents. Two singlets at δ 2.14 and 2.33, each were methyl protons in two acetyl groups. The doublets at δ 5.29 (H-3'b) and 5.33 (H-3'a) were terminal alkene protons which coupling with a proton at δ 6.02 (H-2') with J = 10 and 17 Hz, respectively. The doublet at δ 6.29 (J = 6 Hz) was a proton in CH (H-1') which

coupling with a proton at δ 6.02 (H-2'). The ^{1}H-NMR chemical shifts of compound **9** were shown in table 4.25.

The ^{13}C-NMR spectrum ($CDCl_3$, 100 MHz) (Figure A35) showed that compound **9** consists of 13 carbons. Six carbons in *para* disubstituted aromatic system were at δ 150.4 (C-1), δ 121.7 (C-2, C-6), δ 128.5 (C-3, C-5) and δ 136.4 (C-4). Two signal of the ketone of acetyl appeared at 170.0 and 169.5 ppm. Two signals of methyl in acetyl groups were at 21.3 and 21.2 ppm. Two carbons of terminal alkene exhibited chemical shift at 136.0 (C-2') and 117.1 (C-3'). The ^{13}C-NMR chemical shifts of compound **9** were showed in table 4.18.

The MALDI-TOF mass spectrum (Figure A36) of compound **9** showed the $[M+H]^+$ as 235.01. So the molecular weight of compound **9** was 234.

Table 4.18 ^{1}H and ^{13}C-NMR spectral data of compound **9**

Position	δ_H Compound **9**	δ_H (1'*S*)-1'-Acetoxychavicol acetate (90)	δ_C Compound **9**	δ_C (1'*S*)-1'-Acetoxychavicol acetate (90)
1	-	-	150.4	150.6
2	7.10 (2H, d, *J* = 8 Hz)	7.06 (2H, d, *J* = 8.6 Hz)	121.7	121.6
3	7.40 (2H, d, *J* = 8 Hz)	7.36 (2H, d, *J* = 8.6 Hz)	128.5	128.4
4	-	-	136.4	136.5
5	7.40 (2H, d, *J* = 8 Hz)	7.36 (2H, d, *J* = 8.6 Hz)	128.5	128.4
6	7.10 (2H, d, *J* = 8 Hz)	7.06 (2H, d, *J* = 8.6 Hz)	121.7	121.6
1'	6.29 (1H, d, *J* = 6 Hz)	6.26 (1H, d, *J* = 5.9 Hz)	75.5	75.7
2'	6.02 (1H, m)	5.99 (1H, m)	136.0	136.2
3' a	5.33 (1H, d, *J* = 17 Hz)	5.27 (1H, d, *J* = 16.3 Hz)	117.1	117.0
3' b	5.29 (1H, d, *J* = 10 Hz)	5.23 (1H, d, *J* = 9.6 Hz)		
1-OAc (C=O)	-	-	169.5	169.1
1-OAc (CH_3)	2.33 (3H, s)	2.28 (3H, s)	21.2	21.2
1'-OAc (C=O)	-	-	170.0	169.7
1'-OAc (CH_3)	2.14 (3H, s)	2.09 (3H, s)	21.3	21.2

According to the literature (90) and the above evidences strongly suggested that compound **9** is chavicol acetate. The molecular formula is $C_{13}H_{14}O_4$ and molecular weight is 234 and structure of compound **9** shown in figure 4.11

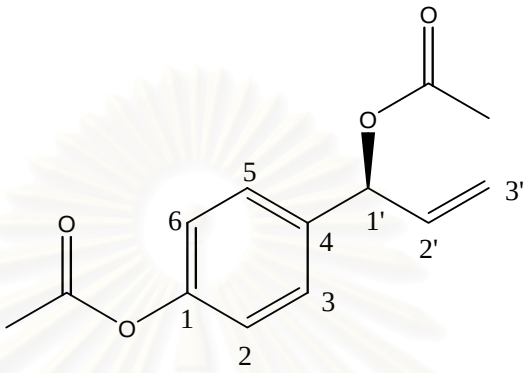

Figure 4.11 Structure of compound **9**

4.3.2 Structure elucidation of compound 10

Compound **10** is a white needle crystal (15 mg) which obtained from the combined crude extract. The UV spectrum of compound **10** exhibited absorption maxima at 211, 234, 322nm.

The IR spectrum (Figure A33) of compound **10** showed a broad absorption band between 3500-3100 cm^{-1} of OH stretching vibration and a strong absorption band at 1758 cm^{-1} which consistent with a carbonyl group. The IR spectrum of compound **10** is summarized in table 4.19.

Table 4.19 The IR absorption band assignment of compound **10**

Wave number (cm^{-1})	Intensity	Vibration
3500-3100	Broad	O-H stretching vibration of hydroxy group
3019	Weak	C - H stretching vibration of aromatic
2890, 2820	Medium	H-C stretching vibration of aldehyde
1645	Strong	C=O stretching vibration of carbonyl conjugated ketone
1579	Medium	C=C stretching vibration of aromatic
1093	Medium	C-O symmetry stretching vibration of C-O-C

The ^{1}H-NMR spectrum (DMSO, 400 MHz) (Figure A38) of compound **10** had two doublets at δ 6.86 and 7.62 ppm, each showed a 1,4-disubstituted in aromatic system with meta coupling (J = 7 Hz), and were integrated for four protons at C-2, 6 and C-3, 5 in this aromatic ring, respectively. Signal at δ 7.67 ppm (multiplet) was attributable to one proton in double bond system with *trans* position. At δ 6.68 ppm showed one proton which coupling with the proton at δ 7.67 ppm with J = 14.5 Hz, and coupling with the aldehyde proton at δ 9.60 ppm with J = 7.7 Hz, respectively. Signal at δ 10.25 ppm (singlet) suggested the presence of phenolic proton.

The ^{13}C-NMR spectrum (DMSO, 100 MHz) (Figure A39) showed that compound **10** consists of 9 carbons. One signal of the carbonyl carbon of aldehyde appeared at 194.6 ppm. The *para* disubstituted aromatic ring contained a total of 4

signals. These were δ 125.7, C-1; δ 131.5, C-2, C-6; δ 116.5, C-3, C-5; δ 161.1, C-4. The remaining two signals were two methine carbon (δ 154.3, C-1'; δ 125.9, C-2'). The ^{13}C-NMR chemical shifts of compound **10** were shown in table 4.26. (Table 4.20)

The MALDI-TOF mass spectrum (Figure A40) of compound **10** showed $[M+H]^+$ at m/z 149.06. Therefore, the molecular weight of compound **10** was 148.

Table 4.20 ^{1}H and ^{13}C-NMR spectral data of compound **10**

Position	δ_H Compound **10**	δ_H *p*-hydroxy cinnamaldehyde (91)	δ_C Compound **10**	δ_C *p*-hydroxy cinnamaldehyde (91)
1	-	-	125.7	126.98
2	7.62 (2H, d, *J* = 5 Hz)	7.50 (2H, d, *J* = 8.5 Hz)	131.5	130.60
3	6.86 (2H, d, *J* = 7 Hz)	6.90 (2H, d, *J* = 8.5 Hz)	116.5	116.12
4	-	-	161.1	158.46
5	6.86 (2H, d, *J* = 7 Hz)	6.90 (2H, d, *J* = 8.5 Hz)	116.5	116.12
6	7.62 (2H, d, *J* = 5 Hz)	7.50 (2H, d, *J* = 8.5 Hz)	131.5	130.60
1'	7.67 (1H, m)	7.42 (1H, d, *J* = 15.9 Hz)	154.3	152.72
2'	6.68 (1H, dd, *J* = 14.5, 7.7 Hz)	6.62 (1H, dd, *J* = 15.9, 7.7 Hz)	125.9	126.56
3'	9.60 (1H, d, *J* = 7.7 Hz)	9.67 (1H, d, *J* = 7.7 Hz)	194.6	193.82
4-OH	10.25 (1H,s)		-	-

According to the literature (91) and the above evidences strongly suggested that compound **10** is *p*-hydroxy cinnamaldehyde. The molecular formula is $C_9H_8O_2$ and molecular weight is 148. The structure of *p*-hydroxy cinnamaldehyde was shown in figure 4.12.

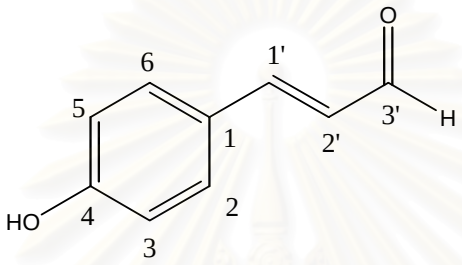

Figure 4.10 Structure of compound **10**

4.3.3 Structure elucidation of compound 11

Compound **11** is white solid (150 mg) which obtained from the combined crude extract. $[\alpha]_D^{25}$ – 3.1 (H_2O, c 0.5).

The IR spectrum (Figure A41) of compound **11** showed a broad absorption band at 3377 cm^{-1} of OH stretching vibration of carboxylic acid and a strong absorption band at 1688 cm^{-1} which consistent with a carbonyl group. The IR spectrum of compound **11** is summarized in table 4.21.

Table 4.21 The IR absorption band assignment of compound **11**

Wave number (cm^{-1})	Intensity	Vibration
3500-2500	Medium	-OH stretching vibration of carboxylic acid
2922	Medium	C-H stretching vibration of aliphatic
1688	Medium	C=O stretching vibration
1221	Medium	C-O stretching vibration

The ^{1}H-NMR spectrum of compound **11** (D_2O, 400 MHz) (Figure A42) had only two signals, two multiplets at δ 2.75 and 3.84 which assigned for the protons in $C\underline{H}_2$ and C<u>H</u>-O, respectively.

The ^{13}C-NMR spectrum (D_2O, 100 MHz) (Figure A43) showed that compound **11** consists of 3 types of carbons. One signal of the carbonyl of carboxylic acid appeared at 174.3 ppm. One signal of carbon which attached to oxygen exhibited the chemical shift at 51.1 ppm. And the last signal of methine carbon appeared at 34.3 ppm. The ^{13}C-NMR chemical shifts of compound **11** were showed in table 4.22.

The MALDI-TOF mass spectrum (Figure A44) of compound **11** showed $[M+H]^+$ at *m/z* 179.01. So the molecular weight of compound **11** was 178.

Table 4.22 ^{1}H and ^{13}C-NMR spectral data of compound **11**

Position	δ_H Compound **11**	δ_C Compound **11**
1	-	174.3
2	2.75, 4H, (m)	51.1
3	3.84, 2H, (m)	34.3
4	3.84, 2H, (m)	34.3
5	2.75, 4H, (m)	51.1
6	-	174.3

The above evidences strongly suggested that the compound **11** had the carboxylic acid functional group (COOH) and hydroxyl group (OH). These results suggested that molecular formula of compound **11** is $(C_3H_5O_3)_n$. From the mass spectrum confirmed that compound **11** has 178 of molecular weight. So the molecular formula of compound **11** was $C_6H_{10}O_6$. Result of ^{13}C-NMR and ^{1}H-NMR spectrum confirmed that compound **11** was 3,4-dihydroxy adipic acid and the structure of this compound shown in figure 4.12.

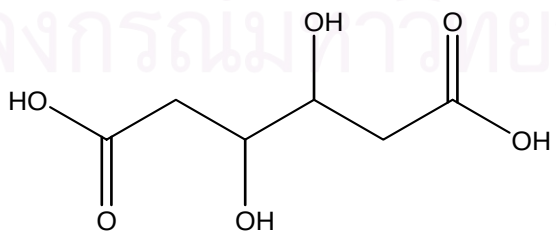

Figure 4.12 Structure of compound **11**

4.4 Structure elucidation of the isolated compounds from *Kaempferia galanga*

4.4.1 Structure elucidation of compound 12

Compound **12** is yellow viscous oil (2037 mg) which obtained from the combined crude extract. The UV spectrum of compound **12** exhibited absorption maxima at 217, 257 nm.

The IR spectrum (Figure A45) of compound **12** showed a strong absorption band at 1630 cm^{-1} which consistent with a carbonyl group. The IR spectrum of compound **12** is summarized in table 4.23.

Table 4.23 The IR absorption band assignment of compound **12**

Wave number (cm^{-1})	Intensity	Vibration
2972, 2828	Weak, weak	C - H stretching vibration of aromatic
1704	Strong	C=O stretching vibration of carbonyl conjugated ketone
1630, 1599	medium	C=C stretching vibration of aromatic
1419, 1361	All medium	C-H stretching vibration of $-CH_3$
1170	Strong	C-O unsymmetry stretching vibration of C-O-C
882, 824	All weak	= C-H out of plane bending vibration of aromatic

The ^{1}H-NMR spectrum ($CDCl_3$, 400 MHz) (Figure A46) of compound **12** was integrated for twelve protons. Signals at δ 7.41 and 7.55 were five aromatic protons with *meta* coupling *J* = 2 Hz that exhibited a monosustituted aromatic system. At δ 6.47 and 7.72 ppm, each showed a proton on C=C with *trans* coupling which exhibited coupling constant of 16 Hz. The δ 4.30 and 1.37 ppm was integrated for CH_2 and CH_3, respectively. The ^{1}H-NMR chemical shifts of compound **12** were shown in table 4.34.

The ^{13}C-NMR spectrum ($CDCl_3$, 100 MHz) (Figure A47) showed that compound **12** consists of 11 carbons. One signal of the ketone appeared at 167.0 ppm (C-3'). The signals of CH_2 and CH_3 of ethyl ester were at 60.5 and 14.3 ppm, respectively. Six carbons of aromatic were at δ 134.4 (C-1), δ 128.2 (C-2, C-6), δ 128.9 (C-3, C-5) and δ 130.3 (C-4). Two signals of methine carbons exhibited the chemical shift at 144.6 (C-1') and 118.2 (C-2') ppm. The ^{13}C-NMR chemical shifts of compound **12** were shown in table 4.24.

The MALDI-TOF mass spectrum (Figure A48) of compound **12** showed $[M+H]^+$ at *m/z* 177.19. So the molecular weight of compound **12** was 176.

Table 4.24 ^{1}H and ^{13}C-NMR spectral data of compound **12**

Position	δ_H Compound **12**	δ_H cinnamic acid ethyl ester (92)	δ_C Compound **12**	δ_C cinnamic acid ethyl ester (92)
1	-	-	134.4	134.3
2	7.55 (2H, d, *J* = 2 Hz)	7.50 (2H, m)	128.2	127.9
3	7.41 (3H, d, *J* = 2 Hz)	7.35 (3H, m)	128.9	128.8
4	7.41 (3H, d, *J* = 2 Hz)	7.35 (3H, m)	130.3	130.1
5	7.41 (3H, d, *J* = 2 Hz)	7.35 (3H, m)	128.9	128.8
6	7.55 (2H, d, *J* = 2 Hz)	7.50 (2H, m)	128.2	127.9
1'	7.72 (1H, d, *J* = 16 Hz)	7.69 (1H, d, *J* = 16.2 Hz)	144.6	144.5
2'	6.47 (1H, d, *J* = 16 Hz)	6.44 (1H, d, *J* = 16.2 Hz)	118.2	118.1
3'	-	-	167.0	166.9
3' $O\underline{CH_2}CH_3$	4.30 (2H, q, *J* = 7 Hz)	4.26 (2H, q, *J* = 7.1 Hz)	60.5	60.4
3' $OCH_2\underline{CH_3}$	1.37 (3H, t, *J* = 7 Hz)	1.33 (3H, t, *J* = 7.1 Hz)	14.3	14.2

According to and the above evidences and the comparison with the literature (92) suggested that compound **12** is cinnamic acid ethyl ester. The molecular formula is $C_{11}H_{12}O_2$ and molecular weight is 176. The structure of compound **12** was shown in figure 4.13.

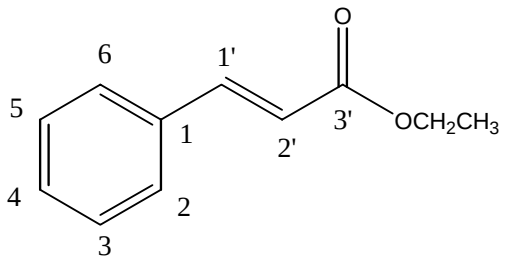

Figure 4.13 Structure of compound **12**

4.4.2 Structure elucidation of compound 13

Compound **13** is a colorless needle crystal (6080 mg) which obtained from the combined crude extract. The UV spectrum of compound **13** exhibited absorption maxima at 211, 275 nm.

The IR spectrum (Figure A49) of compound **13** showed a strong absorption band at 1708 cm^{-1} which consistent with a carbonyl group. The IR spectrum of compound **13** is summarized in table 4.25.

Table 4.25 The IR absorption band assignment of compound **13**

Wave number (cm^{-1})	Intensity	Vibration
2976, 2852	Strong	C - H stretching vibration of aromatic
1708	Strong	C=O stretching vibration of carbonyl conjugated ketone
1633, 1571	Strong, weak	C=C stretching vibration of aromatic
1459, 1365	medium	C-H stretching vibration of $-CH_3$
1034	Medium	C-O symmetry stretching vibration of C-O-C
874, 765	Medium	= C-H out of plane bending vibration of aromatic

The ^{1}H-NMR spectrum ($CDCl_3$, 400 MHz) (Figure A50) of compound **13** was integrated for fourteen protons. Signals at δ 7.51 and 6.93 (all doublets) were the aromatic protons, each signals were integrated for two protons with meta coupling (*J* = 8 Hz), that exhibited a 1,4-disubstituted in aromatic system. At δ 6.34 and 7.67 ppm (all doublets), each showed a proton on C=C with *trans* coupling which exhibited *J* = 16 Hz. The δ 4.27 and 1.37 ppm was integrated for CH_2 and CH_3, respectively. Singlet at δ 3.87 was interpreted for methoxy protons ($4\text{-}OCH_3$). The ^{1}H-NMR chemical shifts of compound **13** were shown in table 4.37.

The ^{13}C-NMR spectrum ($CDCl_3$, 100 MHz) (Figure A51) showed that compound **13** consists of 12 carbons. One signal of the carbonyl carbon appeared at 167.3 ppm (C-3'). Two signals of CH_2 and CH_3 of ethyl ester group were at 60.3 and

14.4 ppm, respectively. Four signals of six aromatic carbons were at δ 127.1 (C-1), δ 129.7 (C-2, C-6), δ 114.3 (C-3, C-5) and δ 161.3 (C-4). Two signals of methine carbons exhibited the chemical shift at 144.2 (C-1') and 115.7 (C-2') ppm. And the last one singlet at δ 55.3 was a methoxy carbon (4-OCH_3). The ^{13}C-NMR chemical shifts of compound **12** were shown in table 4.26.

The MALDI-TOF mass spectrum (Figure A52) of compound **13** showed $[M+H]^+$ at *m/z* 207.12. Therefore, the molecular weight of compound **13** was 206.

Table 4.26 ^{1}H and ^{13}C-NMR spectral data of compound **13**

Position	δ_H Compound **13**	δ_H 4-methoxy cinnamic acid ethyl ester (93)	δ_C Compound **13**	δ_C 4-methoxy cinnamic acid ethyl ester (93)
1	-	-	127.1	127.3
2	7.51 (2H, d, *J* = 8 Hz)	7.46 (2H, d, *J* = 8 Hz)	129.7	129.7
3	6.93 (2H, d, *J* = 8 Hz)	6.88 (2H, d, *J* = 8 Hz)	114.3	114.4
4	-	-	161.3	161.4
5	6.93 (2H, d, *J* = 8 Hz)	6.88 (2H, d, *J* = 8 Hz)	114.3	114.4
6	7.51 (2H, d, *J* = 8 Hz)	7.46 (2H, d, *J* = 8 Hz)	129.7	129.7
1'	7.67 (1H, d, *J* = 16 Hz)	7.63 (1H, d, *J* = 16 Hz)	144.2	144.2
2'	6.34 (1H, d, *J* =16 Hz)	6.29 (1H, d, *J* =16 Hz)	115.7	115.9
3'	-	-	167.3	163.3
3'-$O\underline{CH_2}CH_3$	4.27 (2H, q, *J* = 7 Hz)	4.24 (2H, q, *J* = 7 Hz)	60.3	60.3
3'-$OCH_2\underline{CH_3}$	1.37 (3H, t, *J* = 7 Hz)	1.32 (3H, t, *J* = 7 Hz)	14.4	14.4
4-OCH_3	3.87 (3H, s)	3.81 (3H, s)	55.3	55.3

According to the above evidences and the comparison with the previous report (93) suggested that compound **13** is 4-methoxy cinnamic acid ethyl ester. The molecular formula is $C_{12}H_{14}O_3$ and molecular weight is 206. The structure of compound **13** was shown in figure 4.14.

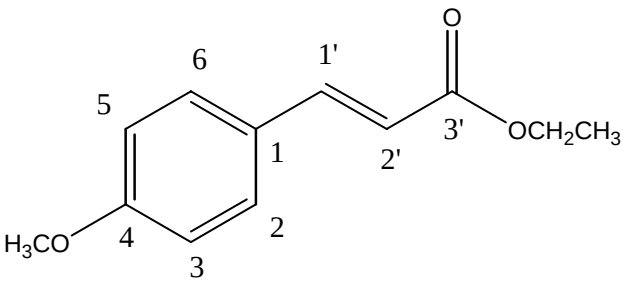

Figure 4.14 Structure of compound **13**

4.4.3 Structure elucidation of compound 14

Compound **14** is a colorless needle crystal (67 mg) which obtained from the combined crude extract. The UV spectrum of compound **14** exhibited absorption maxima at 211, 299 nm.

The IR spectrum (Figure A53) of compound **14** showed a broad absorption band between 3300-2400 cm^{-1} of OH stretching vibration and a strong absorption band at 1676 cm^{-1} which consistent with a carbonyl group. The IR spectrum of compound **14** is summarized in table 27.

Table 4.27 The IR absorption band assignment of compound **14**

Wave number (cm^{-1})	Intensity	Vibration
3300-2400	Medium	OH stretching vibration of carboxylic acid
1676	Strong	C=O stretching vibration of carbonyl conjugated carboxylic acid
1590	Strong	C=C stretching vibration of aromatic
1435, 1315	Strong	C-H stretching vibration of $-CH_3$
1170	Strong	C-O unsymmetry stretching vibration of C-O-C

The ^{1}H-NMR spectrum ($CDCl_3$, 400 MHz) (Figure A54) of compound **14** had four doublets at δ 6.39, 6.99, 7.56 and 7.66 ppm. Signals at δ 6.99 and 7.66 (all doublets with J = 8 Hz) were attributable to four protons in aromatic ring with *para* disubstituents. At δ 6.39 and 7.56 ppm, each showed a proton on C=C with *trans* coupling which exhibited J = 16 Hz. The δ 3.81 ppm was integrated for OCH_3 (4-OCH_3). The ^{1}H-NMR chemical shifts of compound **14** were shown in table 4.40.

The ^{13}C-NMR spectrum ($CDCl_3$, 100 MHz) (Figure A55) showed that compound **14** consists of 10 carbons. One signal of the ketone appeared at 168.3 ppm (C-3'). The signal of OCH_3 was at 55.8 ppm (4-OCH_3). Six aromatic protons were at δ 127.3 (C-1), δ 130.4 (C-2, C-6), δ 114.8 (C-3, C-5) and δ 161.4 (C-4). Two methine carbons exhibited chemical shift at 144.2 (C-1') and 116.9 (C-2'). Result of ^{13}C-NMR

spectrum data of compound **14** were confirmed with 4-methoxy cinnamic acid that shown in table 4.28.

The MALDI-TOF mass spectrum (Figure A56) of compound **14** showed the $[M+H]^+$ at *m/z* 179.08.

Table 4.28 ^{1}H and ^{13}C-NMR spectral data of compound **14**

Position	δ_H Compound **14**	δ_H 4-methoxy cinnamic acid (94)	δ_C Compound **14**	δ_C 4-methoxy cinnamic acid (94)
1	-	-	127.3	128.4
2	7.66 (2H, d, *J* = 8 Hz)	7.53 (2H, d, *J* = 6.77 Hz)	130.4	130.9
3	6.99 (2H, d, *J* = 8 Hz)	6.94 (2H, d, *J* = 6.76 Hz)	114.8	115.4
4	-	-	161.4	163.1
5	6.99 (2H, d, *J* = 8 Hz)	6.94 (2H, d, *J* = 6.76 Hz)	114.8	115.4
6	7.66 (2H, d, *J* = 8 Hz)	7.53 (2H, d, *J* = 6.77 Hz)	130.4	130.9
1’	7.56 (1H, d, *J* = 16 Hz)	7.61 (1H, d, *J* = 16.01 Hz)	144.2	146.2
2’	6.39 (1H, d, *J* = 16 Hz)	6.32 (1H, d, *J* = 16.01 Hz)	116.9	116.6
3’	-	-	168.3	170.8
4-OCH_3	3.81 (3H, s)	3.72 (3H, s)	55.8	55.8

According to the literature (94) and the above evidences suggested that compound **14** is 4-methoxy cinnamic acid. Compound **14** was crystallized from ethyl acetate / hexane to yield colorless needle crystal. The molecular formula is $C_{10}H_{10}O_3$ and molecular weight is 178. The structure of compound **14** was shown in figure 4.15.

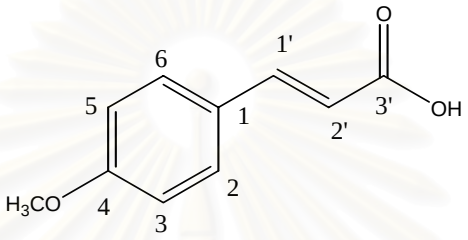

Figure 4.15 Structure of compound **14**

4.5 The inhibitory activity of isolated compounds on HIV-1 protease, HCV protease and HCMV protease

The methanol crude extracts of *Kaempferia parviflora* and *Alpinia galanga* were found to inhibit HIV-1 protease activity by more than 80% at a concentration of 200 μg/ml (Table A2). Compounds **1-8** were isolated from the methanol extract of *Kaempferia parviflora*, and the results of inhibitory activity against HIV-1 protease, HCV protease and HCMV protease shown in table 4.29.

Table 4.29 Inhibition of HIV-1 protease, HCV protease and HCMV protease by compounds **1-8** which isolated from *Kaempferia parviflora*, values are means ± S.D., n = 3

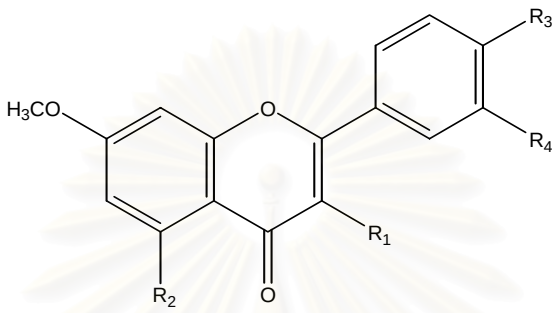

Compounds	R_1	R_2	R_3	R_4	IC_{50} (μM)		
					HIV-1 protease	HCV protease	HCMV protease
1	OCH_3	OH	H	H	66.1 ± 3.2	192.9 ± 9.9	248.6 ± 4.0
2	H	OH	H	H	19.0 ± 3.1	>450	349.1 ± 3.8
3	OCH_3	OH	OCH_3	H	101.1± 10.0	-	-
4	H	OH	OCH_3	H	77.9 ± 9.1	-	-
5	OCH_3	OCH_3	OCH_3	OCH_3	160.1± 5.4	-	-
6	OCH_3	OCH_3	H	H	81.3 ± 7.1	-	-
7	H	OCH_3	H	H	19.5 ± 1.2	-	-
8	H	OCH_3	OCH_3	H	109.9 ± 10.9	-	-

The inhibitory activity of 8 flavonoids on HIV-1 protease was evaluated using fluorescence assay. As the results, compound **1**, **2**, **4**, **6**, and **7** inhibited HIV-1 protease activity in dose dependent manner (IC_{50} less than 100 μM).

Compound **7** had very potent inhibitory activity (IC_{50} = 19.5 ± 1.2 μM). Compound **2** was the most active compound with IC_{50} value of 19.0 ± 3.1 μM. These results suggested that the presence of hydroxy or methoxy group at 5-position of flavonoid nucleus is necessary to enhance HIV-1 protease inhibitory activity. While the substitution of methoxy group at 3-position of flavonoid moiety (compounds **1** and **6**) were less potent (IC_{50} = 66.1 ± 3.2 μM and IC_{50} = 81.3 ± 7.1 μM, respectively). The substitution of methoxy group at 4'- position (compounds **4** and **8**) also reduced the inhibitory effect (IC_{50} = 77.9 ± 9.1 μM and IC_{50} = 109.9 ± 10.9 μM, respectively). Include of disubstitution at 3- and 4' (compounds **3** and **5**) showed the lowest inhibitory activity (IC_{50} = 101.1 ± 9.9 μM and IC_{50} = 160.1 ± 5.4 μM, respectively). These results suggested that the methoxy at position 3 or/and 4' reduce the inhibitory effect.

The kinetic study demonstrated that the mechanism of HIV-1 protease inhibition of compound **2** and compound **7** were a competitive inhibitor with K_i value of 23.5 μM and 32.2 μM, respectively.

Moreover, compound **1** had mild inhibitory activity on HCV and HCMV protease with IC_{50} value of 192.9 ± 9.9 and 248.6 ± 4.0 μM, respectively.

Compounds **9-11** were isolated from the methanol extract of *Alpinia galanga*, and the results of inhibitory activity against HIV-1 protease, HCV protease and HCMV protease shown in table 4.30.

Table 4.30 Inhibition of HIV-1 protease, HCV protease and HCMV protease by compounds **9-11** which isolated from *Alpinia galanga*, values are means ± S.D., n = 3

Compounds	IC_{50} (μM)		
	HIV-1 protease	HCV protease	HCMV protease
9	244.3 ± 21.6	405.0 ± 23.8	316.5 ± 4.9
10	133.4 ± 5.1	500.5 ± 34.6	97.8 ± 5.3
11	-	-	-

Although compounds **9** and **10** had small molecule with molecular weight of 234 and 148, respectively, compounds **9** and **10** had moderate inhibitory activity against HIV-1 protease with IC_{50} value of 244.3 ± 21.6 and 133.4 ± 5.1 μM, respectively. The kinetic study demonstrated that the mechanism of HIV-1 protease inhibition of compound **9** was an uncompetitive inhibitor with K_i value of 5.2 μM and compound **10** was a noncompetitive inhibitor with K_i value of 86.3 μM.

Compounds **9** and **10** exhibited mild inhibitory activity on HCV protease with IC_{50} more than 400 μM. Moreover, compound **10** showed potent inhibition against HCMV protease with IC_{50} value of 97.8 ± 5.3 μM while compound **9** had mild inhibition on this protease enzyme. From the kinetic study of compound **10** on HCMV protease,

the result showed that compound **10** was an uncompetitive inhibitor with K_i value of 3.2 μM.

The inhibition was specific for the different proteases as none of the extracts, or pure compounds inhibited all three enzymes, and when an extract or pure compounds inhibited two proteases it was HIV-1 protease and HCMV protease, two enzymes which are not only structurally unrelated, but that also have completely different active site architectures and catalytic mechanisms.

4.6 The inhibitory activity of isolated compounds from *Kaempferia galanga* and cinnamic acid derivatives on α-glucosidase (95)

Three isolated compounds from *Kaempferia galanga* were tested against α-glucosidase with the *trans*-cinnamic acid derivatives. Compound **12**, **13** and **14** were isolated from the rhizomes of *Kaempferia galanga*. The other *trans*-cinnamic acid derivatives (**15**, **19-28**) were synthesized by the Perkin reaction between aromatic aldehydes and aliphatic carboxylic acids following the procedure of Chiriac et al. And compounds **16-18** were purchased from Fluka Co. Ltd.

From table 4.31, compounds **13**, **14**, **17-21**, **26** and **27** had inhibitory activity against α-glucosidase in dose-dependent manner. The results showed that the compounds **13-14**, **17-21**, **26** and **27** had more potent α-glucosidase inhibitory activity than that of 1-deoxynojirimycin, which was used as the positive inhibitor. While *trans*-

cinnamic acid, its ethyl ester and the 2-hydroxy-*trans*-cinnamic acid were found to be inactive.

Table 4.31 IC_{50} values of *trans*-cinnamic acid and its derivatives for inhibition of α-glucosidase

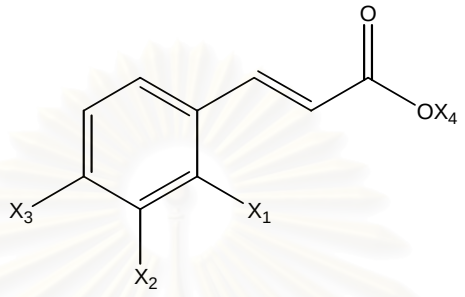

Compounds	X_1	X_2	X_3	X_4	IC_{50} (mM)
12	H	H	H	C_2H_5	>5
13	H	H	OCH_3	C_2H_5	0.05 ± 0.03
14	H	H	OCH_3	H	0.04 ± 0.01
15	H	H	H	H	>5
16	OH	H	H	H	>5
17	H	OH	H	H	1.27 ± 0.51
18	H	H	OH	H	0.20 ± 0.06
19	OCH_3	H	H	H	4.34 ± 0.78
20	H	OCH_3	H	H	0.58 ± 0.15
21	H	H	OPh	H	0.44 ± 0.37
22	H	H	OCH_2Ph	H	>5
23	H	H	OC_4H_9	H	>5
24	H	H	OC_6H_{13}	H	>5
25	H	H	NO_2	H	>5
26	H	H	F	H	0.27 ± 0.06
27	H	H	Cl	H	0.39 ± 0.14
28	H	H	Br	H	>5
1-deoxynojirimycin					5.60 ± 0.42

4-methoxy-*trans*-cinnamic acid (**14**) was the most active compound among tested compounds, while 2-, 3-dimethoxy-*trans*-cinnamic acid (**19** and **20**) were less potent. These results suggested that the presence of hydroxy or methoxy group at 4-position on *trans*-cinnamic acid moiety is necessary to enhance α-glucosidase inhibitory activity. When the α-glucosidase inhibitory activities of compounds **14**, **15** and **18** were compared, it was found that the potency increased in the order of **14**>**18**>**15**. The observation revealed that replacement of the 4-hydroxy substituted in the *trans*-cinnamic acid by a methoxy residue increased α-glucosidase inhibitory activity by 10-fold. Introduction of a methoxy group at *para*-position on *trans*-cinnamate acid ethyl ester (**13**), the IC_{50} values was 0.05 ± 0.03 mM, which was in the same order to that of 4-methoxy-*trans*-cinnamic acid. The evidence supported the previous result (**12** and **15**), that neither the acid group nor the ethyl ester played any important role on α-glucosidase inhibition.

The introduction of 4-phenoxy residue to *trans*-cinnamic acid (**21**) decreased the α-glucosidase inhibitory activity (IC_{50} = 0.44 ± 0.37mM). The compounds having larger alkoxy substituent (**22**–**24**) were found to have no effect on α-glucosidase inhibition (IC_{50} > 5 mM). These results suggested that increasing of the bulkiness, or the chain length of the alkoxy substituent at 4-position may decrease the α-glucosidase inhibitory activity.

While the presence of NO_2 group at 4-position of *trans*-cinnamic acid (**25**) showed no activity (IC_{50} >5 mM), the *trans*-cinnamic acid derivatives having F (**26**) and Cl (**27**) substituent at 4-position gave moderate activity (the IC_{50} values of 0.27 $\pm$ 0.06, 0.39 $\pm$ 0.14 mM, respectively). This observation supported the notion that a decrease in electron diversity of *trans*-cinnamic acid moiety would result in the decrease of α-glucosidase inhibitory activity. On the other hand, 4-bromo-*trans*-cinnamic acid (**28**) had no effect on α-glucosidase inhibiting activity.

The kinetic result demonstrated that the mechanism of α-glucosidase inhibition of 4-methoxy-*trans*-cinnamic acid ethyl ester (**13**) was a competitive inhibitor with K_i value of 0.02 $\pm$ 0.01mM. In contrast, compound **14** was noncompetitive with K_i value of 0.06 $\pm$ 0.01 mM. At this point, the values of K_{max} obtained at 0 and 48.1 μM for compound **13**, and K_i value was calculated using the values of V_{max} obtained at 0 and 55.6 μM for compound **14**, respectively. To date, the microbial α-glucosidase is known to be structurally different to those of mammalial origins. The microbial α-glucosidase inhibitors are not necessarily the mammalial α-glucosidase inhibitors. For example, (+)-catechin, a natural inhibitor of yeast α-glucosidase does not show any inhibitory activity on mammalial α-glucosidase. On the other hand, acarbose and voglibose show very high inhibitory activity on porcine small intestine α-glucosidase, but both of them show very low inhibitory activity on microbial α-glucosidase, suggesting that ongoing experiments should be focused on the inhibitory activity of

these compounds against mammalian intestinal α-glucosidases. Nevertheless, the inhibition of yeast α-glucosidase by *trans*-cinnamic acid derivatives served as an interesting structural activity relationship of this group of inhibitors.

CHAPTER V

CONCLUSION

Methanol crude extracts of medicinal plants in the *Zingiberaceae* family, especially *Curcuma zedoaria*, *Curcuma longa, Kaempferia parviflora* and *Alpinia galanga* exhibit significant inhibition of viral proteases. For all of the studied enzymes there is a great need to identify novel lead compounds and the current study shows that the *Zingiberaceae* family can be a potential source for such compounds. Consequently, medicinal plants can continue to be a rich source of novel compounds for the treatment of human disease and may be useful as complementary treatments to other established anti-viral therapies.

In conclusion, 5-hydroxy-3,7-dimethoxyflavone (**1**), 5-hydroxy-7-methoxyflavone (**2**), 5-hydroxy-3,7,4'-trimethoxyflavone (**3**), 5-hydroxy-7,4'-dimethoxyflavone (**4**), 5-hydroxy-3,7,3',4'-tetramethoxyflavone (**5**), 3,5,7-trimethoxyflavone (**6**), 5,7-dimethoxyflavone (**7**) and 5,7,4'-trimethoxyflavone (**8**) were isolated from *Kaempferia parviflora* by using bioassay guided fractionation. 5-hydroxy-7-methoxyflavone (**2**) and 5,7-dimethoxyflavone (**7**) showed the highest activity against HIV-1 protease inhibition among the flavonoids from *Kaempferia parviflora*. Moreover, 5-hydroxy-3,7-dimethoxyflavone (**1**) had mild inhibitory activity on HCV and HCMV protease.

(1'*S*)-1'-Acetoxychavicol acetate (**9**), *p*-hydroxy-cinnamaldehye (**10**) and 3,4-dihydroxy adipic acid (**11**) were isolated from *Alpinia galanga*. *p*-hydroxy-cinnamaldehye (**10**) had significant inhibitory activity of HIV-1 protease and HCMV protease for the small molecular inhibitors, and should be considered to be a new class of small molecular inhibitors for HIV-1 protease and HCMV protease.

The other approach for anti HIV research, α-glucosidase inhibition, 4-methoxy-*trans*-cinnamic acid (**13**) and 4-methoxy-*trans*-cinnamic acid ethyl ester (**14**) which isolated from *Kaempferia galanga* showed the highest activity against α-glucosidase inhibition among the *trans*-cinnamic acid derivatives.(93)

FURTHER STUDIES

The binding activity of viral proteases with the inhibitors should be evaluated by Biacore assay. And for compound **10**, small molecular HIV-1 protease and HCMV protease inhibitor should be study on the structure and activity relationship.

Further separation will be necessary to isolate the active components and to elucidate their structures and inhibition mechanisms. In addition, it is of interest to determine the inhibitory effects of the extracts are due to a combined effect of several weak inhibitors or the sole effect of a highly potent compound. In order to address these questions, the isolation of the active compounds from effective crude extracts should be isolate by bioassay guided separation.

For the further studies on α-glucosidase inhibitory effects of trans-cinnamic acid derivatives, α-glucosidase from mammalial sources should be used to evaluate the binding activity as well as inhibitory activity of these compounds using X-ray crystallography and *in vivo* experiments.

REFERENCES

1. Xie, L.; Yu, D.; Wild, C.; Allaway, G.; Turpin, J.; Smith, P. C.; and Lee, K. H. Anti-AIDS agents. 52. Synthesis and anti-HIV activity of hydroxymethyl (3'*R*,4'*R*)-3',4'di-*O*-(*S*)-camphanoyl-(+)-*cis*-khellactone derivatives. J. Med. Chem. 47 (2004): 756-760.

2. UNAIDS and WHO. Report on the global AIDS epidemic. (2004): 1-21.

3. De Clercq, E. Chemotherapeutic approaches to the treatment of the acquired immune deficiency syndrome (AIDS). J. Med. Chem. 29 (1986): 1561-1569.

4. Greene, W. C. AIDS and the immune system. Sci. Am.269 (1993): 98-105.

5. Golieb, M. S.; Schroff, R.; Schanker, H. K.; Weisman, J. D.; Fan, P. T.; Wolf, R. A.; and Saxon, A. Pneumocystis carinii pneumonia and mucosal candidiasis ini previously healthy homosexual men: evidence of a new acquired cellular immunodeficiency. N. Eng. J. Med. 305 (1981): 1425-1431.

6. Sanders, C. J. G.; Dijk, M. R. C.; and Borleffs, J. Kaposi's sarcoma. Lancet 364 (2004): 1549-1552.

7. Update on acquire immune deficiency syndrome (AIDS)--United States. MMWR Morb. Mortal Wkly. Rep. 31 (1982): 507-508.

8. Clavel, F.; Guetard, D.; Bru-Vezinet, F.; Chammaret, S.; Rey, M.; Santos-Ferreira, M. O.; Laurent, A. G.; Dauguet, C.; Katlama, C.; Rouzioux, C.; Klatzmann, D.; Champalimaud, J. L.; Montagnier, L. Isolation of a new human retrovirus from West African patients with AIDS. Science 233 (1986): 343-346.

9. Franchetti, P.; Perlini, P.; Abu Sheikha, G.; Cappellacci, L.; Grifantini, M.; Loi, A. G.; DeMontis, A.; Pani, A.; Marongiu, M. E.; La Colla, L. Potent and selective inhibitors of human immunodeficiency virus protease structurally related to L-694, 746. Antiviral Chem. Chemother. 9 (1998): 303-309.

10. Gao, f.; Bailes, E.; Robertson, D. L.; Chen, Y.; Rodenburg, C. M.; Michael, S. F.; Cummins, L. B.; Arthur, L. O.; Peeters, M.; Shaw, G. M.; Sharp, P. M.; Hahn, B. H. Origin of HIV-1 in the chimpanzee *Pan Troglodytes Troglodytes.* Nature 397 (1999): 436-441.

11. Chen, Z.; Kuckay, A.; Sodora, D. L.; Telfer, P.; Reed, P.; Gettie, A.; Kanu, J. M.; Sadek, R. F.; Yee, J.; Ho, D. D.; Zhang, L.; Marx, P. A. Human immunodeficiency virus type 2 (HIV-2) seroprevalence and characterization of a distinct HIV-2 genetic subtype from the natural range of simian immunodeficiency virus-infected sooty mangabeys, J. Virol. 71 (1997): 3953-3960.

12. Quinn, T. C. Acute primary HIV infection. JAMA 278 (1997): 58-62.

13. Daar, E. S.; Moudgil, T.; Meer, R. D.; Ho, D. D. Transient high levels of viremia in patients with primary human immunodeficiency virus type 1 infection. N. Engl. J. Med. 324 (1991: 961-964.

14. Ho, D. D.; Neumann, A. U.; Perelson, A. S.; Chen, W.; Leonard, J. M.; Markowitz, M. Rapid turnover of plasma virions and CD4 lymphocytes in HIV-1 infection. Nature 373 (1995): 123-126.

15. Wei, X.; Ghosh, S. K.; Taylor, M. E.; Johnson, V. A.; Emini, E. A.; Deutsch, P.; Lifson, J. D.;; Bonhoeffer, S.; Nowak, M. A.; Hahn, B. H.; et al. Viral dynamics in human immunodeficiency virus type 1 infection. Nature 373 (1999): 117-122.

16. Fauci, A. S. the human immunodeficiency virus-infectivity and mechanisms of pathogenesis. Science 239 (1988) 617-622.

17. Markowitz, M. H. HIV pathogenesis and viral dynamics. Antiviral Therapy 2 (1997): 7-17.

18. Author, L. O.; Bess, J. W., Jr.; Sowder, R. C., 2nd; Benveniste, R. E.; Mann, D. L., Chermann, J. C.; Henderson, L. E. Cellular proteins bound to immunodeficiency viruses: implications for pathogenesis and vaccines. Science 258 (1992): 1935-1938.

19. Turner B G; Summers, M. F. Structural biology of HIV. J. Mol. Biol. 285 (1999): 1-32.

20. Janvier, K.; Pei, C.; Le Rouzic, E.; Schwarz, O.; Benichou, S. HIV auxiliary proeins : an interface between the virus and the host. AIDS (2000): S21-30.

21. Ratner, L. HIV life cycle and genetic approaches. Prospect. Drug. Discovery Des. 1 (1993): 2-22.

22. Garg, R.; Gupa, S. P.; Gao, H.; Babu, M. S.; Debnath, A. K.; Hansch, C. Comparative quantitative structure-activity relationship studies on anti-HIV drugs. Chem. Rev. 99 (1999): 4112-4121.

23. De Clercq, E.; Toward improved anti-HIV chemotherapy: Therapeutic strategies for intervention with HIV infections. J. Med. Chem. 38 (1995): 2491-2517.

24. Jones, P. S.; Strategies for antiviral drug discovery. Antiviral Chem. Chemother. 9 (1998): 283-302.

25. Abrams, D. I. Treatment options in Zidovudine intolerance of fairlure. AIDS 8 (1994): S3-7.

26. Richman, D. D.; Fischl, M. A.; Grieco, M. H.; Gottlieb, M. S.; et al. The toxicity of azidothymidine (AZT) in the treatment of patients with AIDS-related complex. A double-blind, Placebo-controlled trial. N. Eng. J. Med. 317 (1987): 192-197.

27. Kramer, R. A.; Schaber, M. D.; Skalka, A. M.; Ganguly, K.; Wong-Staal, F.; Reddy, E. P. HTTLV-III gag protein is processed in yeast cells by the virus pol-protease. Science 231 (1986): 1580-1585.

28. Roberts, N. A.; Martin, J. A.; Kinchington, D.; Broadhurst, A. V.; et al. Rational design of peptide based HIV proteinase inhibitors. Science 248 (1990): 358-364.

29. Flexner, C. HIV-protease inhibitors. Drug therapy 338 (1998): 1281-1292.

30. Walli, R.; Herfort, O.; Michl, G. M.; Demant, T.; et al. Treatment with protease inhibitors associated with peripheral insulin resistance and impaired oral glucose tolerance in HIV-1 infected patients. AIDS 12 (1998): F167-173.

31. Carr, A.; Samaras, K.; Burton, S.; Law, M.; Freund, J.; Chisholm, D. J.; Cooper, D. A. A syndrome of peripheral lipodystrohy, hyperlipidaemia and insulin resistance in patients receiving HIV protease inhibitors. AIDS 12 (1998): F51-58.

32. Martinez, E.; Casamitjana, R.; Conget, I.; Gatell, J. M. Protease inhibitor-associated hyperinsulinaemia. AIDS 23 (1998): 2077-2079.

33. Markowitz, M.; Mo, H.; Kempf, D. J.; Norbeck, D. W.; et al. Selection and analysis of human immunodeficiency virus type 1 variants with increased resistance to ABT-38, a novel protease inhibitor. J. Virol. 69 (1995): 701-706.

34. Condra, J. H.; Schleif, W. A,; Blahy, O. M.; Gabryelski, L. J.; et al. In vivo emergence of HIV-1 variants resistant to multiple protease inhibitors. Nature 374 (1995): 569-571.

35. Ridky, T.; Leis, J. Development of drug resistance to HIV-1 protease inhibitors. J. Biol. Chem. 270 (1995):29621-29623.

36. Richman, D. D. HIV chemotherapy. Nature 410 (2001): 995-1001.

37. Carpenter, C. C.; Fischl, M. A.; Hammer, S. M.; et al. Antiretroviral therapy for HIV infection in 1998: updated recommendations of the international AIDS society-USA panel. JAMA 280 (1998): 78-86.

38. Erikson, J. W.; Gulnik, S. V.; Markowitz, M. Protease inhibitors: resistance, cross-resistance, fitness and the choice of initial and salvage therapies. AIDS 13 (1999): S189-S204.

39. Giannini, C.; and Brechot, C. Hepatitis C virus biology. Cell Death and Differentiation.10 (2003): S27-S38.

40. Alberi, A.; Benvegnu, L.; Boccao, S.; Ferrari, A.; and Sebastiani, G. Natural history of initially mild chronic hepatitis C. Digestive and Liver Disease. 36 (2004): 646-654.

41. Han, W; Hu ; Jiang X.; Wasseran , Z. R.; and Decicco, C. P. Glycine α-ketoamides as HCV NS3 protease inhibitors. Bioorg. Med. Chem. Lett. 13 (2003): 1111-1114.

42. Hegde V. R.; Pu, H.; Pattel, M.; Das, P. R.; Butkiewicz, N; et al. Two antiviral compounds from the plant *Stylogne cauliflora* as inhibitors of HCV NS3 protease. Bioorg. Med. Chem. Lett. 13 (2003): 2925-2928.

43. Dai, J. R.; Carte, B. K.; Sidebotttom, P. J.; et al. Circumdatin G, a new alkaloid from the fungus *Aspergillus ochraceus*. J. Nat. Prod. 6 (2001): 125-126.

44. Perni, R. B. NS3.4A protease as a target for interfering with hepatitis C virus replication. Drug News Perspect. 13 (2000): 69-77.

45. Bonneau, P. R.; Hasani, F.; Plouffe, C.; Malenfant, E.; et al. Inhibition of human cytomegalovirus protease by monocyclic β-lactam derivatives: Kinetic characterization using a fluorescent probe. J. Am. Chem. Soc. 121 (1999): 2965-2973.

46. Fujikawa, T.; Numazaki, K.; Asanuma, H.; and Tsutsumi, H. Human cytomegalovirus infection during pregnancy and detection of specific T cells by intracellular cytokine staining. Int. J. Infect. Dis. 7 (2003): 215-221.

47. Shu, Y. Z.; Ye, Q.; Kolb, J. M.; Huang, S.; Veitch, J. A.; Lowe, S. E.; and Manly, S. P. Bripiodionen, a new inhibitor of human cytomegalovirus protease from *Streptomyces* sp. WC76599. J. Nat. Prod. 60 (1997): 529-532.

48. Smith, D. G.; Gribble, A. D.; Haigh, D.; Ife, R. J.; Lavery, P.; et al. The inhibition of human cytomegalovirus (HCMV) protease by hydroxylamine derivatives. Bioorg. Med. Chem. Lett. 9 (1999): 3137-3142.

49. Cos, P.; Maes, L.; Berghe, D. V.; et al. Plant substances as anti-HIV agents selected according to their putative mechanism of action. J. Nat. Prod. 67 (2004): 284-293.

50. Garg, R.; Gupta, S.P.; Gao, H.; et al. Comparative quantitative structure-activity relationship studies on anti-HIV drugs. Chem. Rev. 99 (1999): 3525-3601.

51. Asano, N. Glycosidase inhibitors: update and perspectives on practical use Glycobiology 13 (2003): 93R-104R.

52. Jacob, G. S. Glycosylation inhibitors in biology and medicine. Current Opinion in Structural Biology 5 (1995): 605-611.

53. Nishioka, T.; Kawabata, J.; and Aoyama, Y. Baicalein, an alpha-glucosidase inhibitor from *Scutellaria baicalensis*. J. Nat. Prod. 61 (1998): 1413-1415.

54. Nakao, Y.; Maki, T.; Matsunaga, S.; et al. Penarolide sulfates A_1 and A_2, new alpha-glucosidase inhibitors from a marine sponge *Penares* sp. Tetrahedron 56 (2000): 8977-8987.

55. Lee, D. S.; Lee, S. H.; Genistein, a soy isoflavone, is a potent α-glucosidase inhibitor. FEBS Letters. 501 (2001): 84-86.

56. Takada, K.; Uehara, T.; Nakao, Y.; et al. Schulzeines A-C, new alpha-glucosidase inhibitors from the marine sponge *Penares schulzei*. J. Am. Chem. Soc. 126 (2004): 187-193.

57. Kashman, Y.; Gustafson, K. R.; Fuller, R. W.; et al. The calanolides, A novel HIV-inhibitory class of coumarin derivatives from the tropical rain-forest tree, Calophyllum lanigerum. J. Med. Chem. 35 (1992): 2735-2743.

58. Chang, F. R.; Yang, P. Y.; Lin, J. Y.; Lee, K. H.; and Wu, Y. C. Bioactive kaurane diterpenoids from *Annona glabra*. J. Nat. Prod. 61 (1998): 437-439.

59. Corbett, J. W.; Gearhart, L. A.; Ko, S. S.; et al. Novel 2,2-dioxide-4,4-disubstituted-1,3-H-2,1,3-benzothiadiazines as non-nucleoside reverse transcriptase inhibitors. Bioorg. Med. Chem. Lett. 10 (2000): 193-195.

60. Corbett, J. W.; Pan, S.; Markwalder, J. A.; et al. 3, 3a-dihydropyrano [4,3,2-de] quinazolin-2(1H)-ones are potent non-nucleoside reverse transcriptase inhibitors. Bioorg. Med. Chem. Lett. 11 (2001): 211-214.

61. Potts, B. C. M.; and Faulkner, D. J. Didemnaketals A and B, HIV-1 protease inhibitors from the Ascidian *Didemnum* sp. J. Am. Chem. Soc. 113 (1991): 6321-6322.

62. Mazumder, A.; Wang, S.; Neamati, N.; et al. Antiretroviral agents as inhibitors of both human immunodeficiency virus type 1 integrase and protease. J. Med. Chem. 39 (1996): 2472-2481.

63. El Mekkawy, S.; Meselhy, M. R.; Nakamura, N.; et al. Anti HIV-1 and anti HIV-1-protease substances from *Ganoderma lucidum*. Phytochemistry. 49 (1998): 1651-1657.

64. Xu, H. X.; Wan, M.; Dong, H.; et al. Inhibitory activity of flavonoids and tannins against HIV-1 protease. Biol. Pharm. Bull. 23 (2000): 1072-1076.

65. Chu, M.; Mierzwa, R.; He, L.; et al. Isolation and structure of SCH 351633: A novel hepatitis C virus (HCV) NS3 protease inhibitor from the fungus *Penicillium griseofulvum*. Bioorg. Med. Chem. Lett. 9 (1999): 1949-1952.

66. Yoakim, C.; Ogilvie, W. W.; Cameron, D. R.; et al. β-lactam derivatives as inhibitors of human cytomegalovirus protease. J. Med. Chem. 41 (1998): 2882-2891.

67. Welch, A. R.; McNally, L. M.; and Gibson. W. Cytomegalovirus assembly protein nested gene family: four 3'-coterminal transcripts encode four in-frame, overlapping proteins. J. Virol. 65 (1991): 4091-4100.

68. Qian-Cutrone, J.; Kolb, J. M.; Mcbrien, K.; et al. Quanolirones I and II, two new human cytomegalovirus protease inhibitors produced by streptomyces sp. WC76535. J. Nat. Prod. 61 (1998): 1379-1382.

69. Guo, B.; Dai, J. R.; Ng, S.; et al. Cytonic acids A and B: Novel tridepside inhibitors of hCMV protease from the endophytic fungus Cytonaema species. J. Nat. Prod. 63 (2000): 602-604.

70. Grandi, M. J. D.; Curran, K. J.; Baum, E. Z.; et al. Pyrimido[1,2-b]-1,2,4,5-tetrazin-9-ones as HCMV protease inhibitors: a new class of heterocycles with flavin-like redox properties. Bioorg. Med. Chem. Lett. 13 (2003): 3483-3486.

71. Collins, R. A.; Ng, TT. B.; Fong, W. P.; Wan, C. C.; and Yeung, H. W. A comparison of human immunodeficiency virus type 1 inhibition by partially purified

aqueous extracts of Chinese medicinal herbs. Life Sciences. 60 (1997): 345-351.

72. Lam, T. L.; Lam, M. L.; Au, T. K.; Ip, D. T. M.; Ng, T. B.; Fong, W. P.; and Wan, D. C. C. A comparison of human immunodeficiency virus type-1 protease inhibition activities by the aqueous and methanol extracts of Chinese medicinal herbs. Life Sciences. 67 (2000): 2889-2896.

73. Gronowitz, J. S.; Lennerstrand, J.; Petterson, A.; Neumuller, M.; Johansson, M.; and Kallander, C. F. R. Determination of IC_{50} values and the mechanism of action of HIV-1 RT inhibitors, by the use of carrier bound template-primer, template, or primer, with ^{125}I-IUTP as substrate. Antivir. Chem. Chemother. 3 (1992): 203-213.

74. Danielson, U. H.; Lindgren, M. T.; Markgren, P. O.; and Nillroth, U. Investigation of an allosteric site of HIV-1 proteinase involved in inhibition by Cu2+. Adv Exp Med Biol. 436 (1998): 99-103.

75. Nillroth, U.; Vrang, L.; Markgren, P. O.; Hultén, J.; Hallberg, A., Danielson, U. H. Human immunodeficiency virus type 1 proteinase resistance to symmetric cyclic urea inhibitor analogs. Antimicrob. Agents Chemother. 41 (1997) 2383-2388.

76. Johansson, A.; Poliakov, A.; Akerblom, E.; Lindeberg, G.; Siniwarter, S.; Samuelsson, B.; Danielson, U. H.; and Hallberg, A. Tetrapeptides as potent protease inhibitors of hepatitis C virus full-length NS3 (protease-helicase/NTPase). Bioorg. Med. Chem. Lett. 10 (2002): 3915-3922.

77. Poliakov, A.; Johansson, A.; Akerblom, E.; Oscarsson, K.; Samuelsson, B.; Hallberg, A.; and Danielson, U. H. Structure-acivity relationships for the selectivity of hepatitis C virus NS3 protease inhibitors. Biochimmica et Biophysica Acta. 1672 (2004): 51-59.

78. Holskin, B. P.; Bukhtiyarova, M.; Dunn, B. M.; Baur, P.; Chastonay, J.;. Pennington, M. W. A continuous fluorescence-based assay of human cytomegalovirus protease using a peptide substrate, Anal Biochem 227 (1995) 148-155.

79. Geitmann, M.; Danielson, U. H.; Detection of conformational changes in the human cytomegalovirus protease upon substrate binding using optical biosensor technology, Anal. Biochem. 332 (2004) 203-214.

80. Matsui, T.; Yoshimoto, C.; Osajima, K.; Oki, T.; and Osajima, Y. In vivo survey of α-glucosidase inhibitory food components. Biosci. Biotech. Biochem. 60 (1996): 2019-2022.

81. Tan, G. T.; Pezzuto, J. M.; Kinghorn, A. G.; and Hughes, S. H. Evaluation of natural products as inhibitors of human immunodeficiency virus type 1 (HIV-1) reverse transcriptase. J. Nat. Prod. 54 (1991): 143-154.

82. Mabry, T. M.; Kagan, J.; and Rösler, H. NMR spectra of trimethylsilyl ethers of flavonoid glycosides. Phytochemsitry 4 (1965): 177-183.

83. Mabry, T. M.; Kagan, J.; and Rösler, H. Baptisia flavonoids: nuclear magnetic resonance analysis. Phytochemistry 4 (1965): 487-493.

84. Jaipetch, T.; Reutrakul, V.; Tuntiwachwuttikul, P.; and Santisuk, T. Flavonoids in the black rhizomes of *Boesenbergia pandurata.* Phytochemistry 22 (1983): 625-626.

85. Astudillo, L.; Avila, F.; Morrison, R.; Gutierrez, M.; Bastida, J.; Codina, C.; and Schmeda-Hirschmann, G. Biologically active compounds from Chilean propolis. Boletin de la Sociedad Chilena de Quimica 45 (2000).

86. Vidari, G.; Finzi, P. V.; and De Bernardi, M. Flavonols and quinines in stems of *Aframomum giganteum* Phytochemistry 10 (1971): 3335-3339.

87. Silva, M.; and Mundaca, J. M. Flavonoid and triterpene constituents of *Baccharis rhomboidalis* Phytochemistry 10 (1971): 1942-1943.

88. Matsuda, H.; Morikawa, T.; Toguchida, I.; and Yoshikawa, M. Structural requirements of flavonoids and related compounds for aldose reductase inhibitory activity Chem. Pharm. Bull. 50 (2002): 788-795.

89. Franca, N. C.; Gottlieb, O. R.; Magalhaes, M. T.; and et al. Tri-O-methylgalangin from *Aniba riparia* Phytochemistry 15 (1976): 572-573.

90. Noro, T.; Sekiya, T.; Katoh, M.; and et al. Inhibitors of xanthine oxidase from *Alpinia galanga* Chem. Pharm. Bull. 36 (1988): 244-248.

91. Stange Jr. R. R.; Sims, J. J.; Midland, S. L.; and McDonald, R. E. Isolation of a phytoalexin, trans-*p*-coumaryl aldehyde, from *Cucurbita maxma*, Cucurbitaceae Phytochemistry 52 (1999): 41-43.

92. Chen, Y.; Huang, L.; Ranade, M. A.; and Zhang, X. P. Iron (III) and ruthenium porphyrin complex-catalyzed selective olefination of aldehydes with ethyl diazoacetate. J. Org. Chem. 68 (2003): 3714-3717.

93. Kosuge, T.; Yokota, M.; Sugiyama, K.; Saito, M.; Iwata, Y.; Kakura, M.; and Yamamoto, T. Studies on anticancer principles in Chinese medicines. II.[1)] Cytotoxic principles in *Biota orientalis* (L.) ENDL. and *Kaempferia galanga* L. Chem. Pharm. Bull. 33 (1985): 5565-5567.

94. Tan, C. Y. K.; and Weaver, D. F. A one-pot synthesis of 3-amino-3-arylpropionic acids. Tetrahedron 58 (2002): 7449-7461.

95. Adisakwattana, S.; Sookkongwaree, K.; Roengsumran, S.; Petsom, A.; Ngamrojnavanich, N.; Chavasiri, W.; Deesamer, S.; and Yibchok-anun, Y. Structure-activity relationships of trans-cinnamic acid derivatives on α-glucosidase inhibition. Bioorg. Med. Chem. Lett. 14 (2004): 2893-2896.

APPENDICES

Table A1 Inhibition of HIV-1 reverse transcriptase by methanol and aqueous extracts from *Zingiberaceae* medicinal herbs. Extracts of the specified part were tested at 20 and 200 μg/ml, values are means ± S.D., n = 3

Name	Used part	% HIV-1 RT inhibition			
		Methanol extracts		Aqueous extracts	
		20 μg/ml	200 μg/ml	20 μg/ml	200 μg/ml
Curcuma aromatica	Fresh rhizome	-	9.2±2.1	-	28.1±3.2
Curcuma sp. (En leung)	Dried rhizome	-	-	12.0±1.6	34.3±3.4
Kaempferia galanga	Dried rhizome	-	-	16.7±1.8	32.3±2.8
Curcuma zedoaria	Fresh rhizome	16.6±2.3	26.7±3.7	15.1±1.7	55.1±4.5
Curcuma longa	Fresh rhizome	10.2±1.6	30.6±2.5	14.6±2.5	59.9±4.6
Kaempferia parviflora	Fresh rhizome	7.6±1.5	25.2±2.1	7.7±2.3	19.9±3.5
Boesenbergia pandurata	Fresh rhizome	3.5±1.0	18.3±1.9	-	5.5±2.1
Curcuma sp. (Kamin Dum)	Fresh rhizome	5.2±1.4	15.7±1.6	5.8±1.9	35.6±5.3
Zingiber zerumbet	Fresh rhizome	5.7±1.8	11.8±1.8	9.8±2.6	12.9±2.3
Zingiber officinale	Fresh rhizome	8.2±1.7	28.1±2.3	29.6±2.8	69.3±5.8
Alpinia galanga	Fresh rhizome	3.9±1.5	19.5±2.4	14.8±2.9	34.3±3.6

Table A2 Inhibition of HIV-1 protease by methanol and aqueous extracts from *Zingiberaceae* medicinal herbs. Extracts of the specified part were tested at 20 and 200 μg/ml, values are means ± S.D., n = 3

Name	Used part	% HIV-1 protease inhibition			
		Methanol extracts		Aqueous extracts	
		20 μg/ml	200 μg/ml	20 μg/ml	200 μg/ml
Curcuma aromatica	Fresh rhizome	2.4 ± 0.7	43.2 ± 1.2	0.7 ± 0.1	3.9 ± 3.3
Curcuma sp. (En leung)	Dried rhizome	19.3 ± 0.3	47.7 ± 1.3	19.7 ± 2.3	40.0 ± 5.8
Kaempferia galanga	Dried rhizome	1.5 ± 0.8	4.9 ± 1.4	0.7 ± 0.7	22.1 ± 1.2
Curcuma zedoaria	Fresh rhizome	18.6 ± 2.7	97.8 ± 1.5	26.5 ± 3.4	89.8 ± 1.2
Curcuma longa	Fresh rhizome	67.8 ± 5.6	92.9 ± 0.9	35.3 ± 3.5	97.0 ± 1.9
Kaempferia parviflora	Fresh rhizome	37.1 ± 0.4	81.5 ± 0.8	15.2 ± 0.6	48.3 ± 7.8
Boesenbergia pandurata	Fresh rhizome	22.1 ± 2.1	64.6 ± 2.0	35.7 ± 1.7	57.9 ± 2.0
Curcuma sp. (Kamin Dum)	Fresh rhizome	6.6 ± 3.3	14.5 ± 3.2	0.4 ± 0.1	6.1 ± 2.9
Zingiber zerumbet	Fresh rhizome	9.9 ± 2.8	17.8 ± 1.4	5.0 ± 0.6	8.5 ± 0.5
Zingiber officinale	Fresh rhizome	14.8 ± 2.7	46.0 ± 8.6	17.6 ± 0.6	26.8 ± 0.7
Alpinia galanga	Fresh rhizome	97.5 ± 0.4	98.2 ± 1.0	16.5 ± 0.1	37.9 ± 1.0

Table A3 Inhibition of HCV proteases by methanol and aqueous extracts from *Zingiberaceae* medicinal herbs. Extracts of the specified part were tested at 20 and 200 μg/ml, values are means ± S.D., n = 3

Name	Used part	% HCV protease inhibition			
		Methanol extracts		Aqueous extracts	
		20 μg/ml	200 μg/ml	20 μg/ml	200 μg/ml
Curcuma aromatica	Fresh rhizome	3.5 ± 2.7	44.1 ± 6.1	68.0 ± 1.8	80.9 ± 0.5
Curcuma sp. (En leung)	Dried rhizome	53.1 ± 3.8	83.4 ± 1.9	38.2 ± 1.7	78.3 ± 1.4
Kaempferia galanga	Dried rhizome	3.5 ± 2.7	20.9 ± 6.4	8.3 ± 0.1	29.4 ± 3.9
Curcuma zedoaria	Fresh rhizome	68.9 ± 2.4	84.7 ± 6.2	50.6 ± 9.9	81.3 ± 1.3
Curcuma longa	Fresh rhizome	44.6 ± 6.1	84.9 ± 2.8	65.1 ± 5.8	84.5 ± 5.9
Kaempferia parviflora	Fresh rhizome	17.7 ± 2.8	71.9 ± 2.3	56.7 ± 2.3	87.2 ± 2.6
Boesenbergia pandurata	Fresh rhizome	33.9 ± 3.5	82.0 ± 1.2	54.0 ± 0.9	84.8 ± 2.1
Curcuma sp. (Kamin Dum)	Fresh rhizome	3.6 ± 0.6	45.8 ± 3.3	26.2 ± 1.6	95.6 ± 1.0
Zingiber zerumbet	Fresh rhizome	47.2 ± 3.5	85.4 ± 5.5	7.9 ± 4.4	71.8 ± 5.5
Zingiber officinale	Fresh rhizome	53.6 ± 0.8	96.0 ± 1.4	43.0 ± 9.7	93.1 ± 2.2
Alpinia galanga	Fresh rhizome	58.7 ± 1.8	82.8 ± 0.9	12.3 ± 0.8	75.7 ± 5.2

Table A4 Inhibition of HCMV proteases by methanol and aqueous extracts from *Zingiberaceae* medicinal herbs. Extracts of the specified part were tested at 20 and 200 μg/ml, values are means ± S.D., n = 3

Name	Used part	% HCMV protease inhibition			
		Methanol extracts		Aqueous extracts	
		20 μg/ml	200 μg/ml	20 μg/ml	200 μg/ml
Curcuma aromatica	Fresh rhizome	30.0 ± 6.4	77.7 ± 1.3	5.5 ± 4.3	51.0 ± 0.9
Curcuma sp. (En leung)	Dried rhizome	44.5 ± 0.5	94.7 ± 4.4	4.3 ± 0.9	2.1 ± 0.4
Kaempferia galanga	Dried rhizome	22.3 ± 0.8	45.6 ± 1.7	6.7 ± 1.7	22.9 ± 0.4
Curcuma zedoaria	Fresh rhizome	32.1 ± 1.6	94.8 ± 2.8	13.1 ± 4.7	57.5 ± 0.2
Curcuma longa	Fresh rhizome	68.6 ± 1.2	97.3 ± 2.4	1.8 ± 0.9	54.1 ± 3.2
Kaempferia parviflora	Fresh rhizome	29.6 ± 4.0	74.7 ± 3.5	11.3 ± 6.5	33.8 ± 7.3
Boesenbergia pandurata	Fresh rhizome	47.9 ± 3.6	96.2 ± 0.6	13.1 ± 3.0	19.2 ± 3.9
Curcuma sp. (Kamin Dum)	Fresh rhizome	5.2 ± 1.7	65.5 ± 5.6	6.1 ± 4.3	12.5 ± 1.3
Zingiber zerumbet	Fresh rhizome	20.5 ± 2.4	39.0 ± 0.3	0.9 ± 0.4	5.5 ± 4.3
Zingiber officinale	Fresh rhizome	4.0 ± 1.5	57.2 ± 5.8	5.8 ± 0.4	11.9 ± 8.2
Alpinia galanga	Fresh rhizome	77.1 ± 0.3	96.6 ± 0.3	5.2 ± 3.0	10.7 ± 3.9

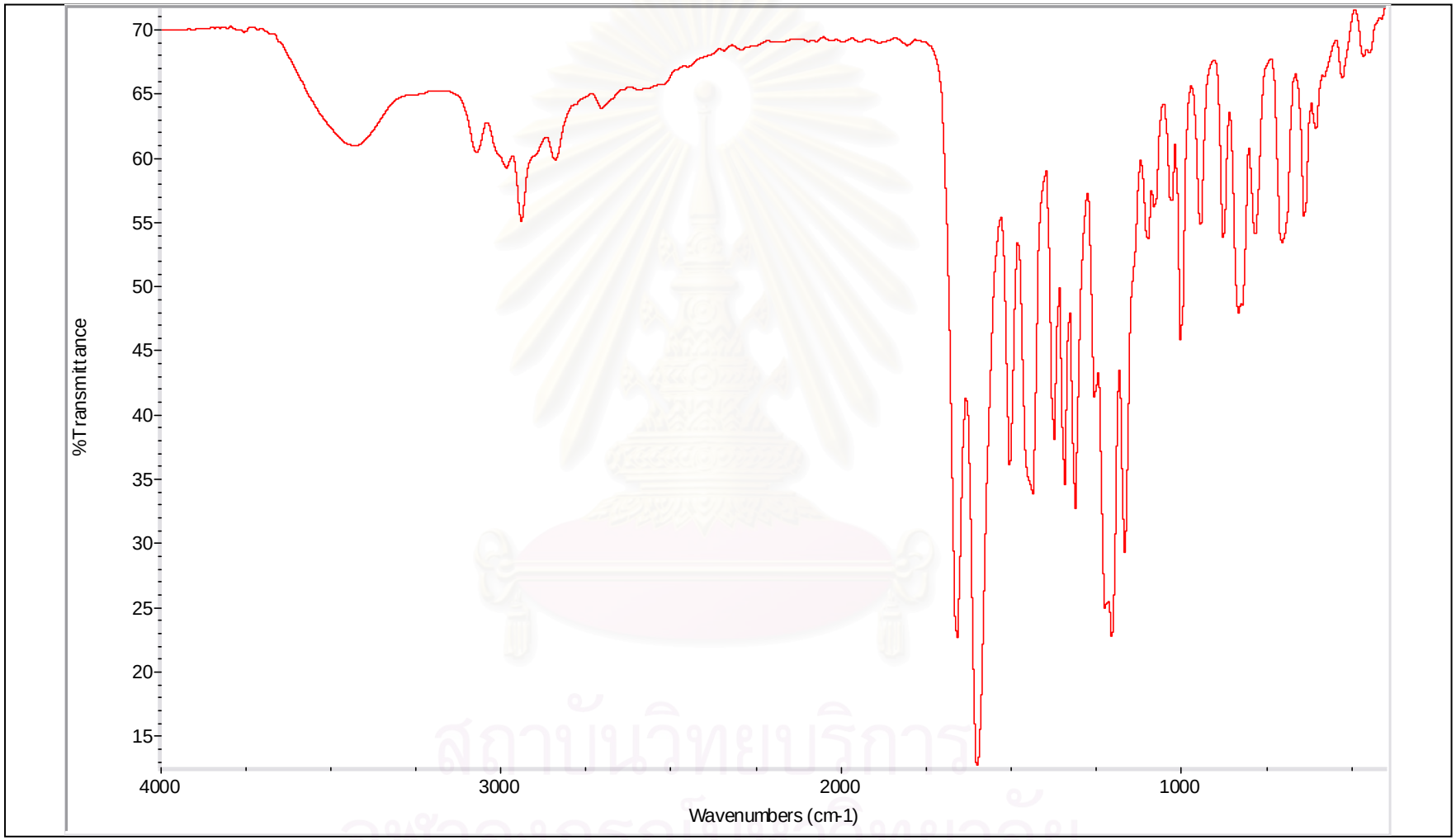

Figure A1 The IR spectrum of compound **1**

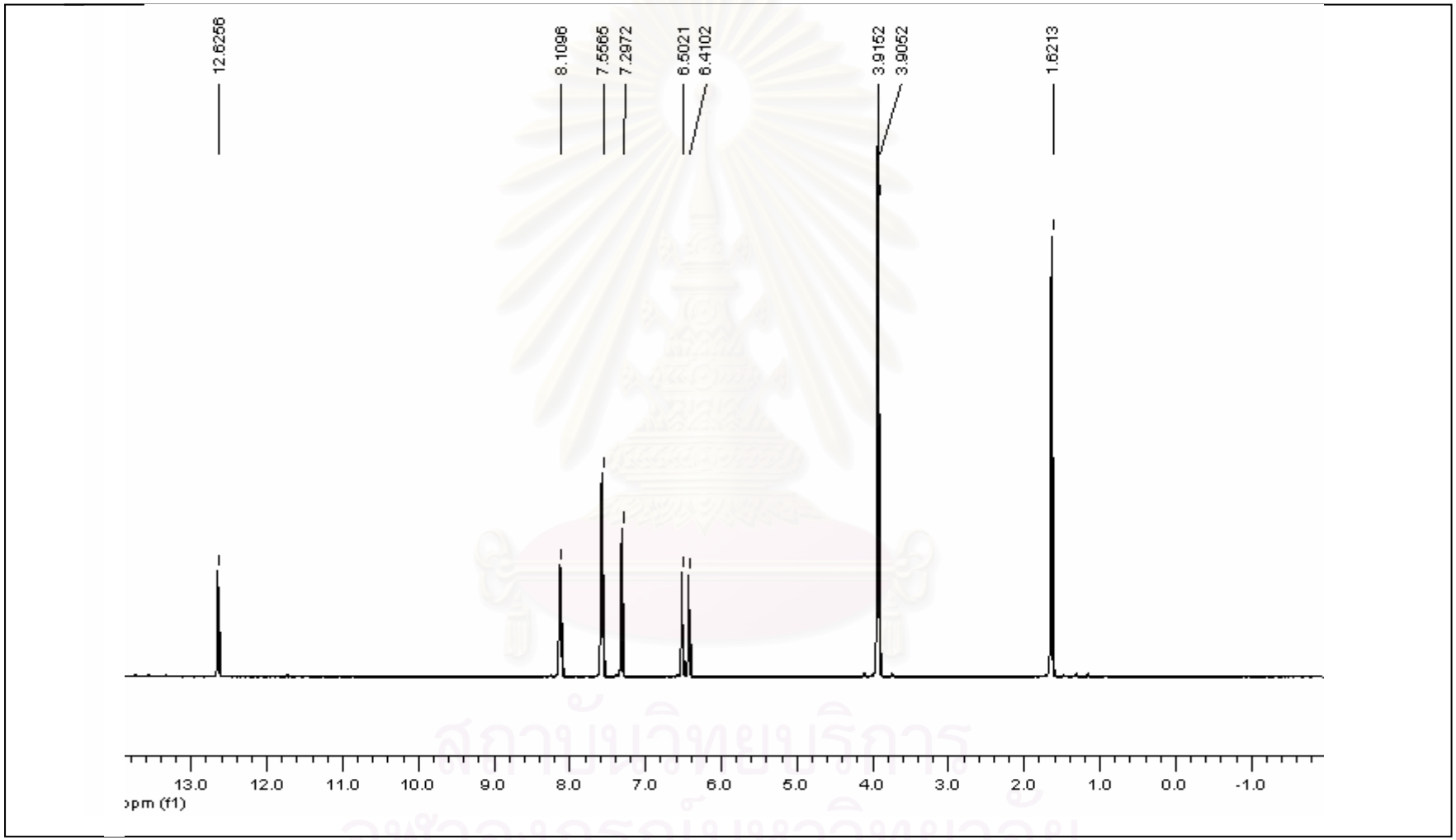

Figure A2 The ^{1}H-NMR spectrum of compound **1**

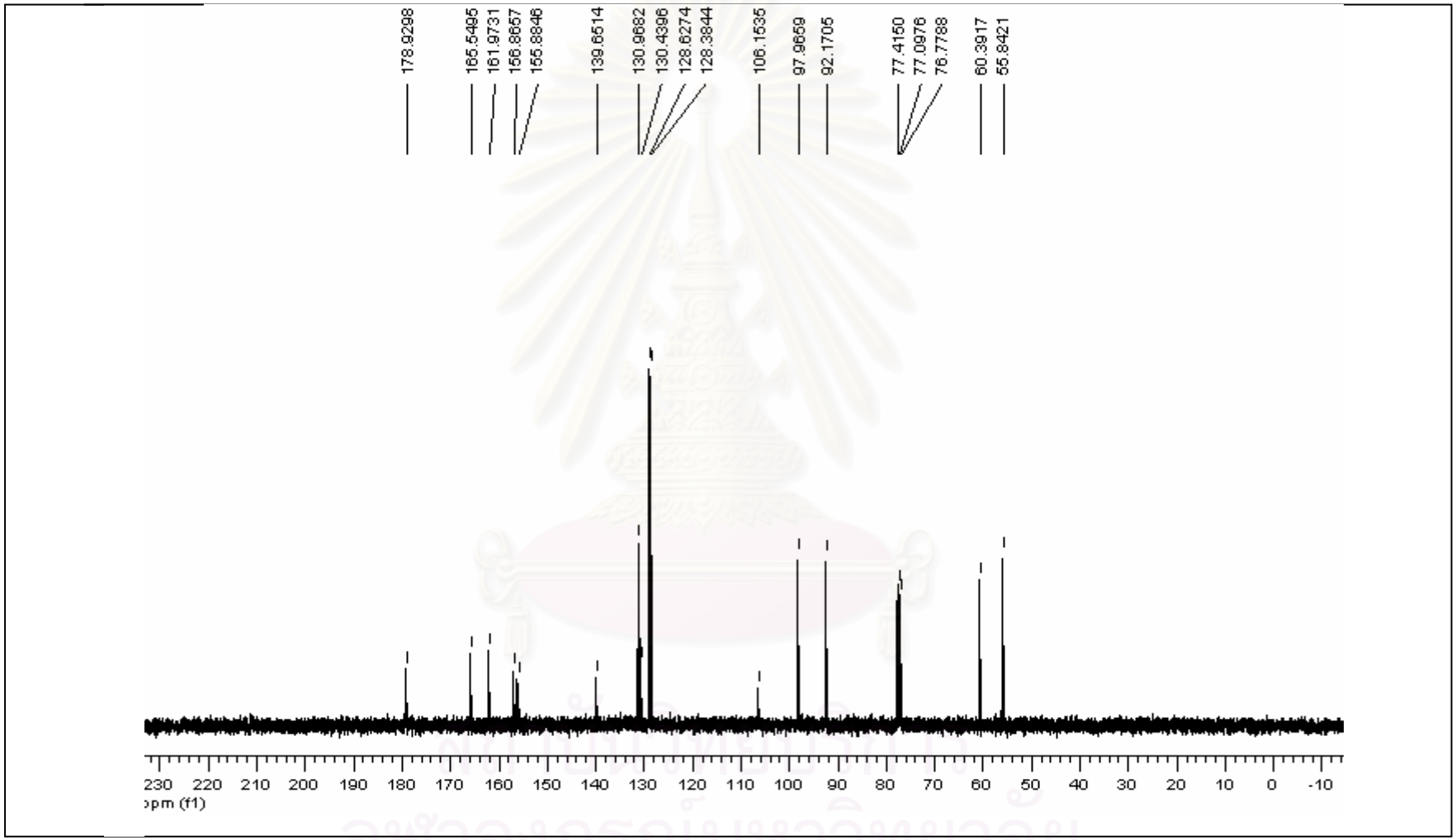

Figure A3 The ^{13}C-NMR spectrum of compound **1**

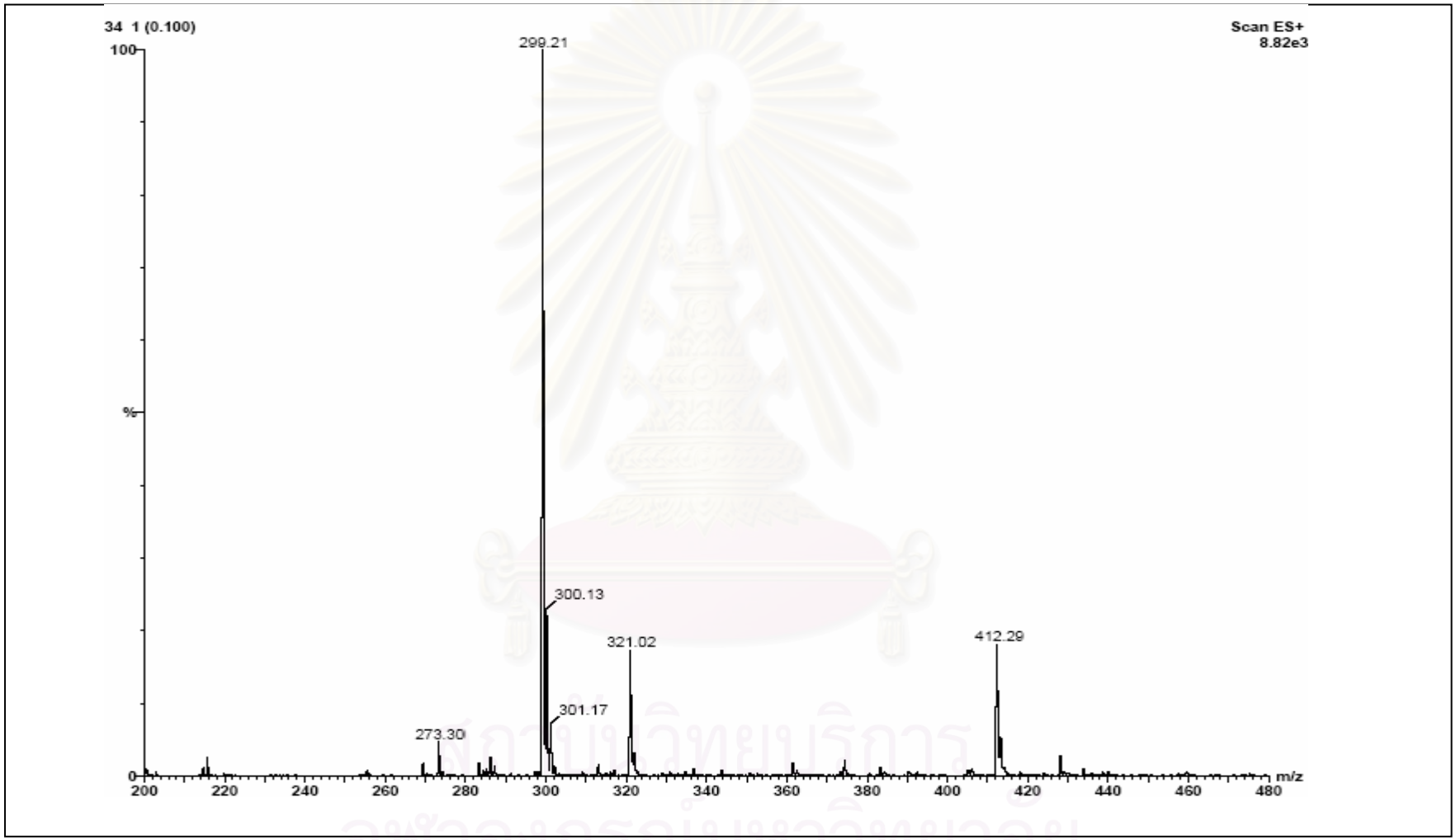

Figure A4 The mass spectrum of compound **1**

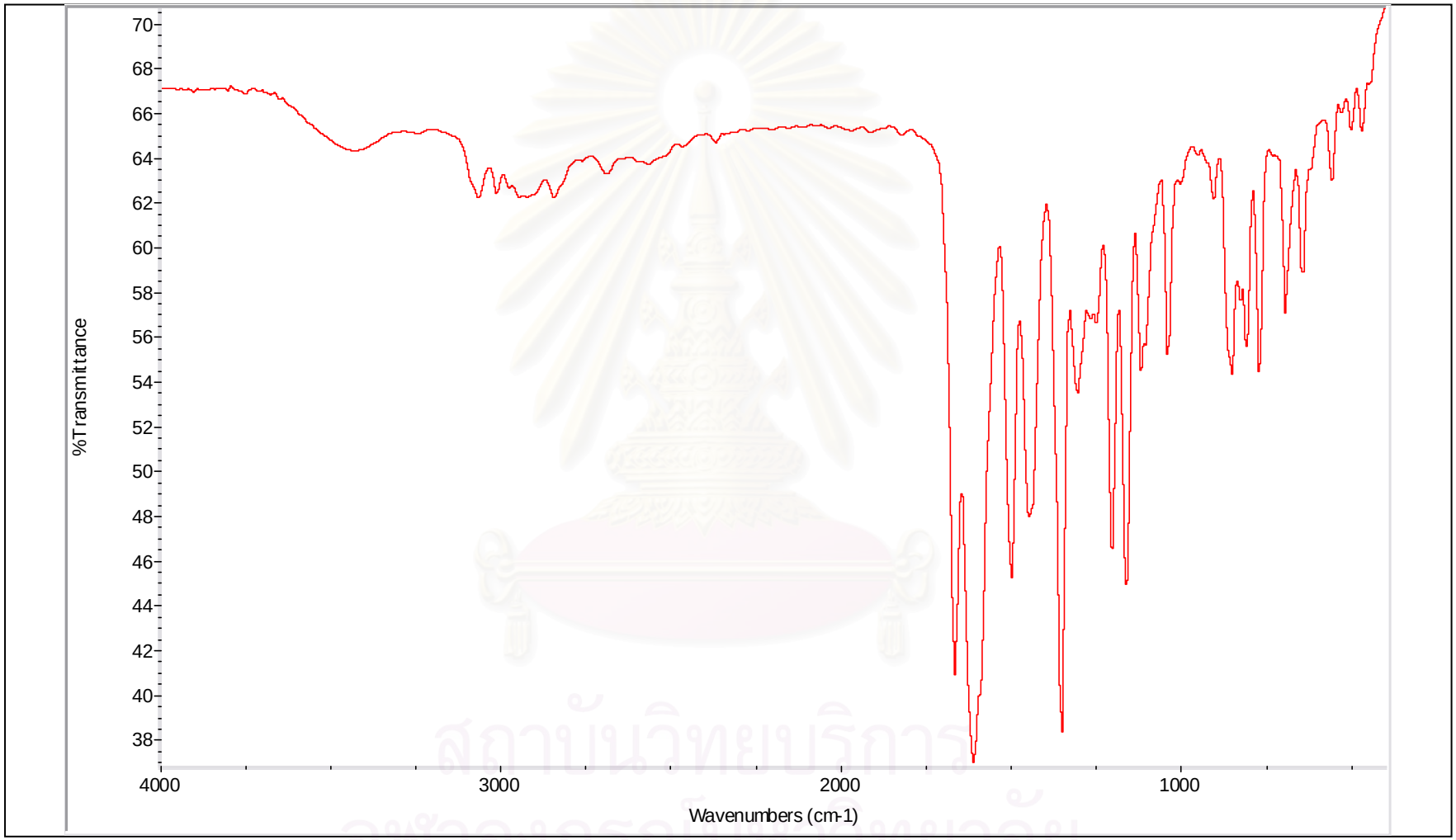

Figure A5 The IR spectrum of compound **2**

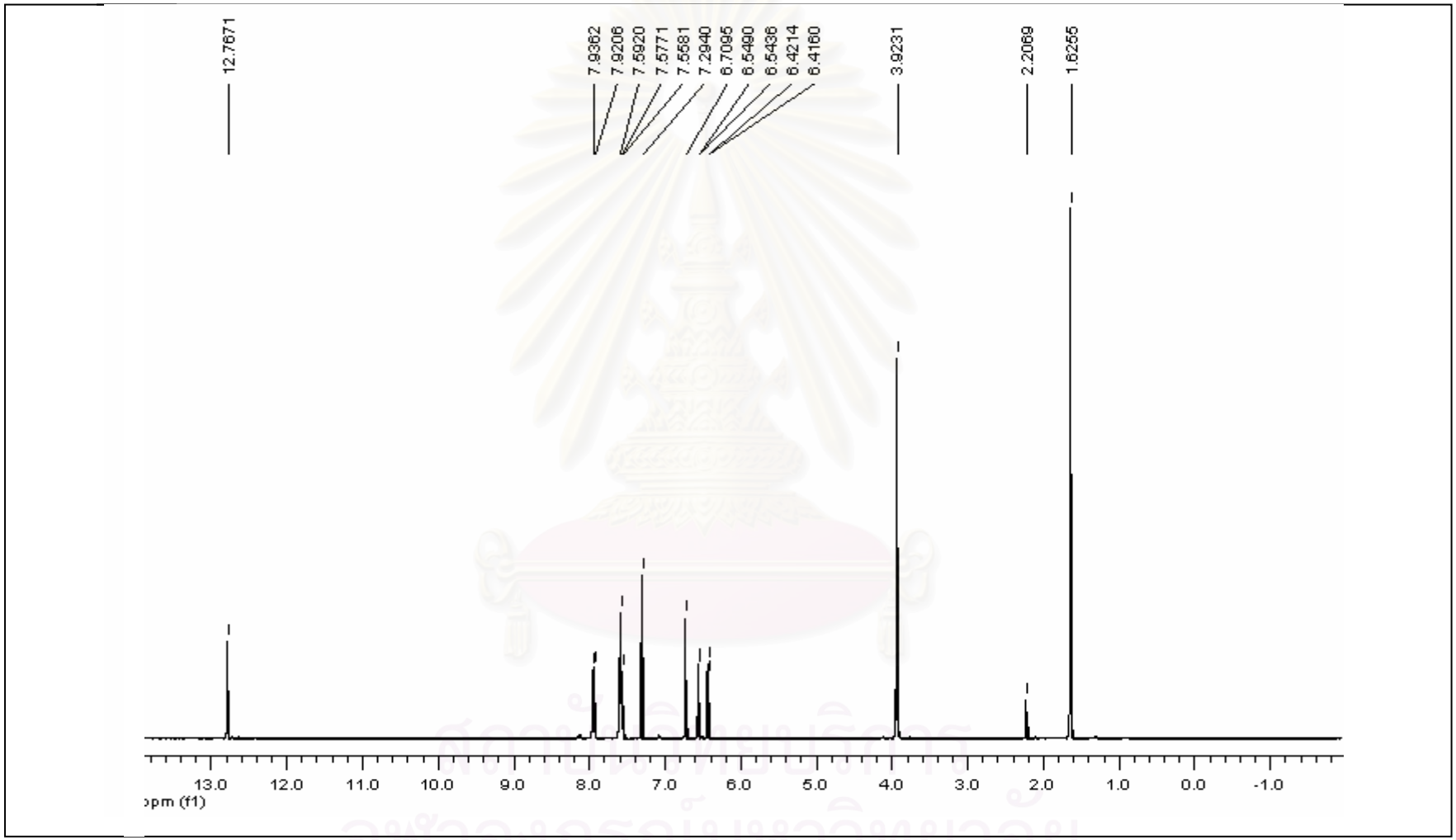

Figure A6 The ^{1}H-NMR spectrum of compound 2

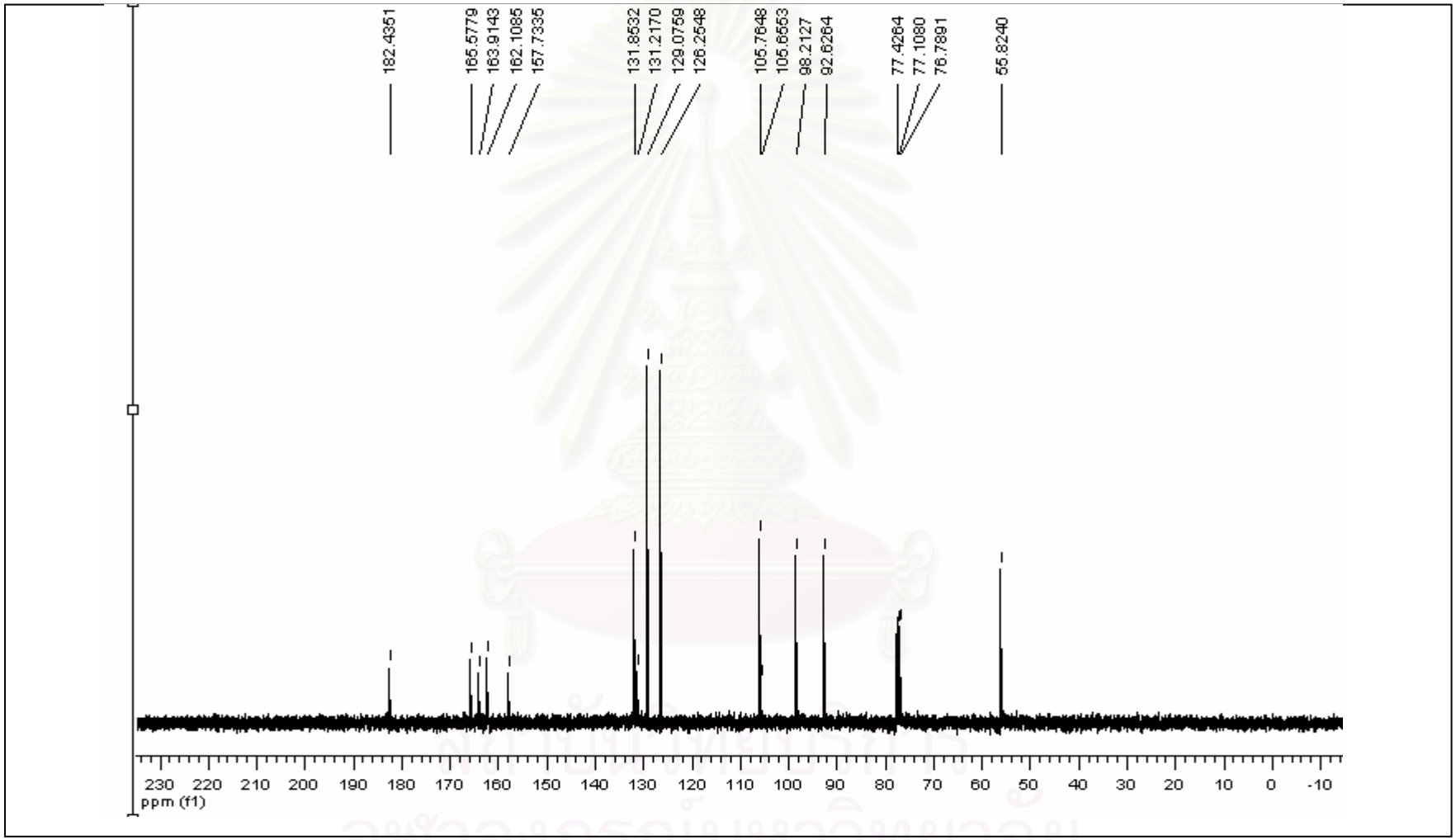

Figure A7 The ^{13}C-NMR spectrum of compound **2**

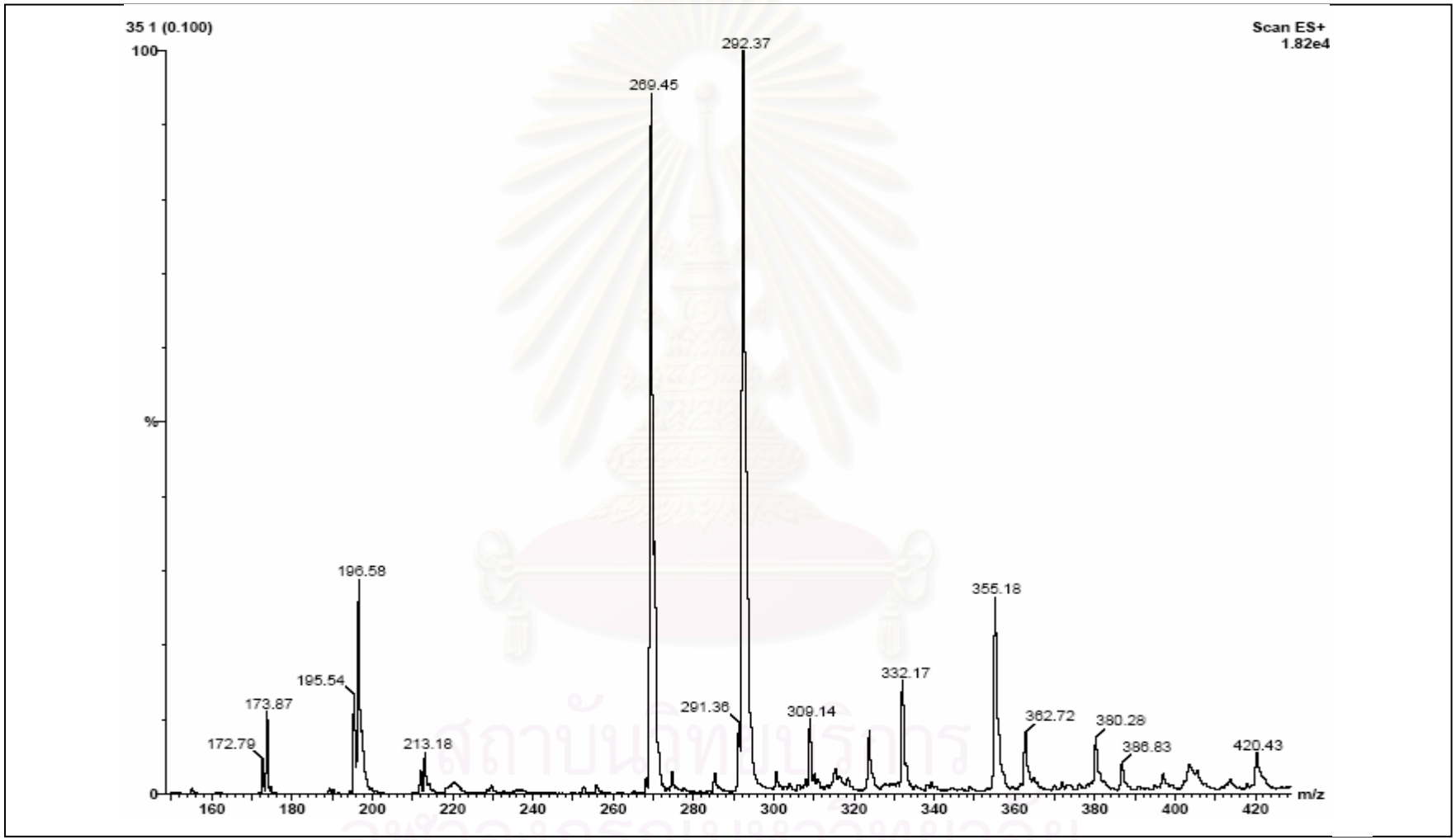

Figure A8 The mass spectrum of compound **2**

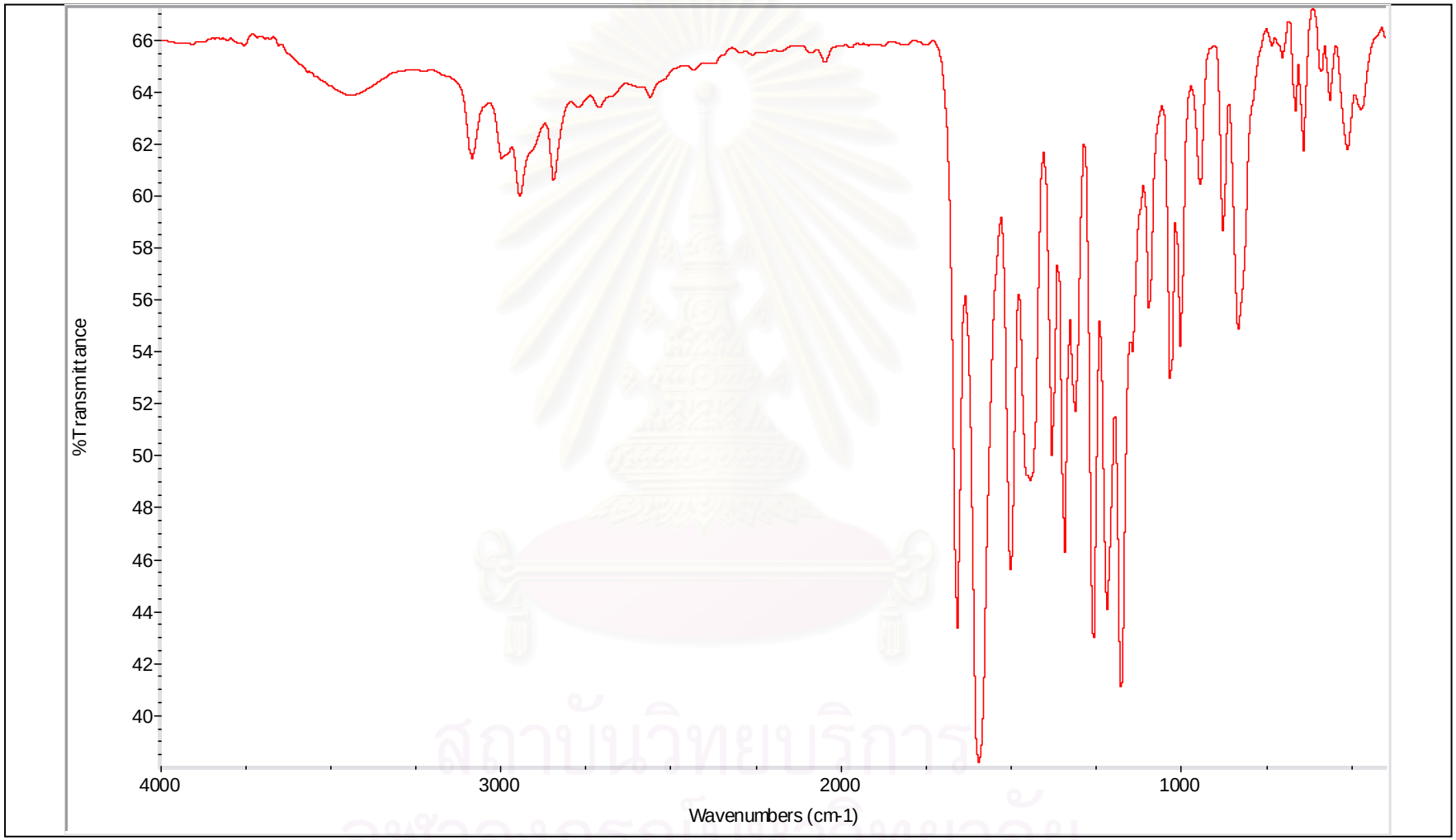

Figure A9 The IR spectrum of compound **3**

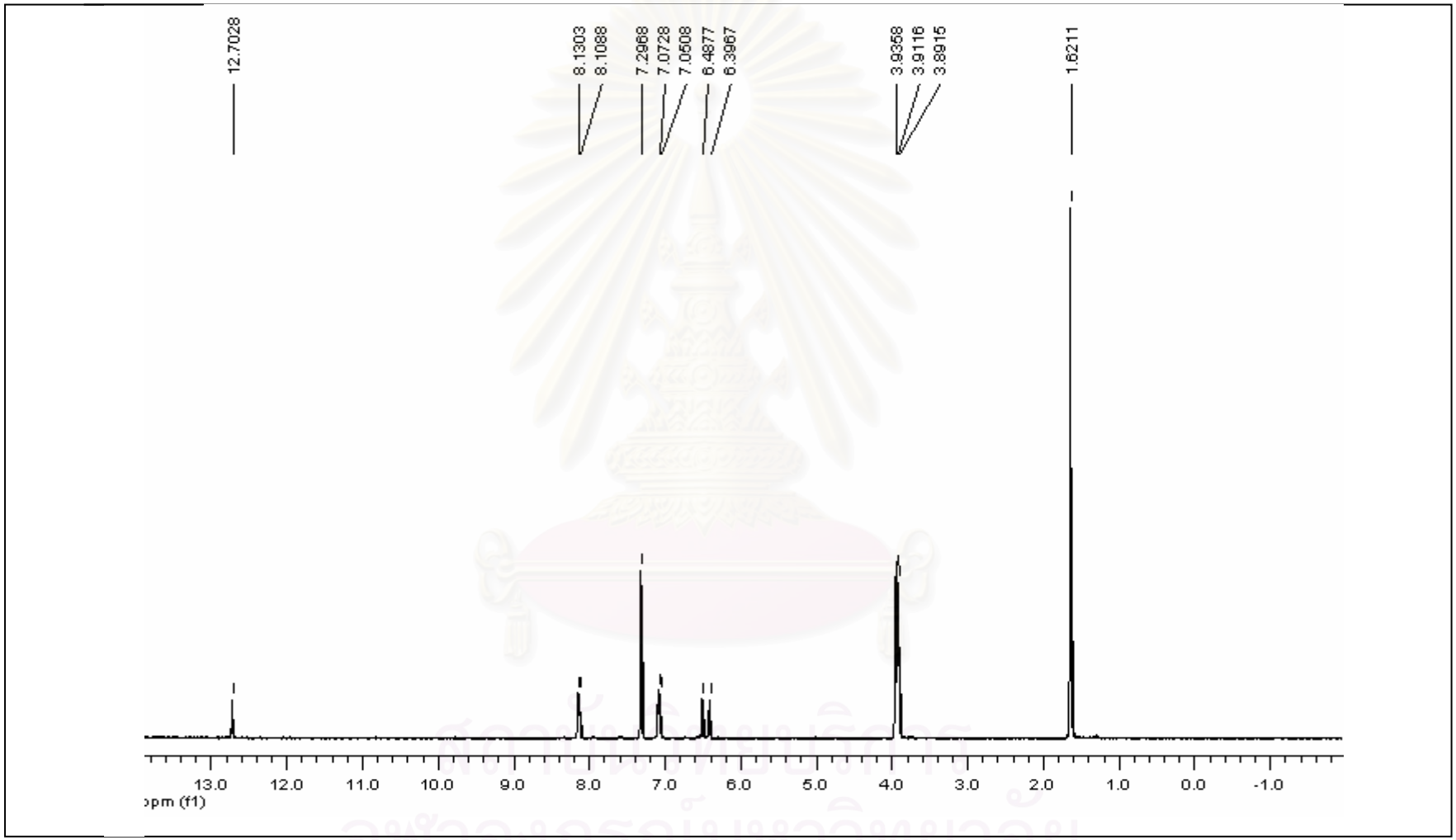

Figure A10 The ^{1}H-NMR spectrum of compound 3

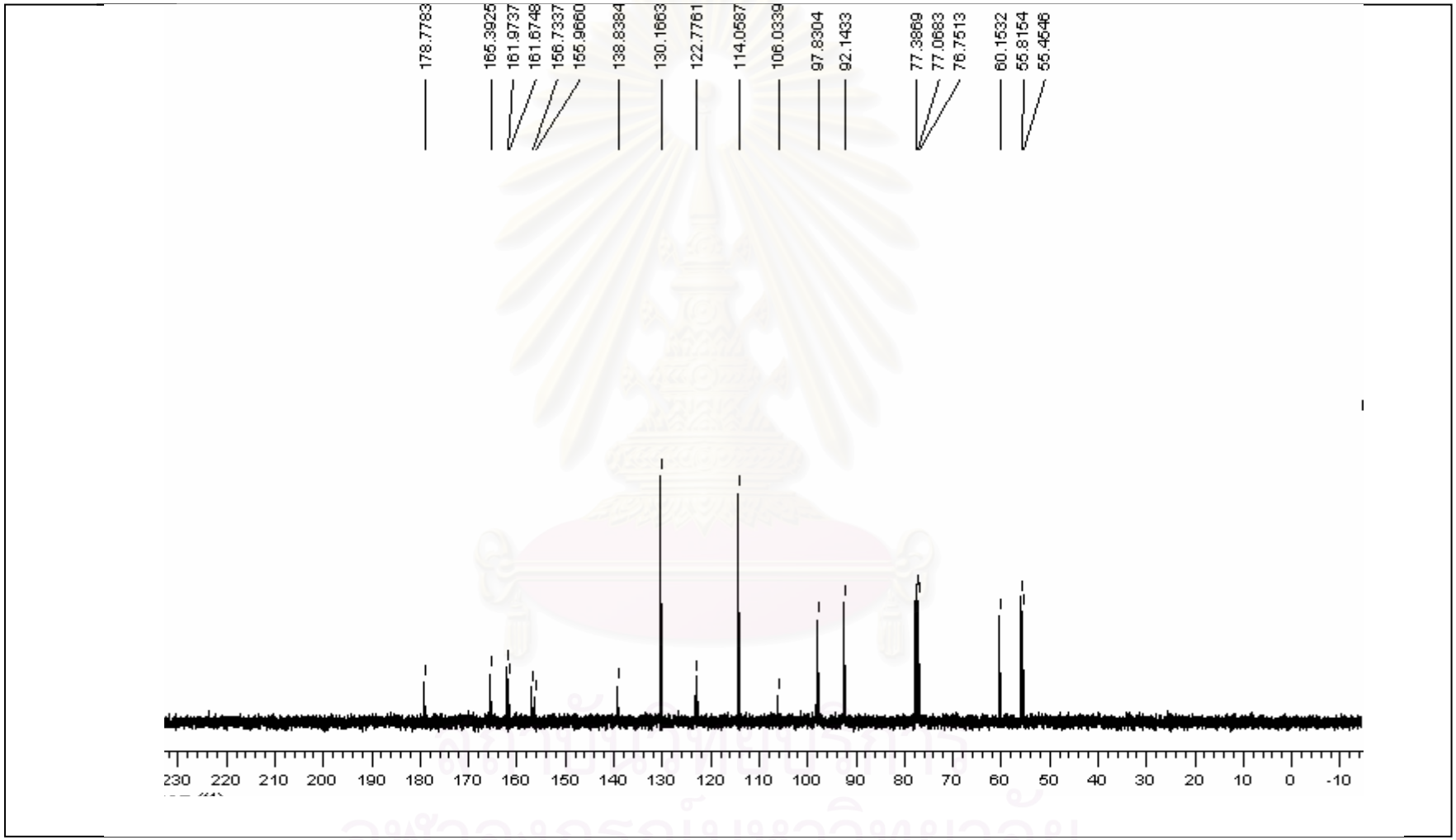

Figure A11 The ^{13}C-NMR spectrum of compound **3**

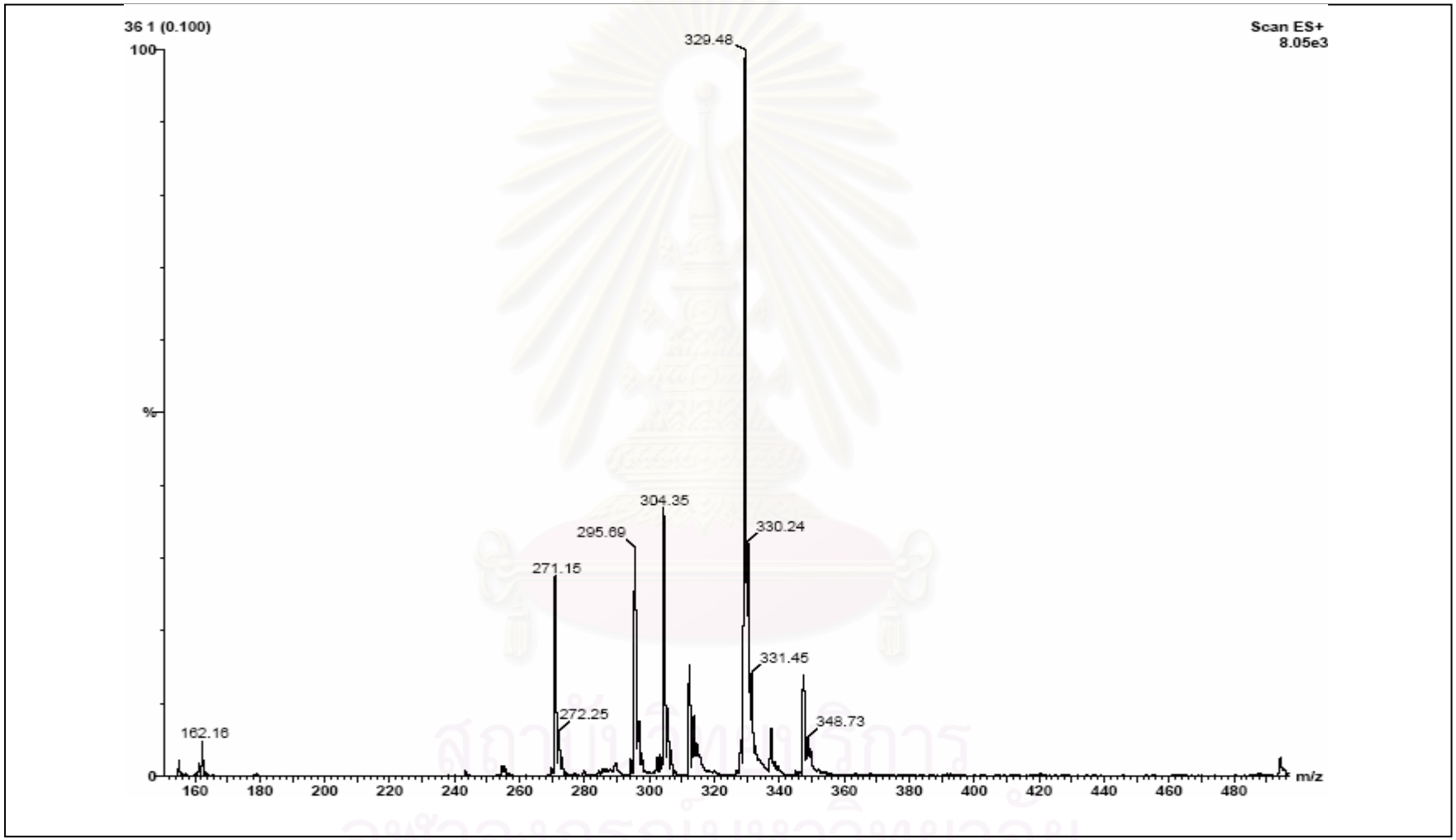

Figure A12 The mass spectrum of compound 3

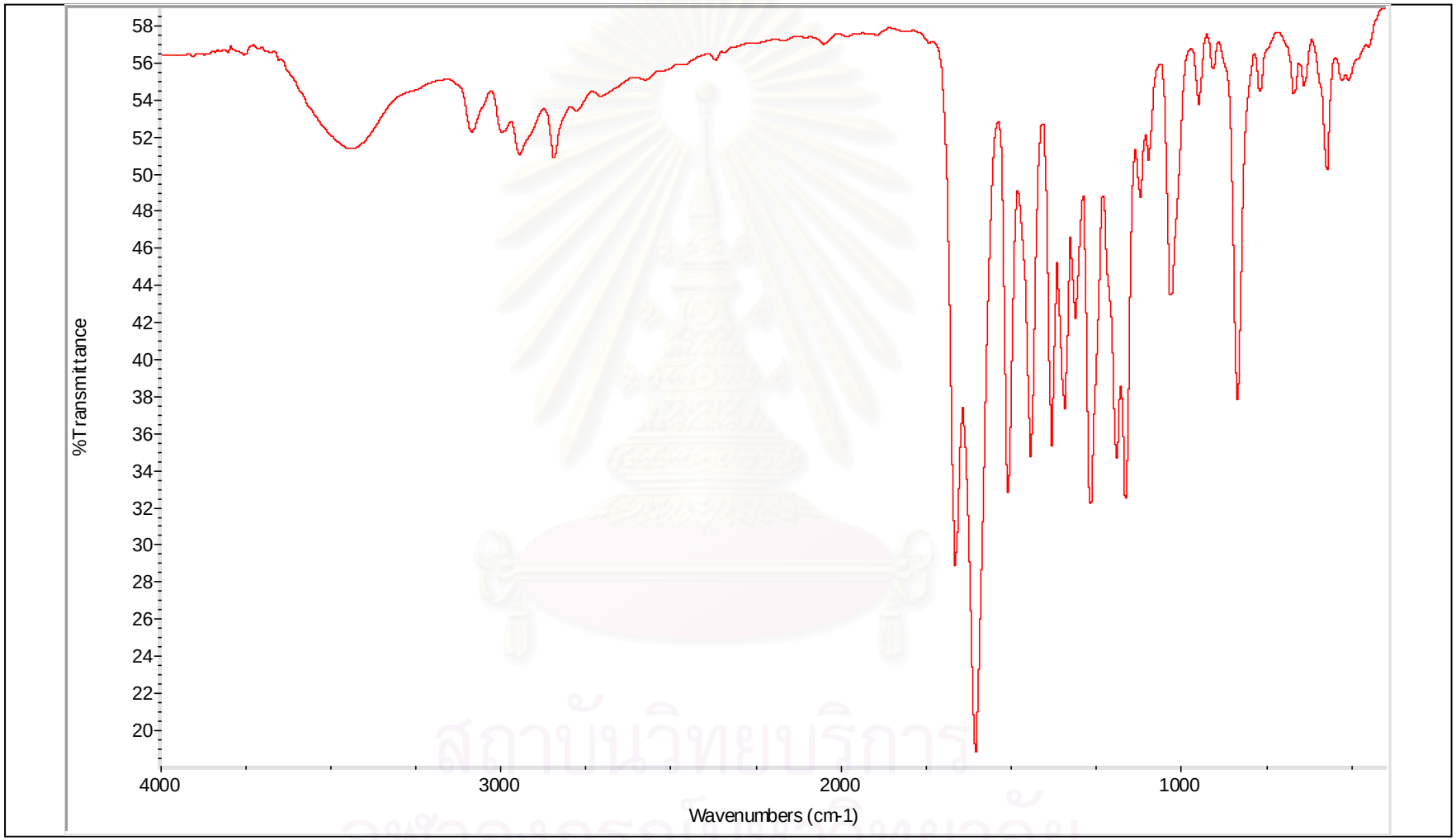

Figure A13 The IR spectrum of compound **4**

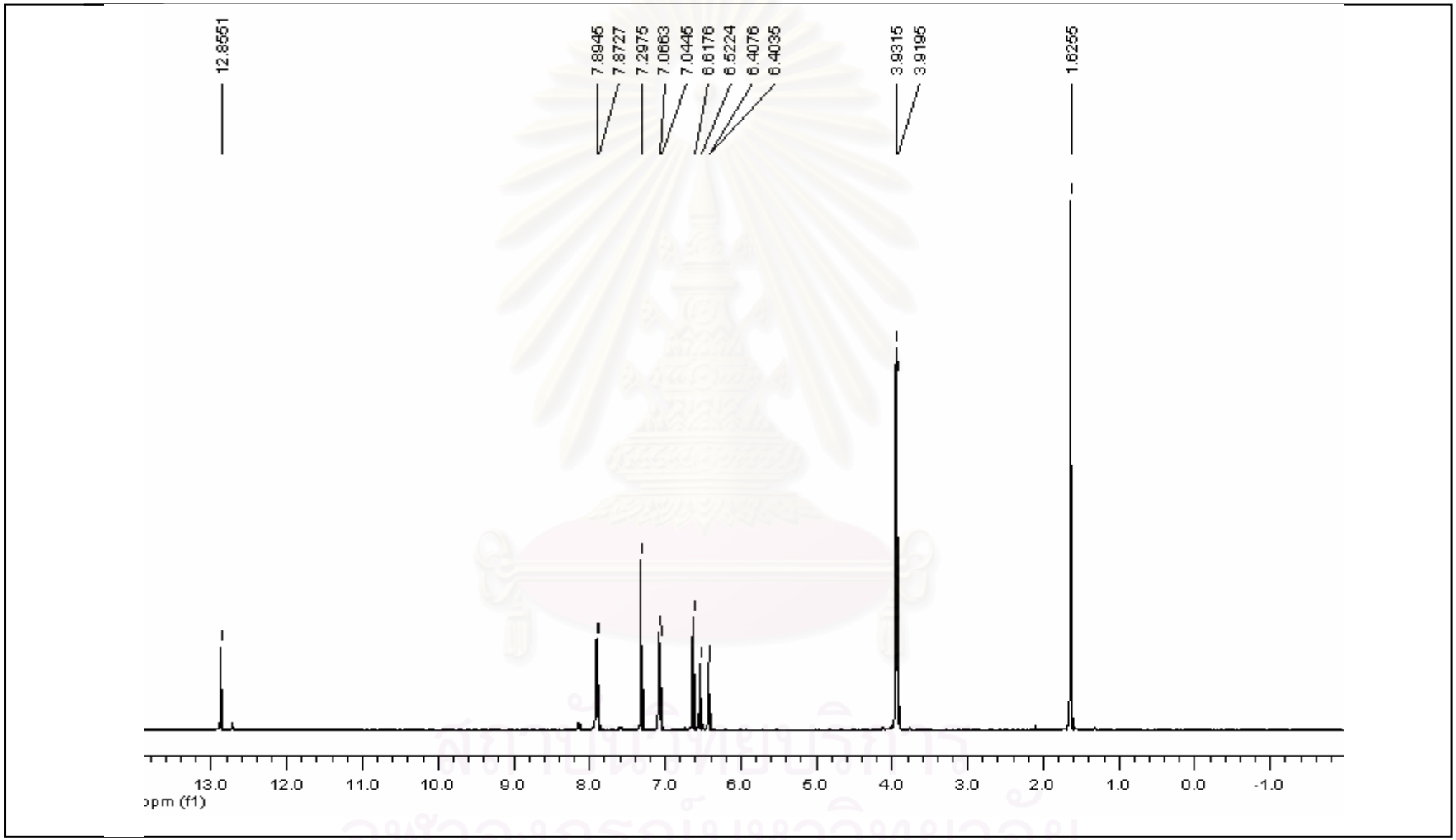

Figure A14 The ^{1}H-NMR spectrum of compound **4**

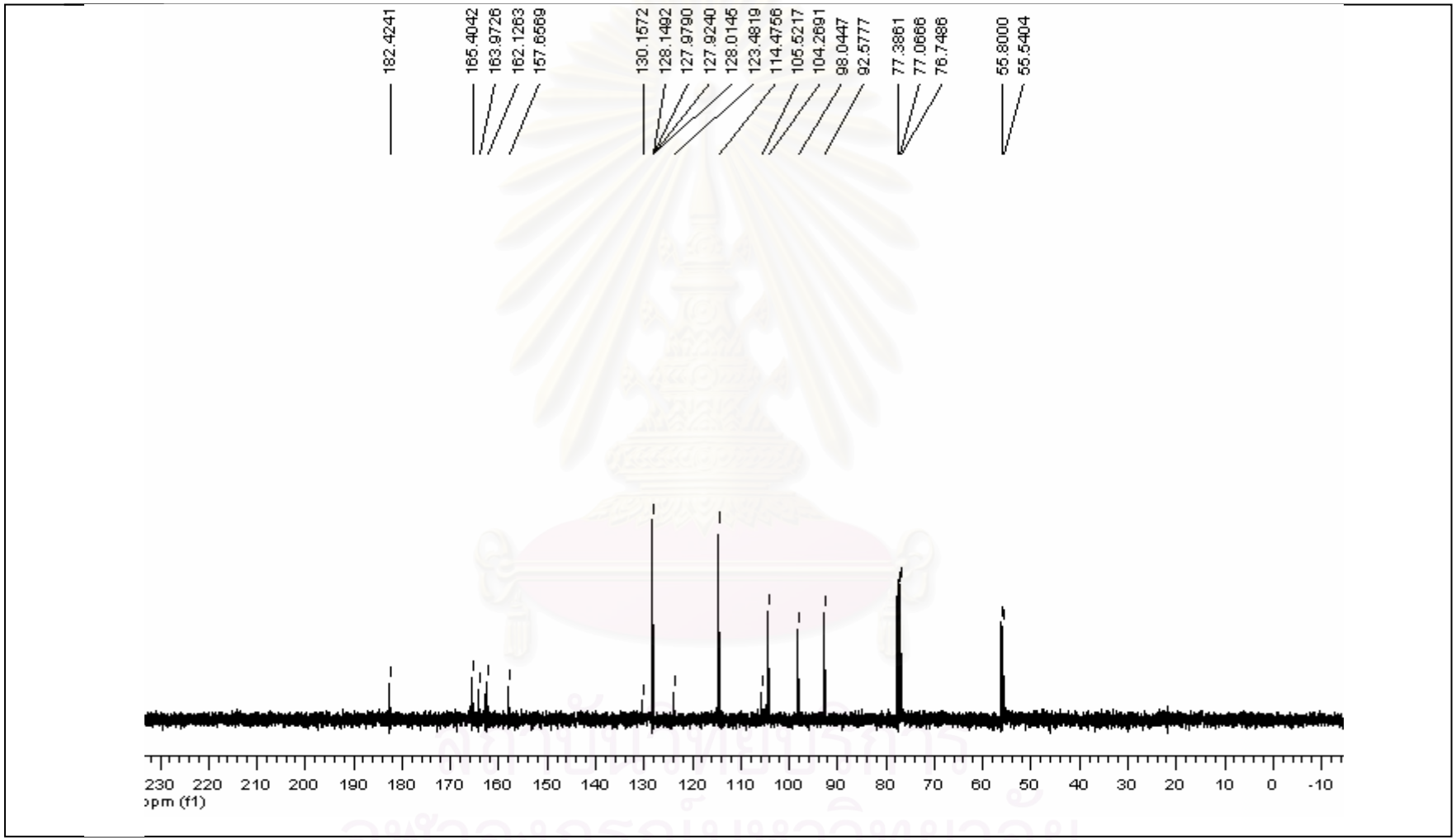

Figure A15 The ^{13}C-NMR spectrum of compound 4

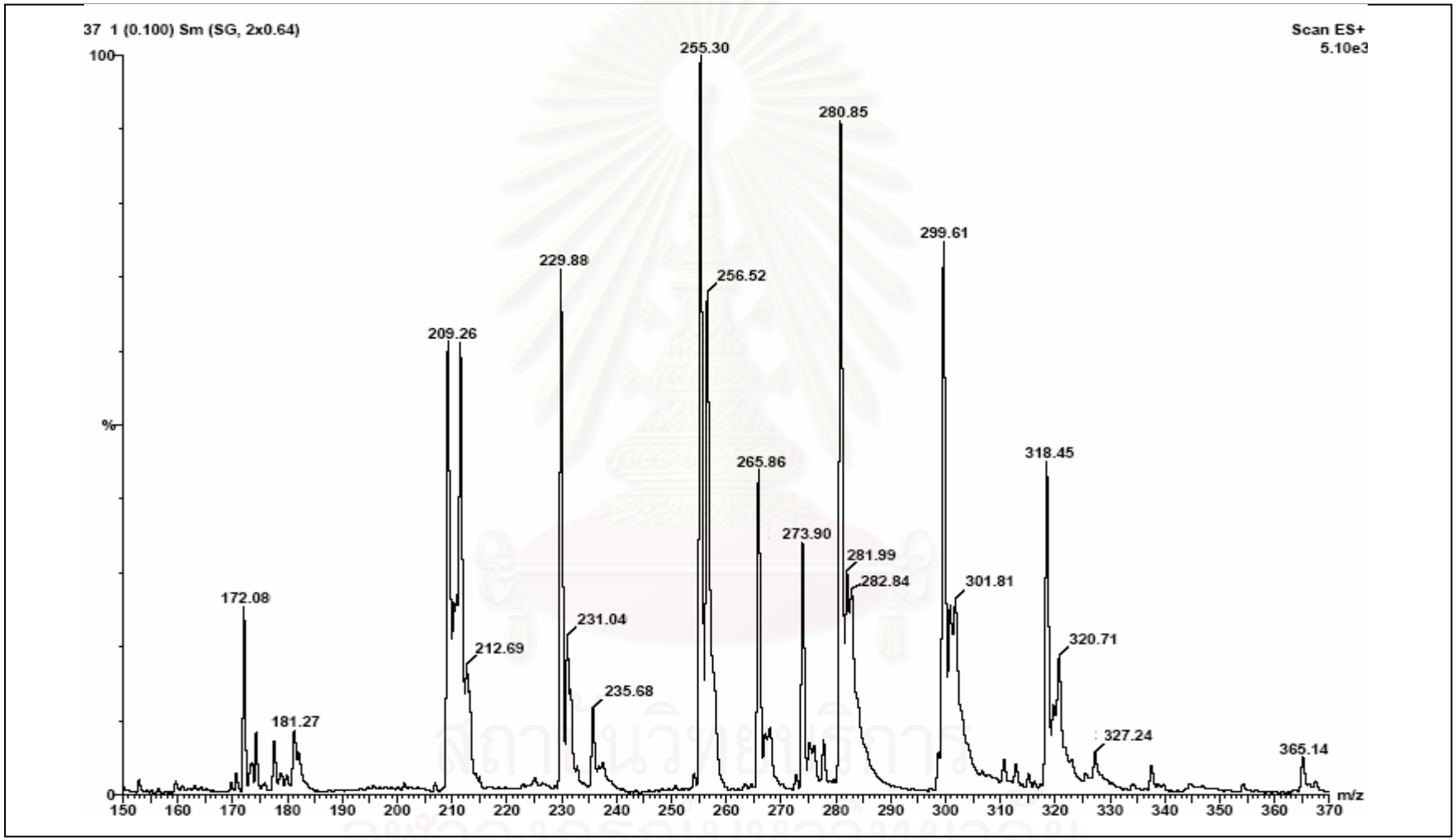

Figure A16 The mass spectrum of compound 4

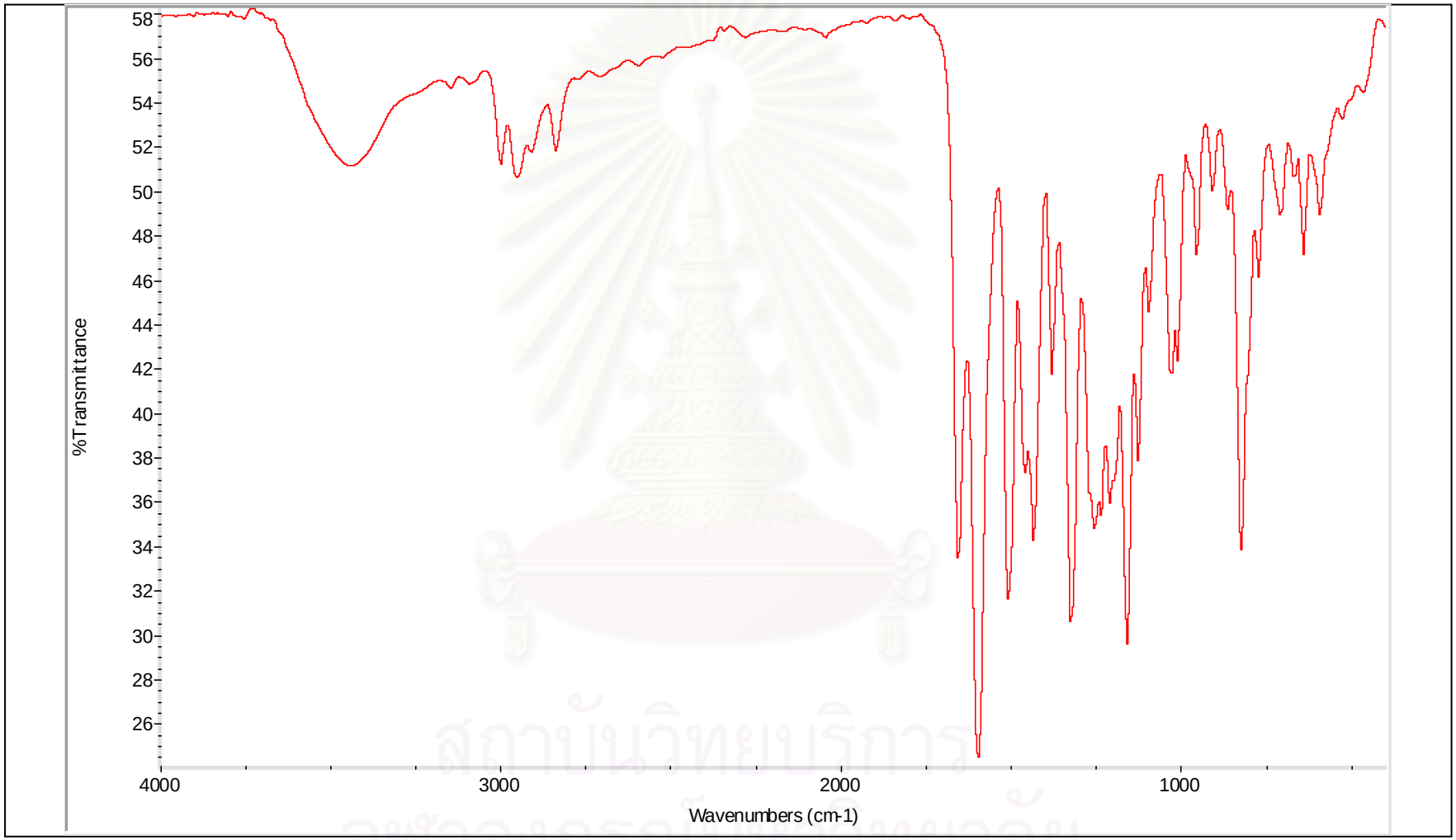

Figure A17 The IR spectrum of compound **5**

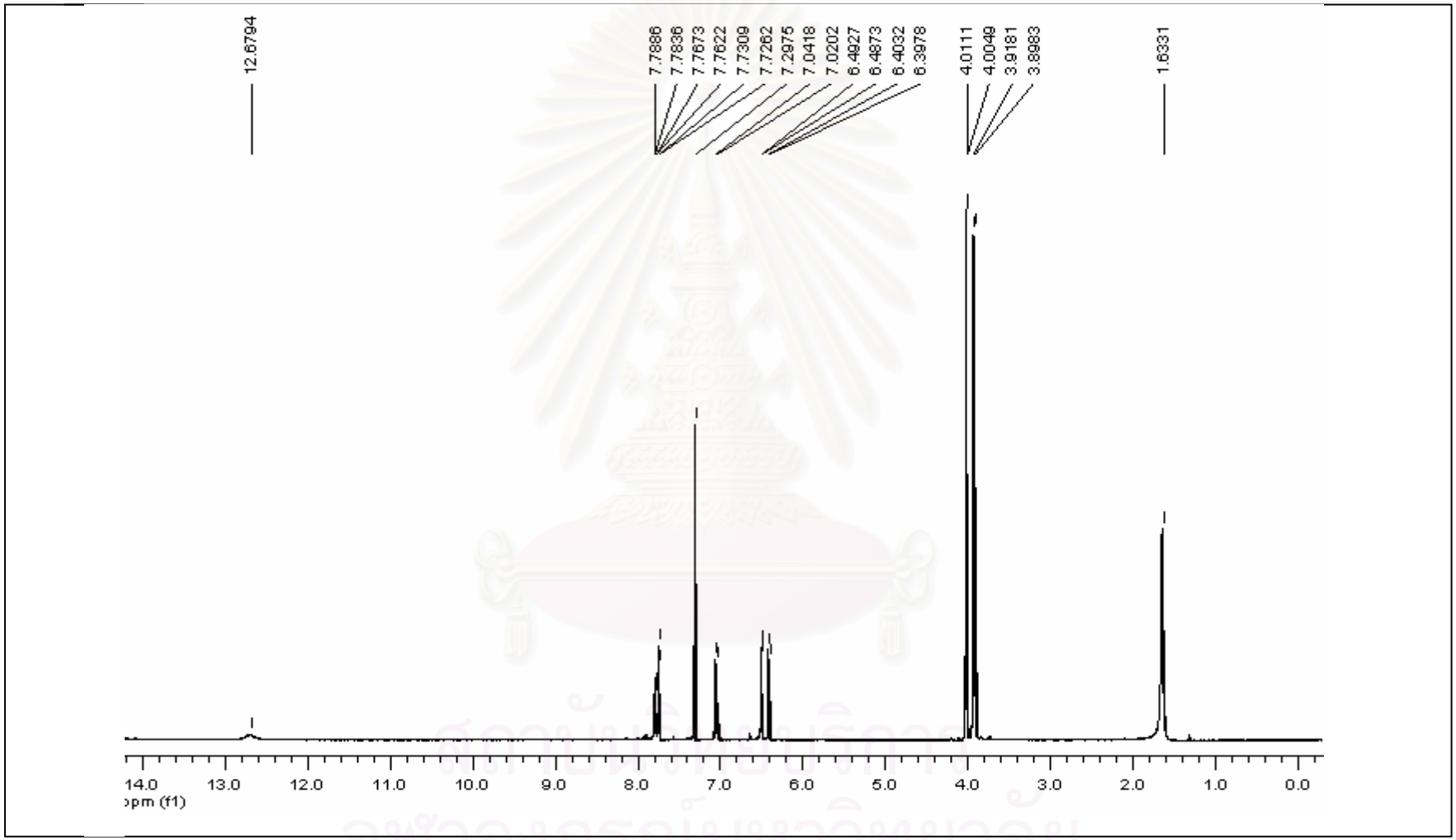

Figure A18 The ^{1}H-NMR spectrum of compound 5

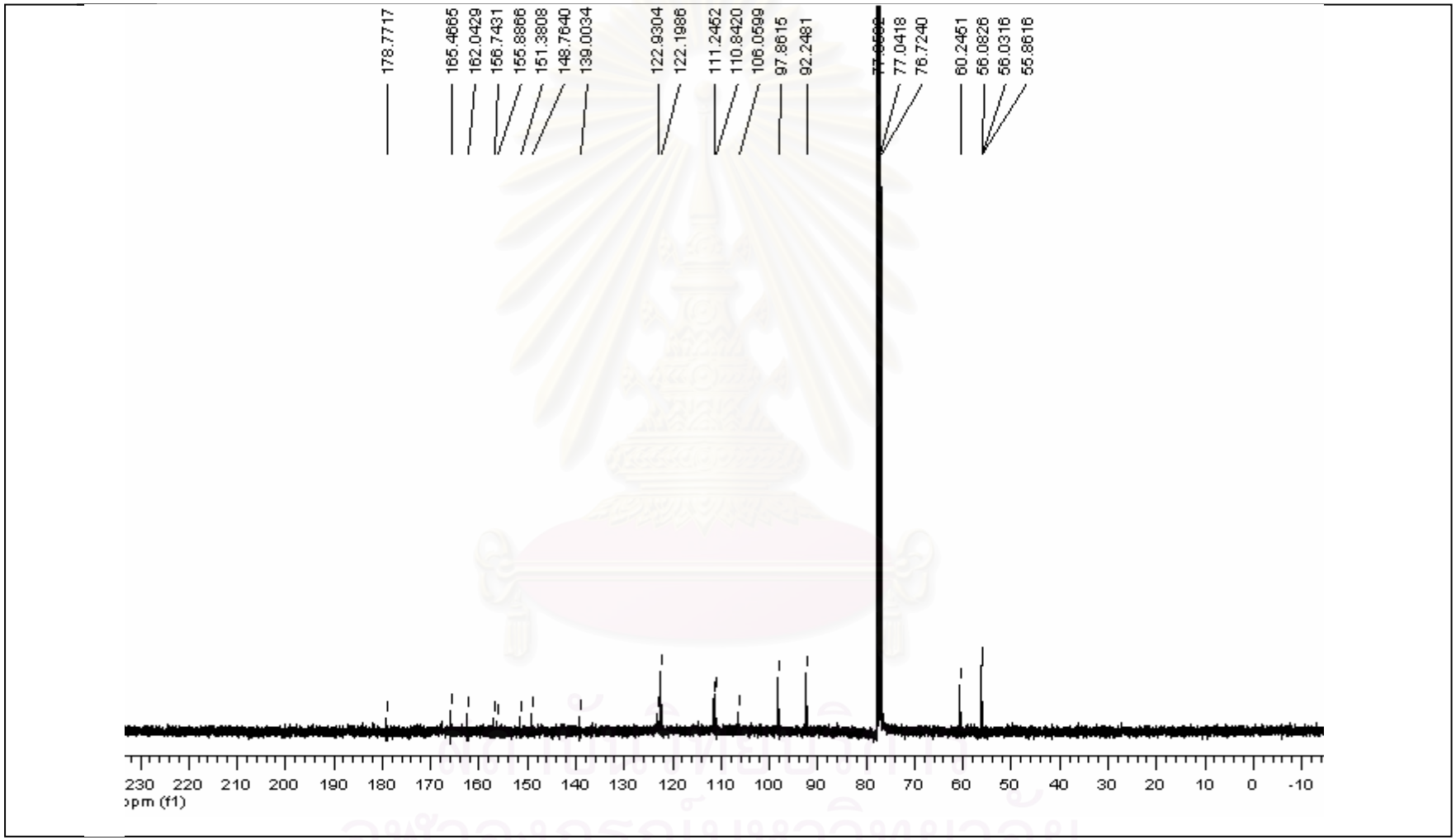

Figure A19 The ^{13}C-NMR spectrum of compound 5

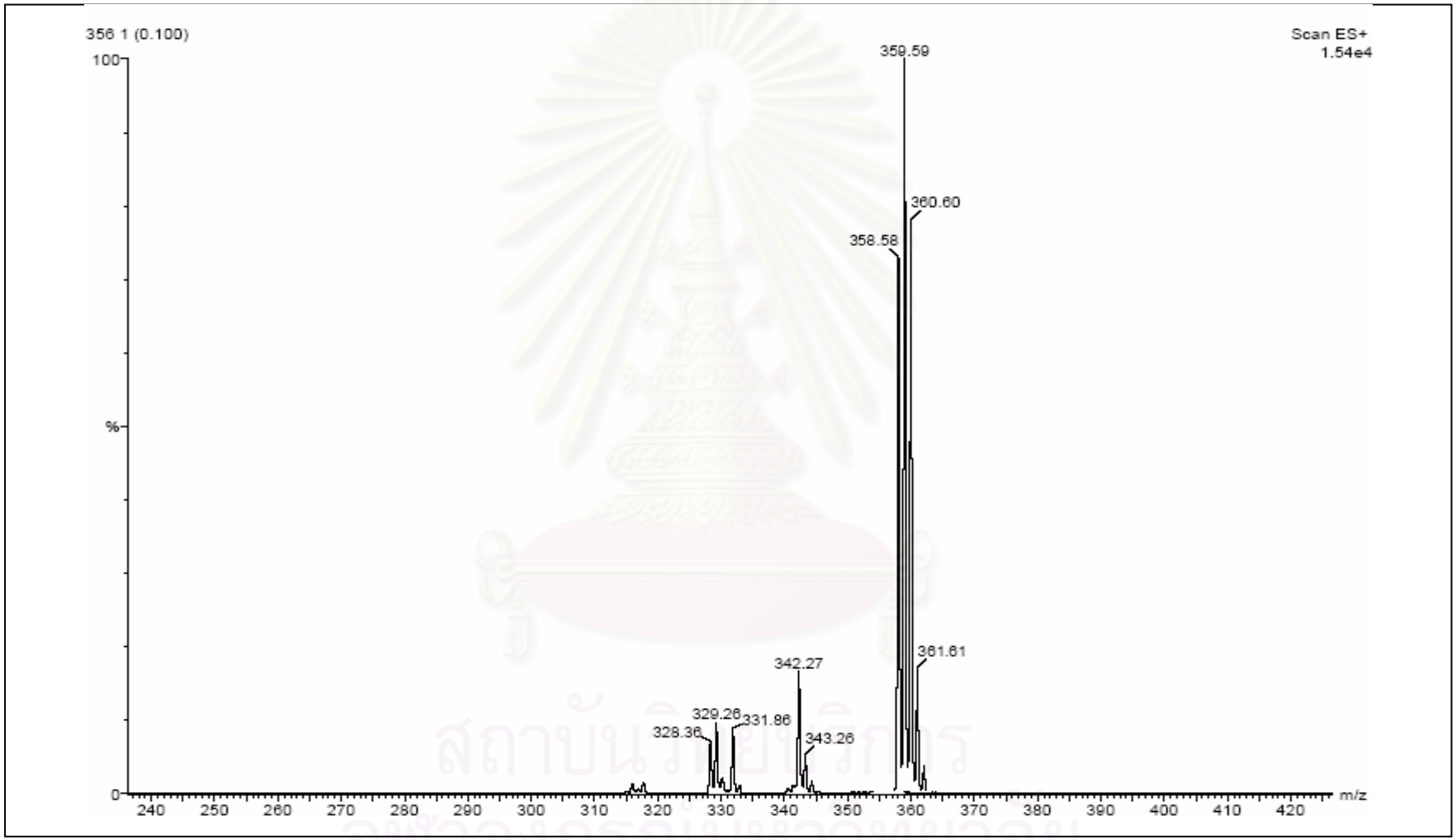

Figure A20 The mass spectrum of compound **5**

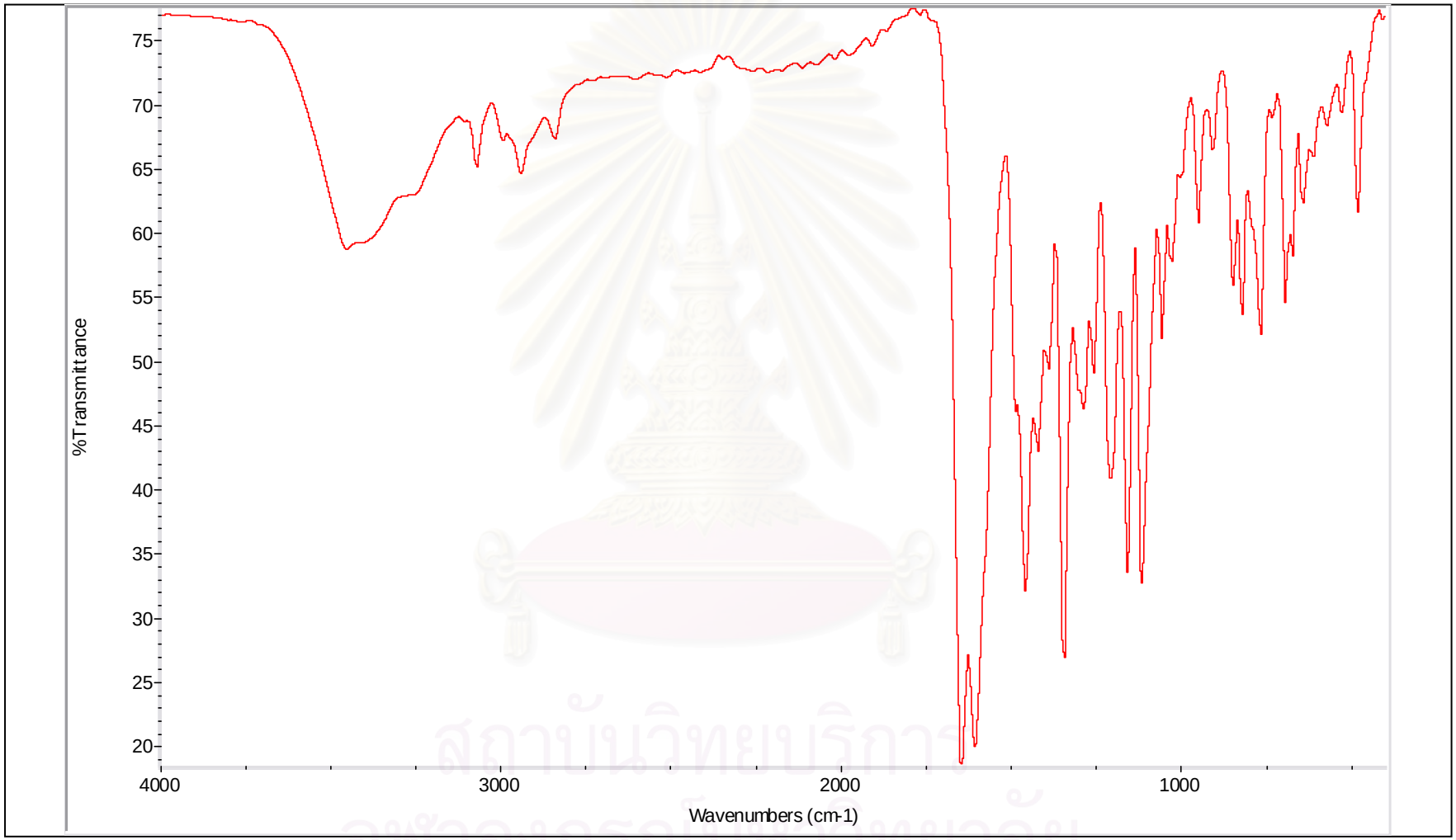

Figure A21 The IR spectrum of compound **6**

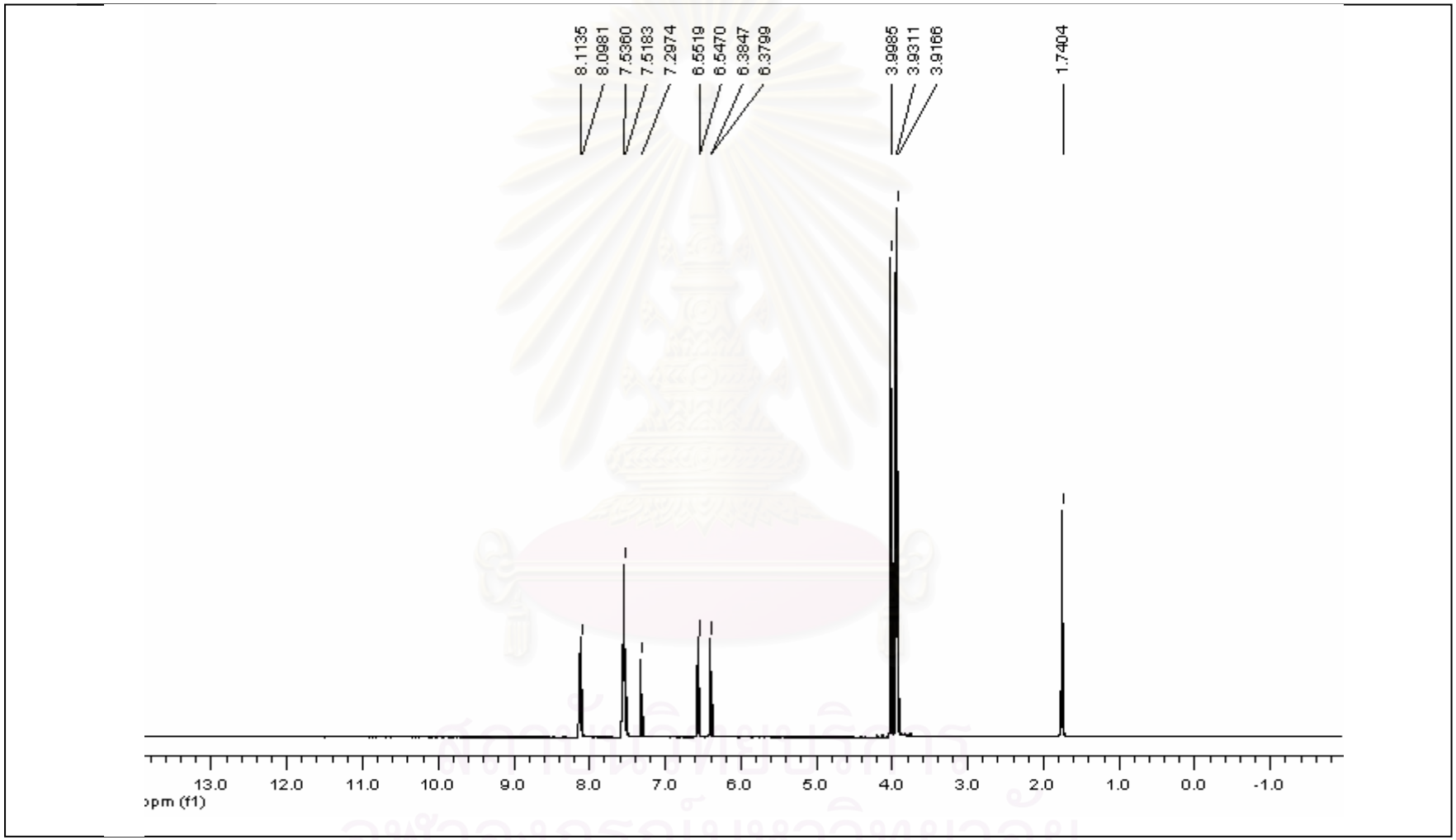

Figure A22 The ^{1}H-NMR spectrum of compound 6

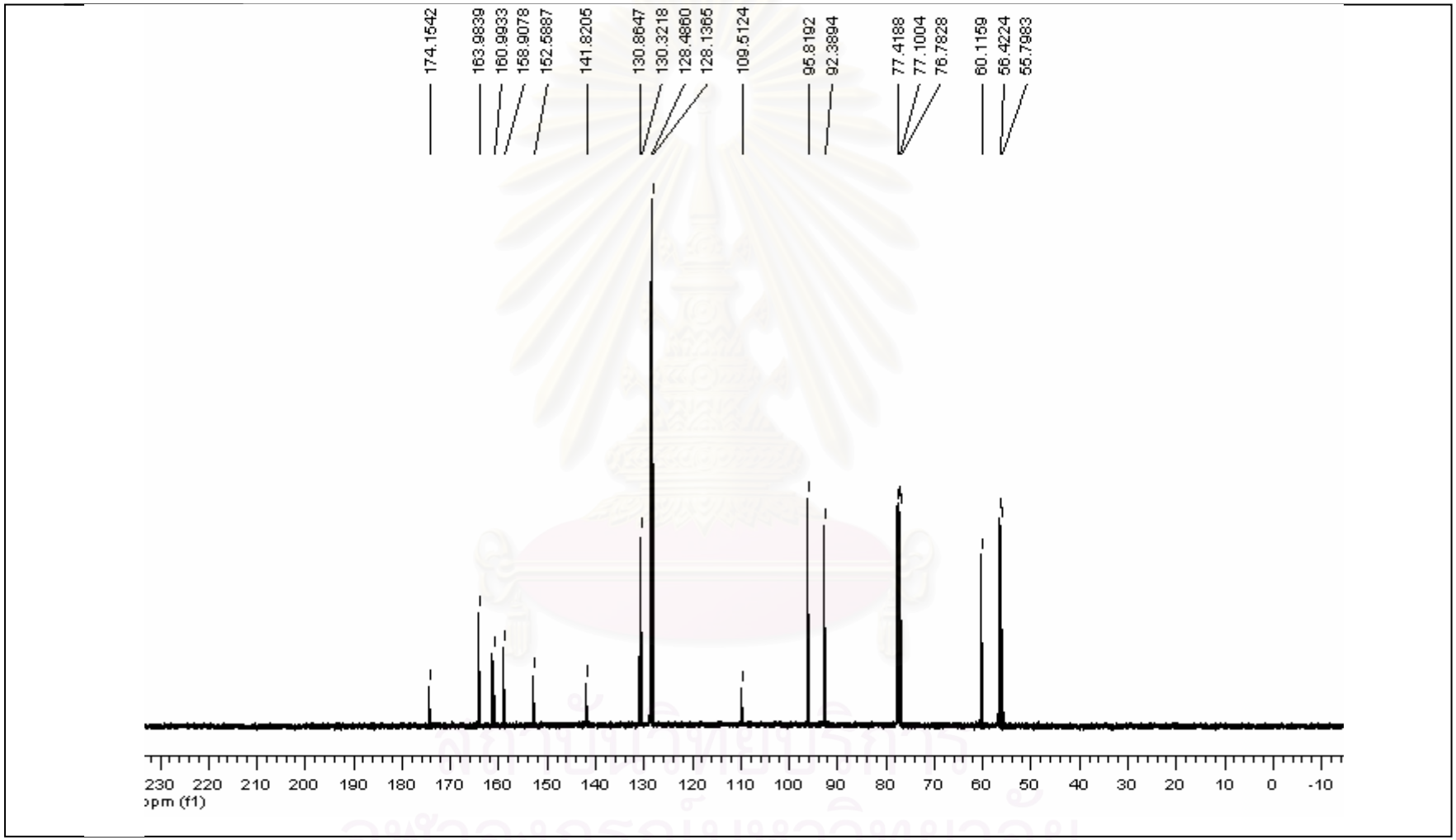

Figure A23 The ^{13}C-NMR spectrum of compound **6**

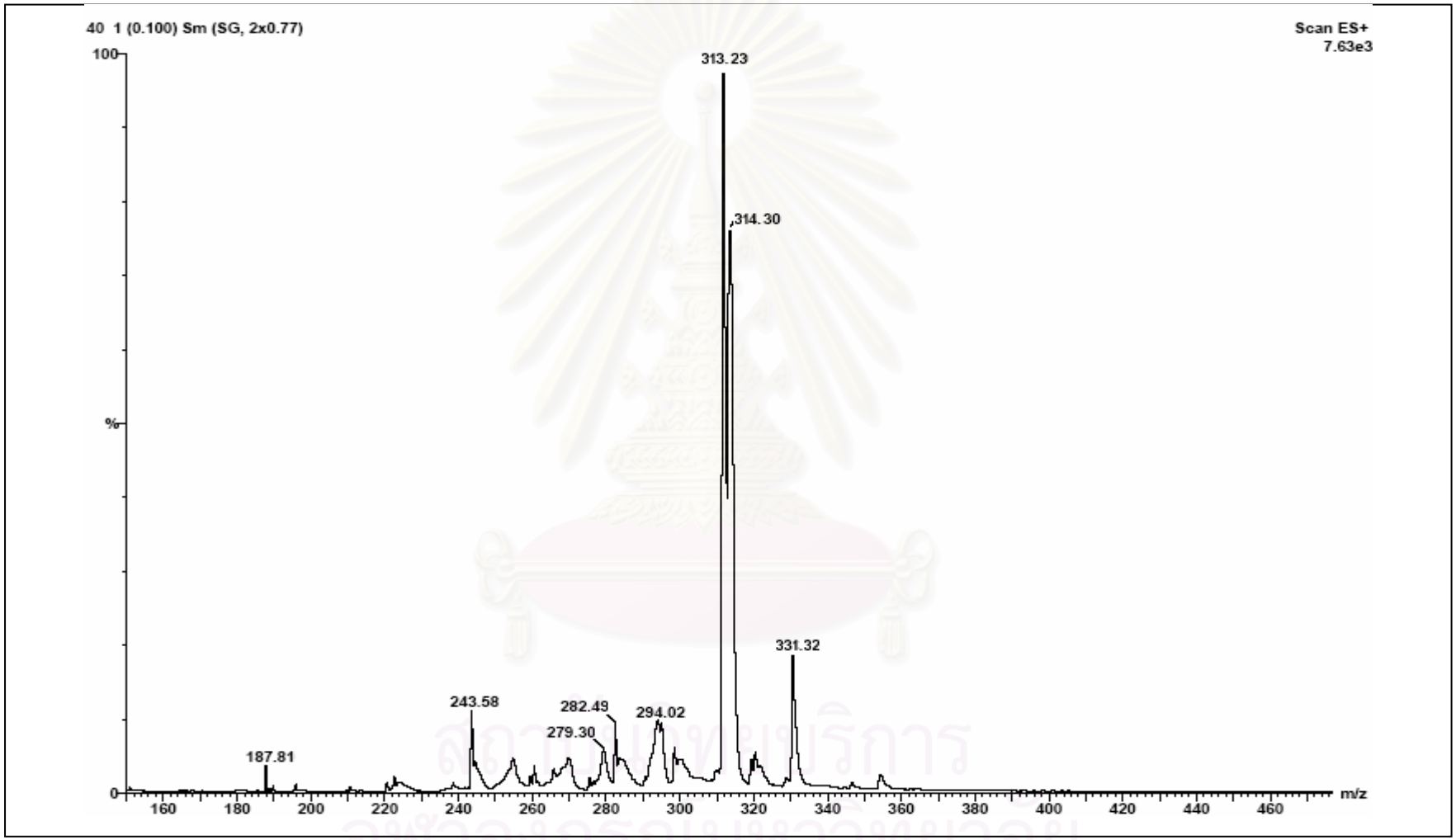

Figure A24 The mass spectrum of compound 6

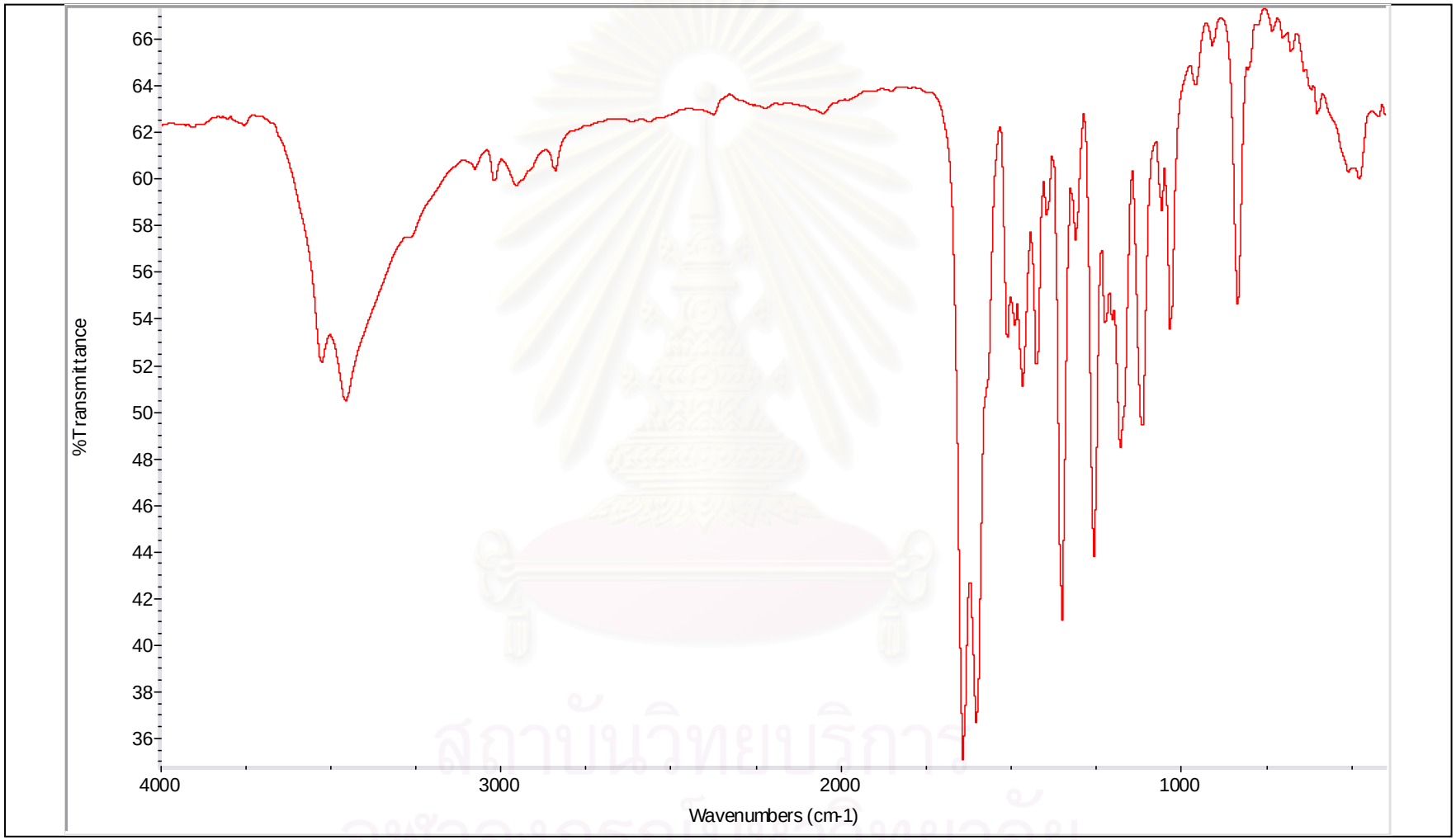

Figure A25 The IR spectrum of compound **7**

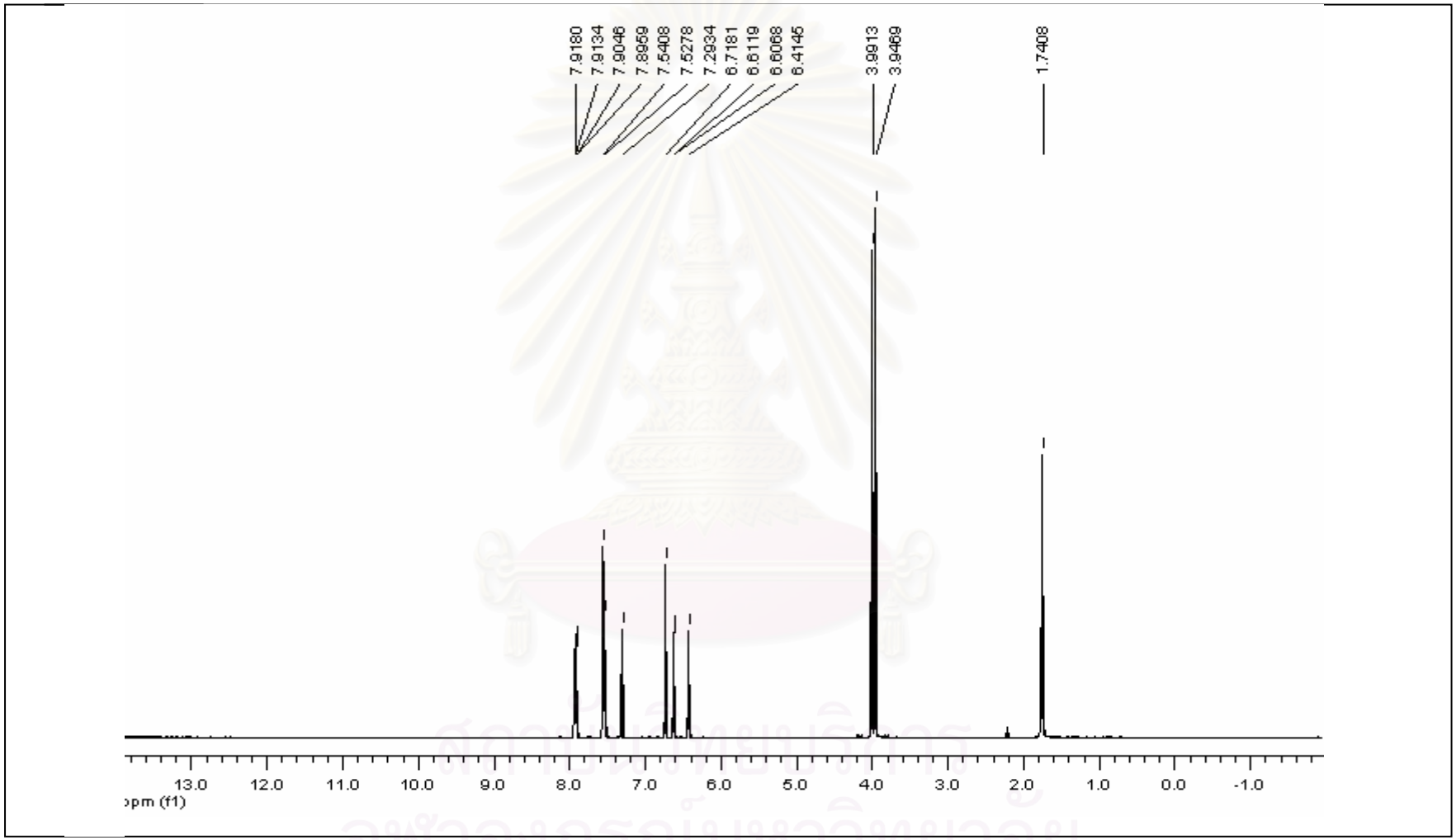

Figure A26 The ^{1}H-NMR spectrum of compound 7

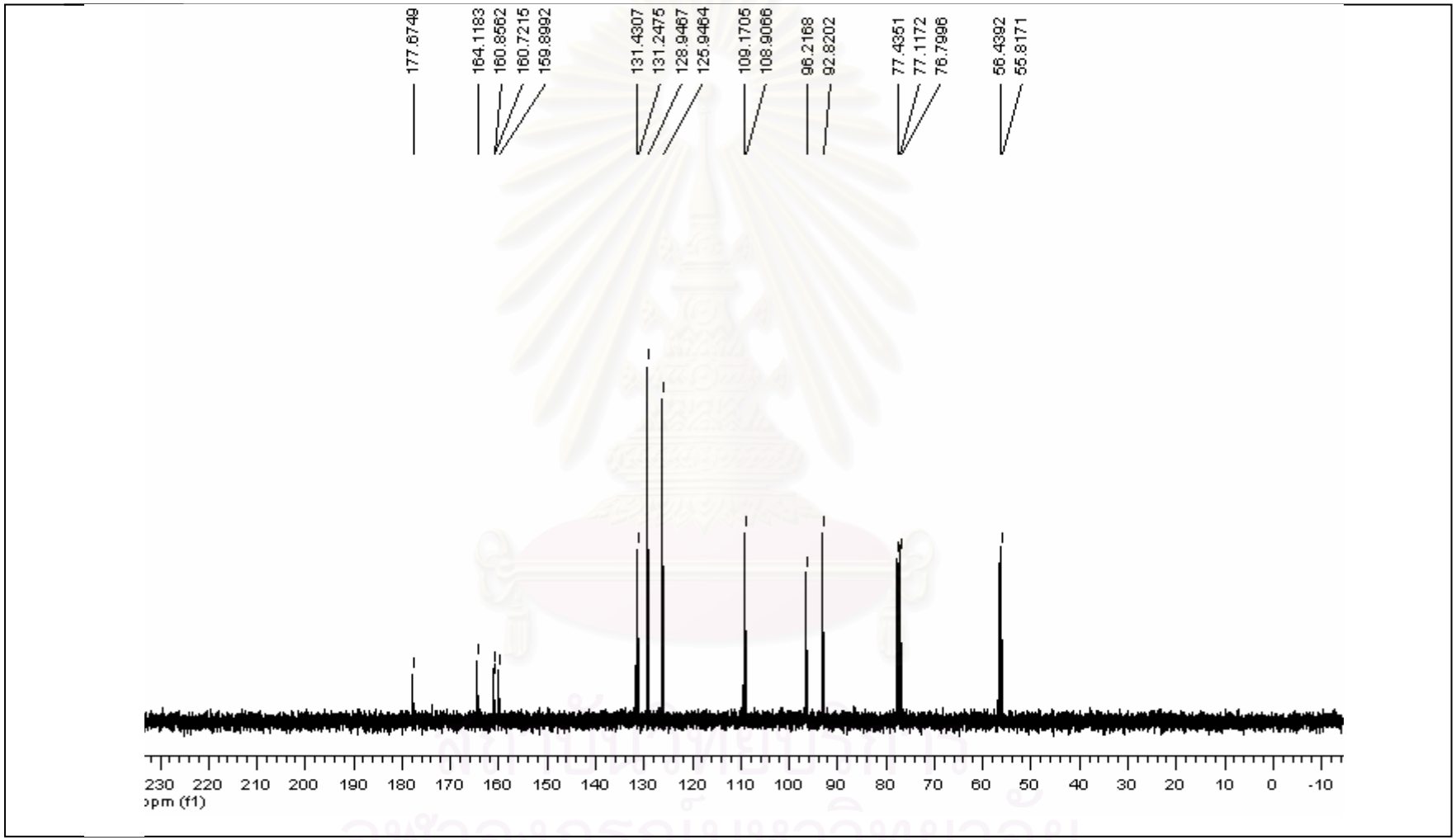

Figure A27 The ^{13}C-NMR spectrum of compound **7**

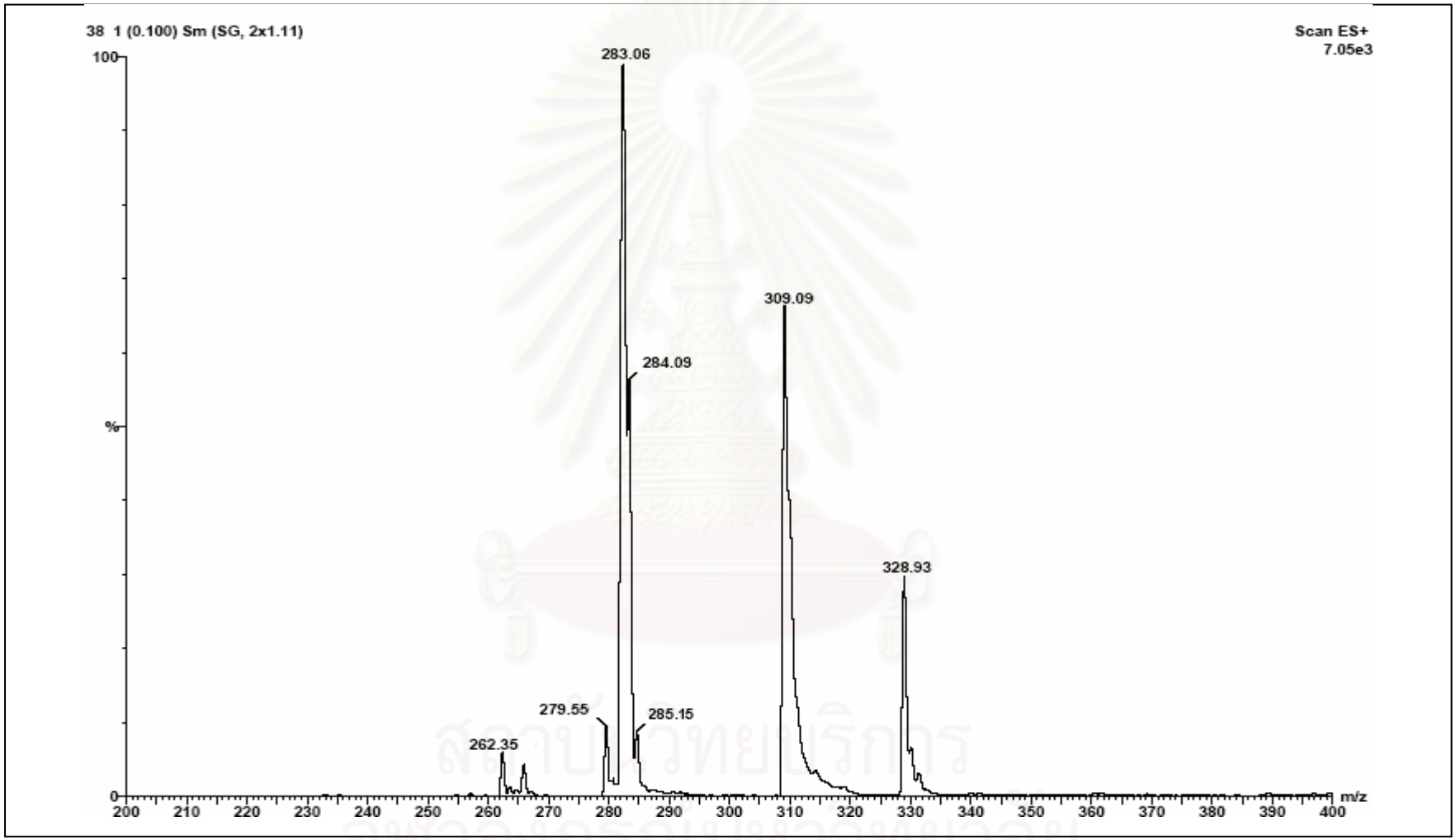

Figure A28 The mass spectrum of compound 7

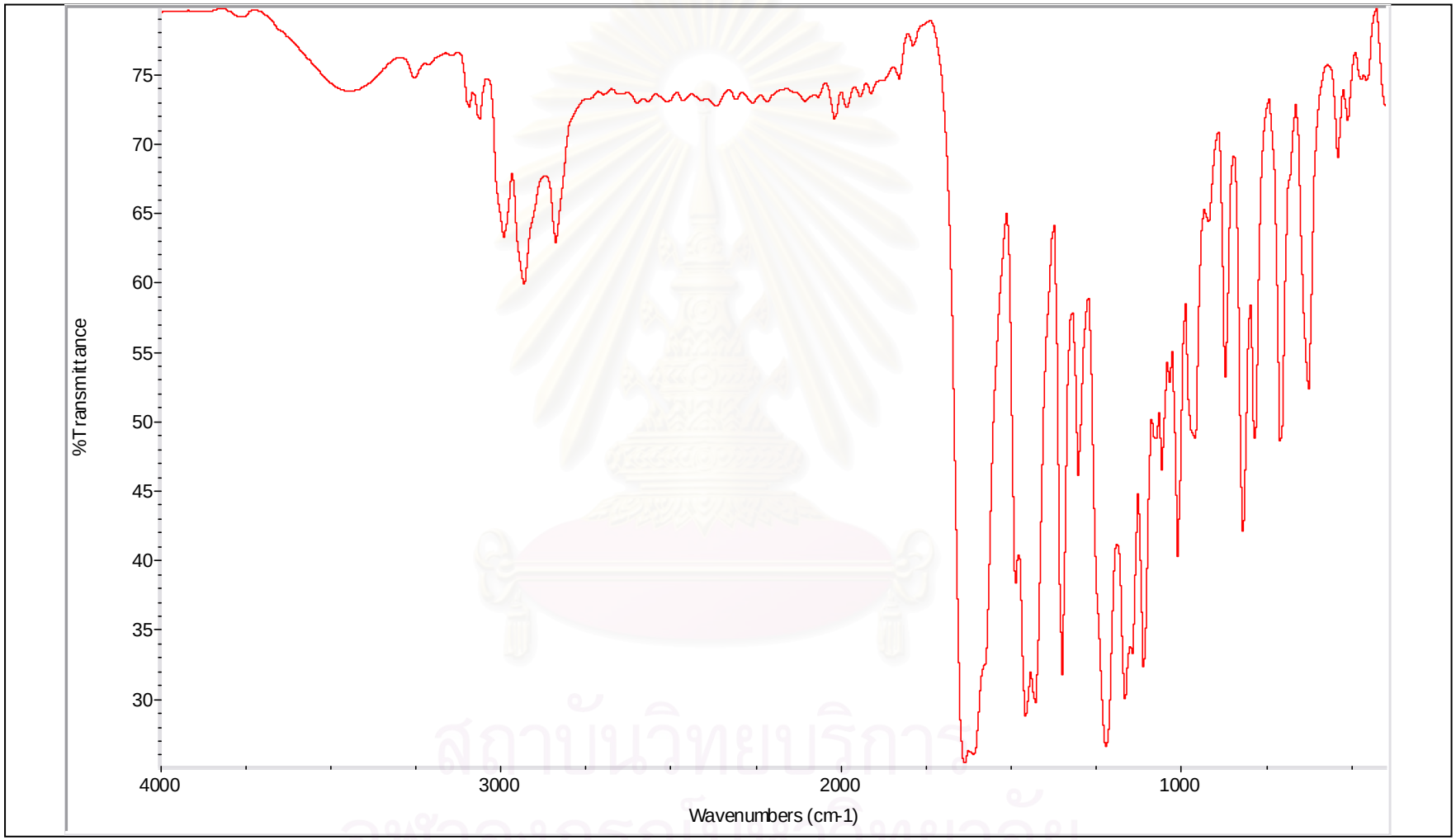

Figure A29 The IR spectrum of compound **8**

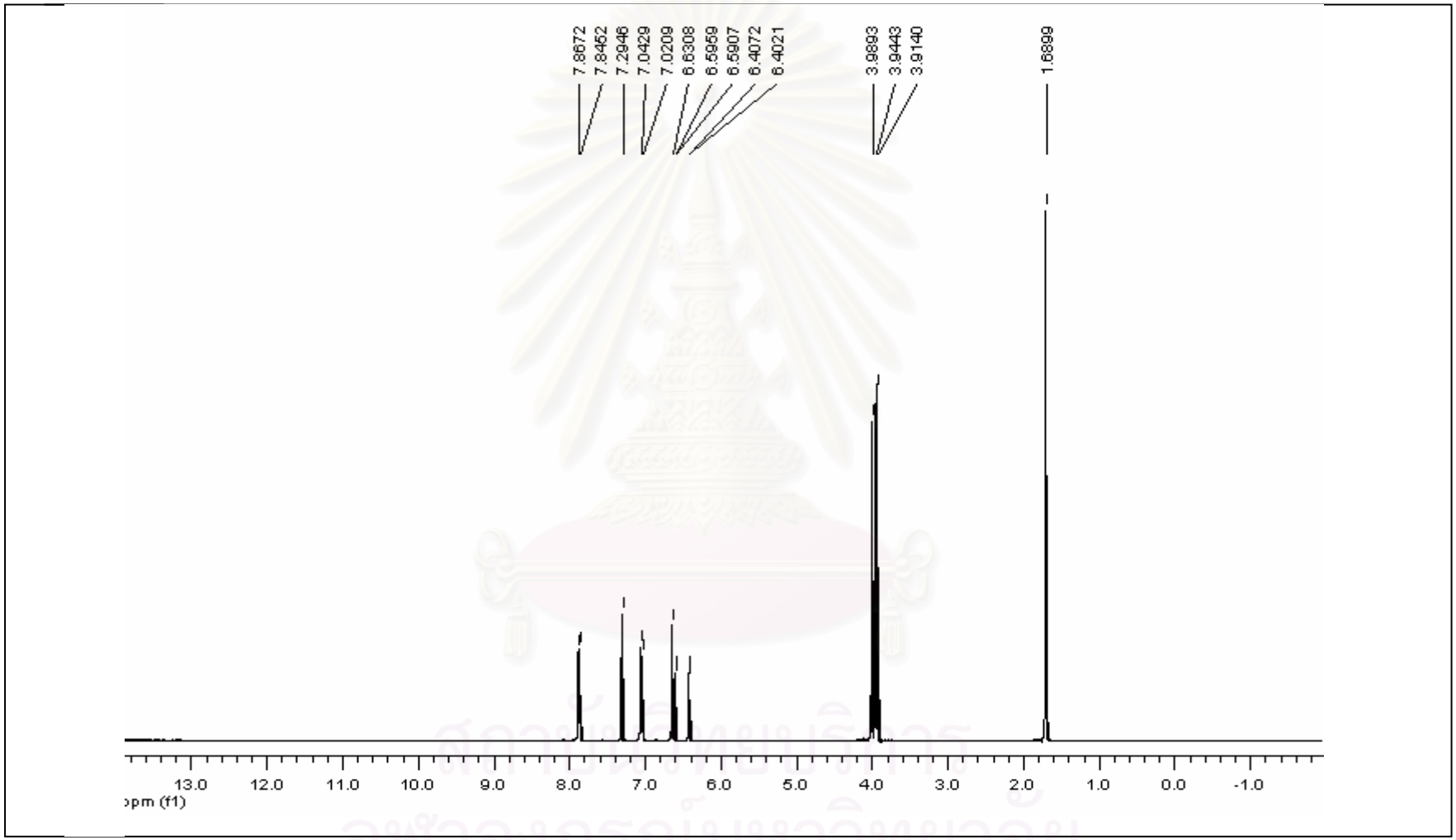

Figure A30 The ^{1}H-NMR spectrum of compound 8

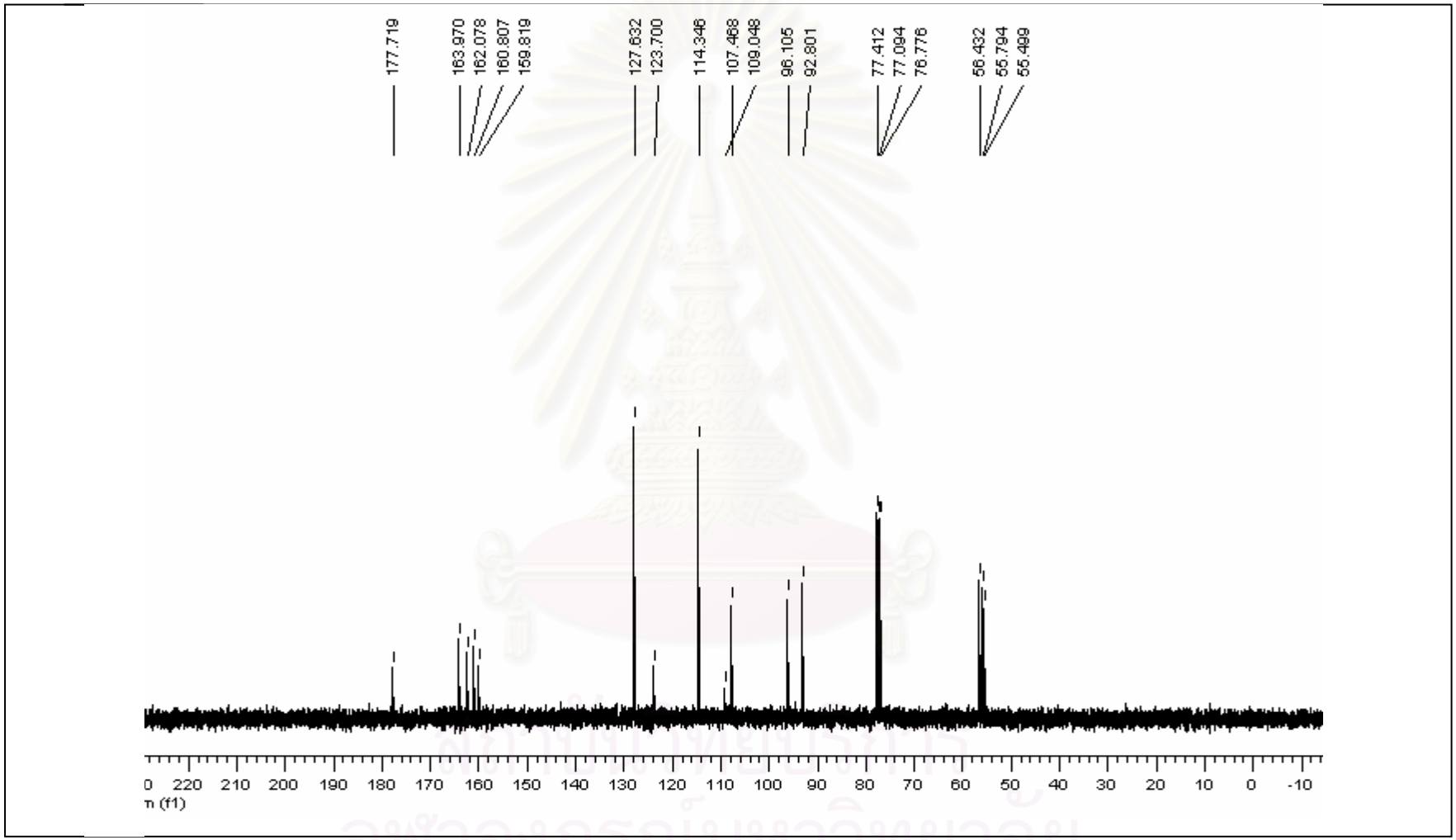

Figure A31 The ^{13}C-NMR spectrum of compound **8**

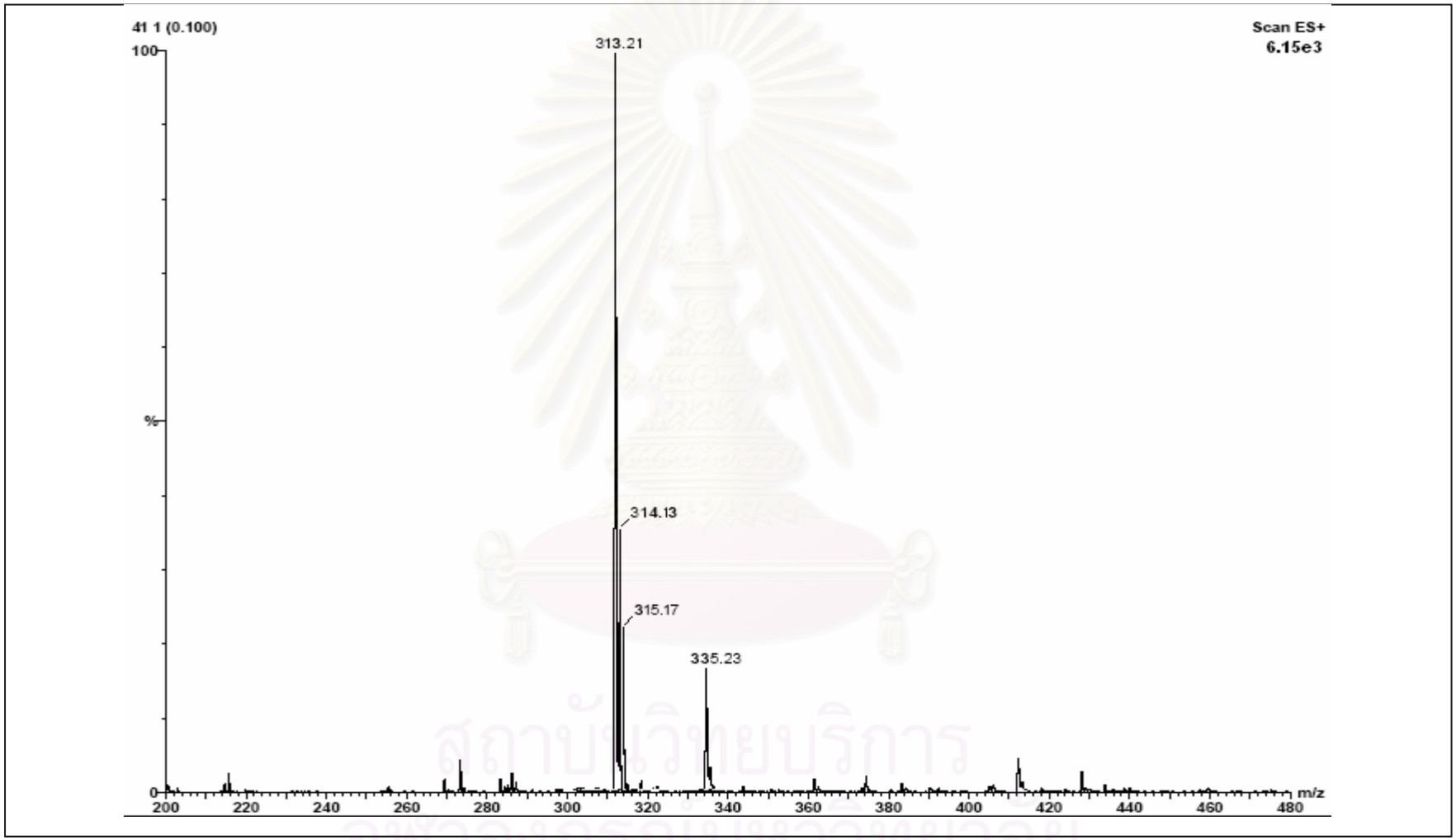

Figure A32 The mass spectrum of compound 8

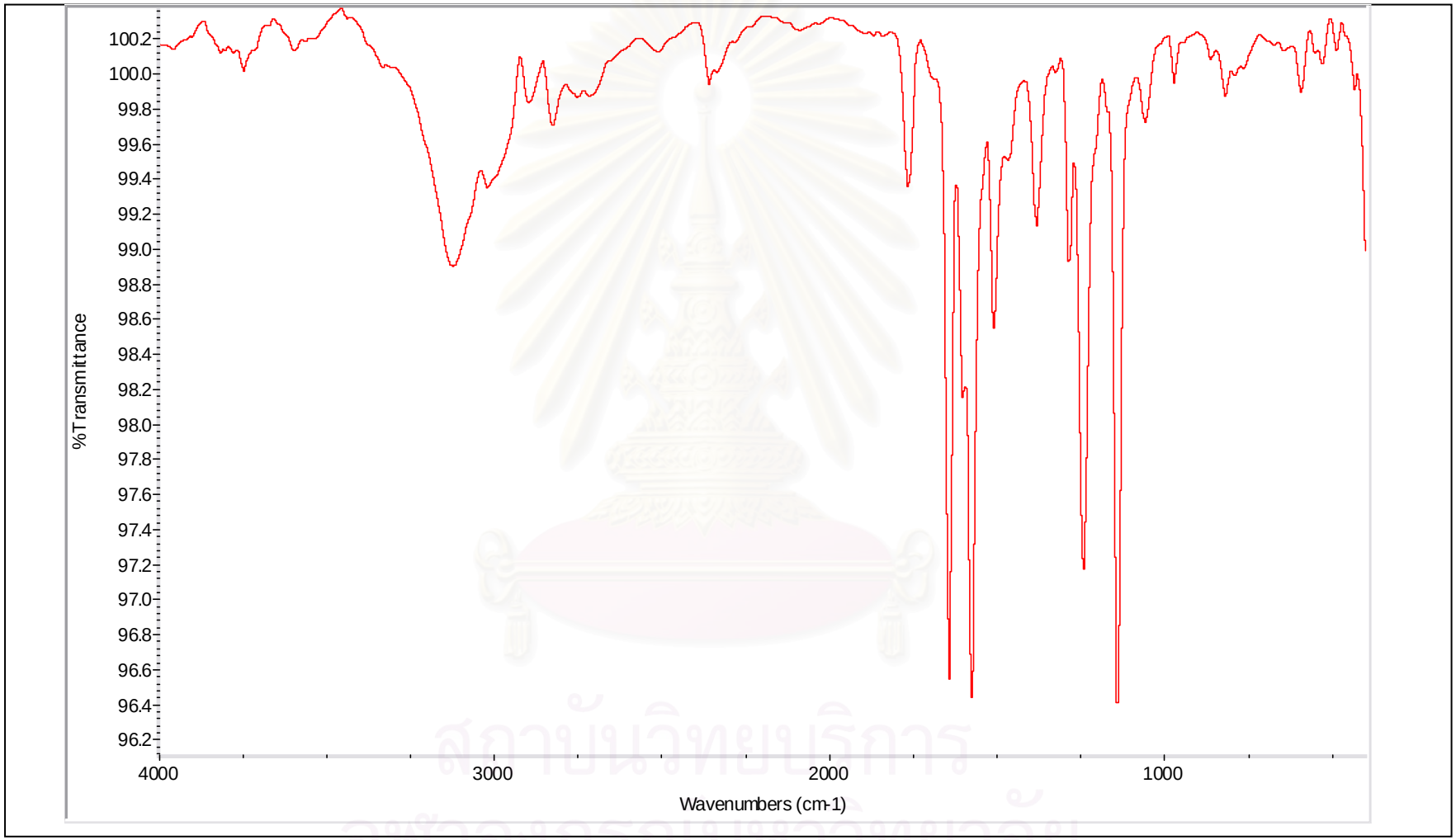

Figure A33 The IR spectrum of compound **9**

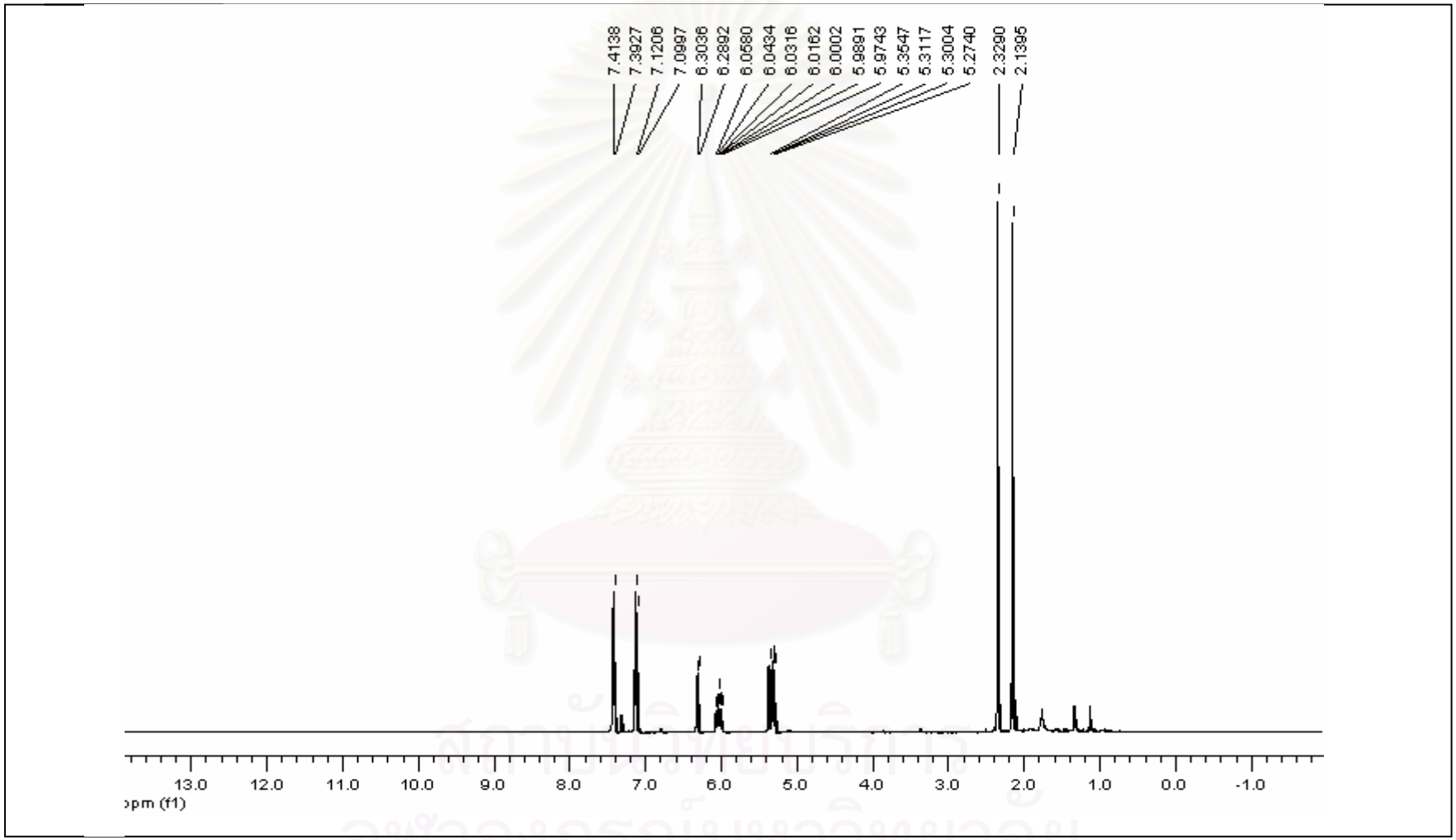

Figure A34 The ^{1}H-NMR spectrum of compound 9

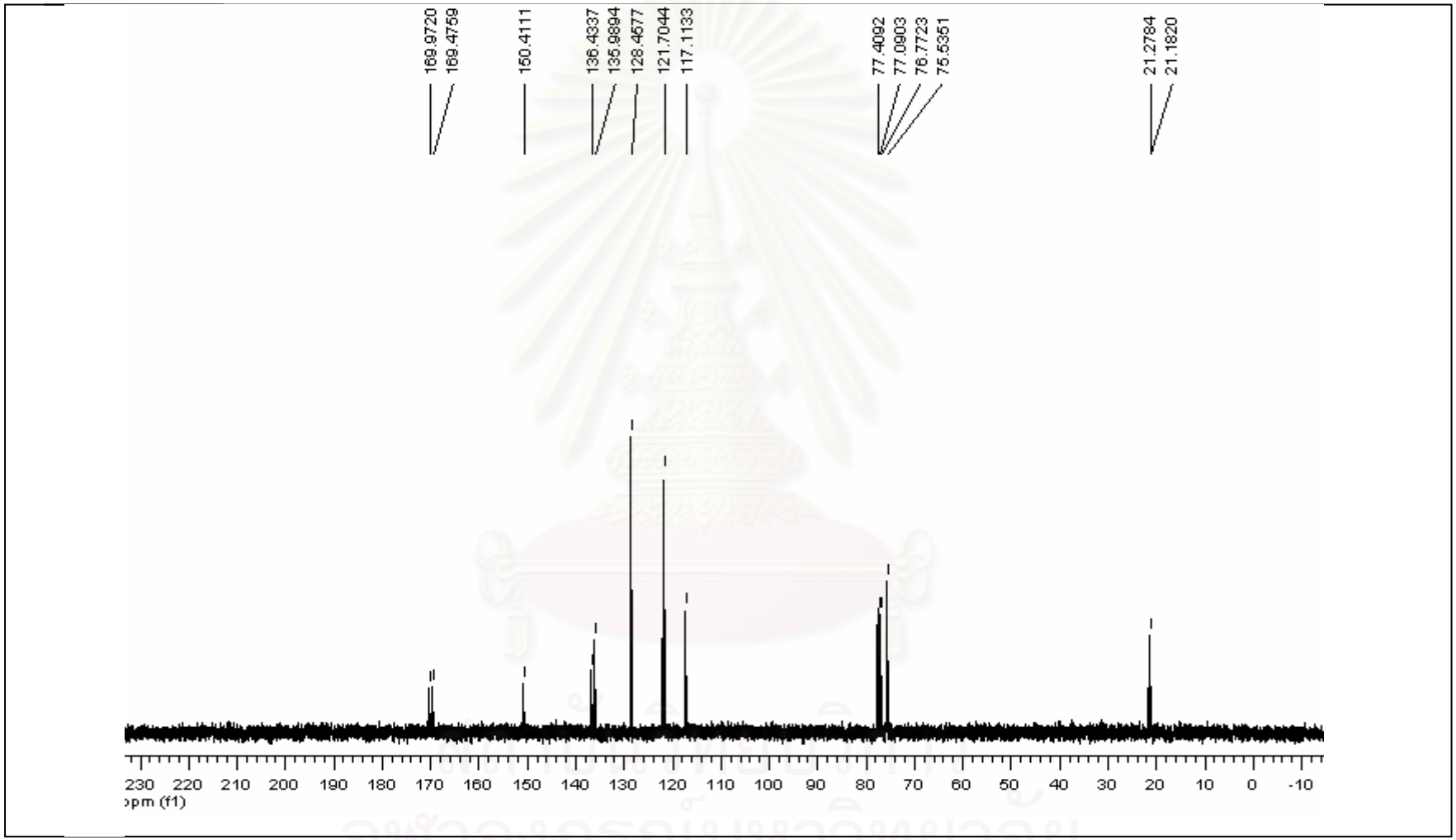

Figure A35 The ^{13}C-NMR spectrum of compound 9

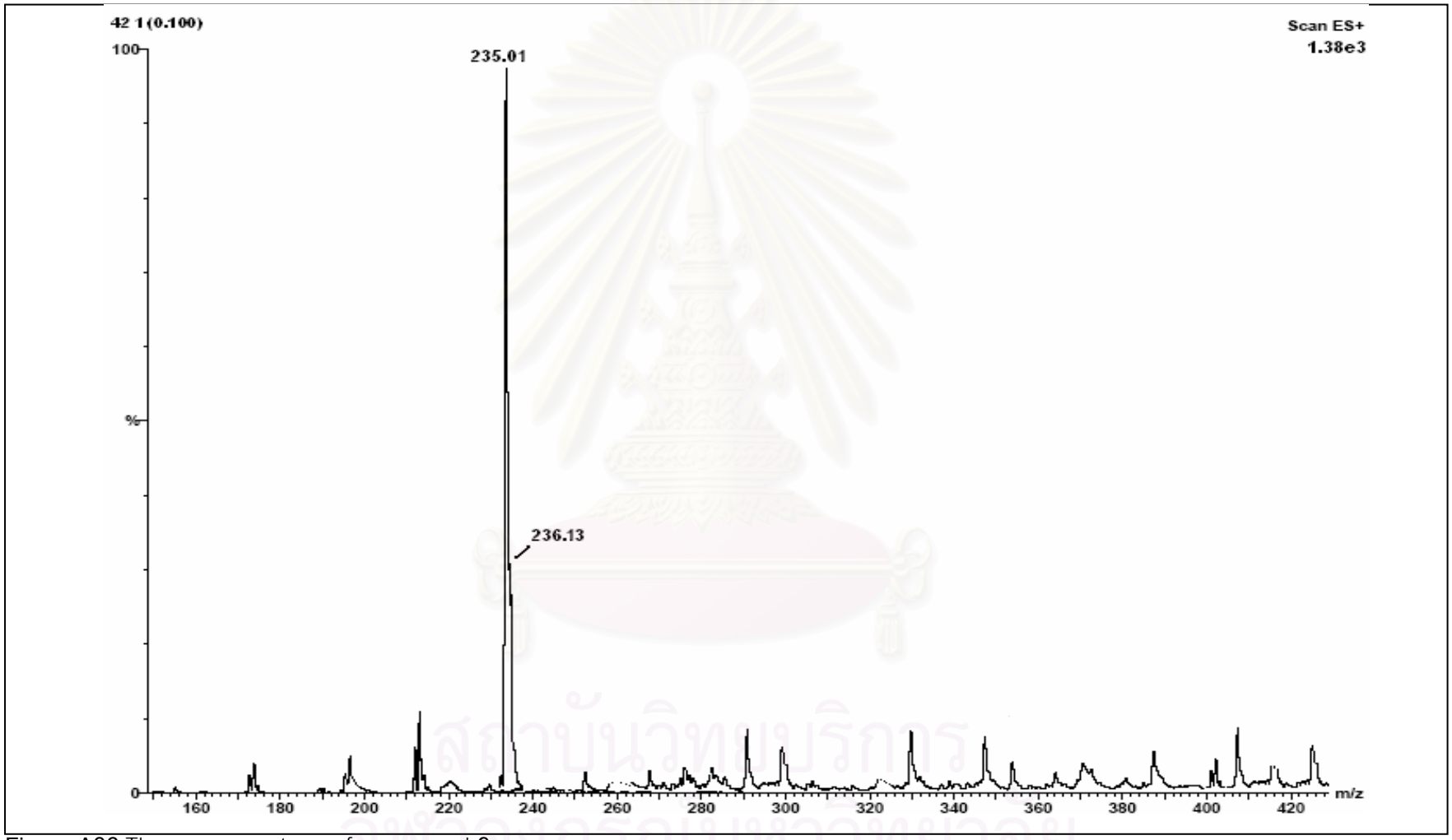

Figure A36 The mass spectrum of compound 9

Figure A37 The IR spectrum of compound **10**

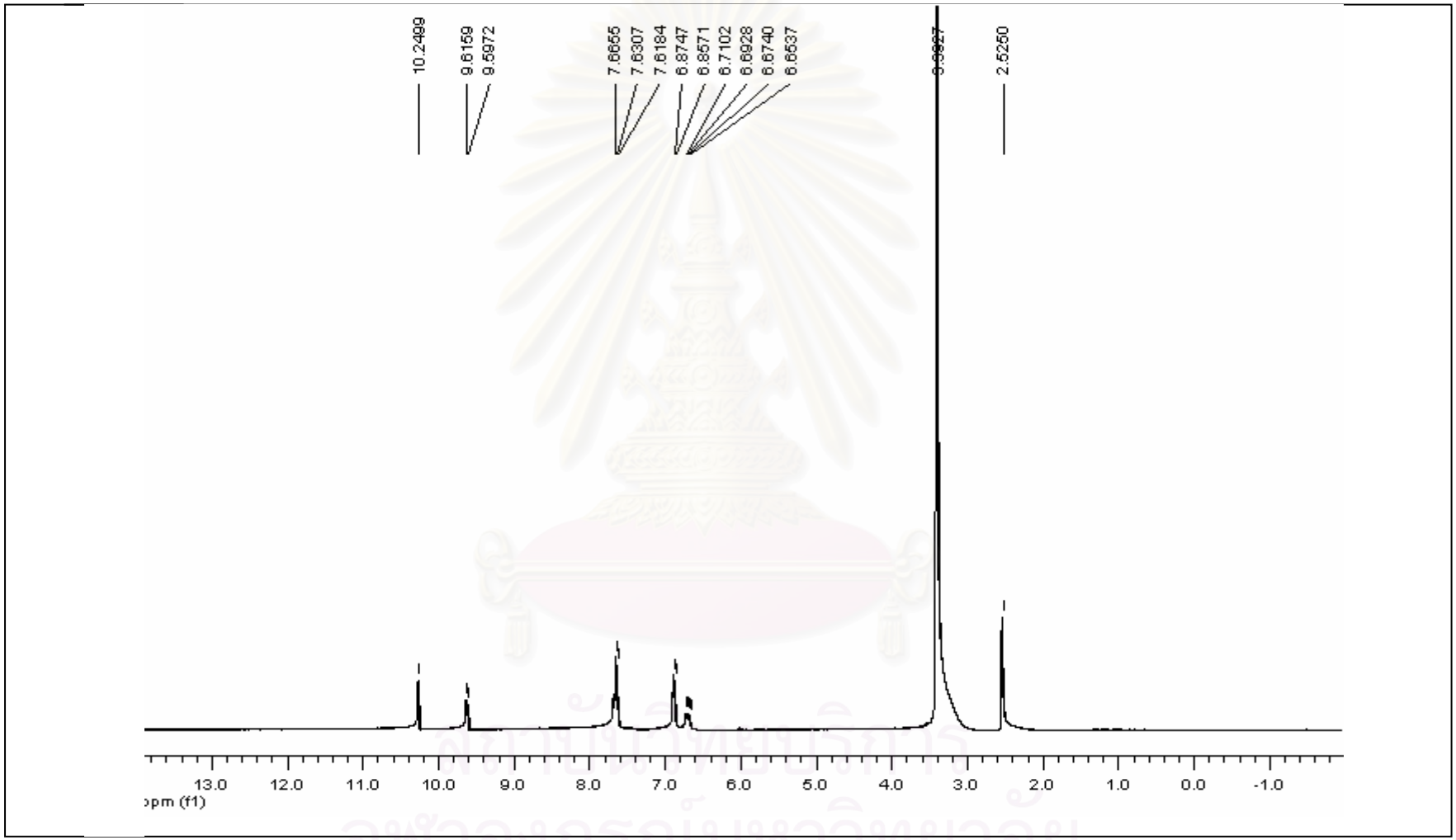

Figure A38 The ^{1}H-NMR spectrum of compound **10**

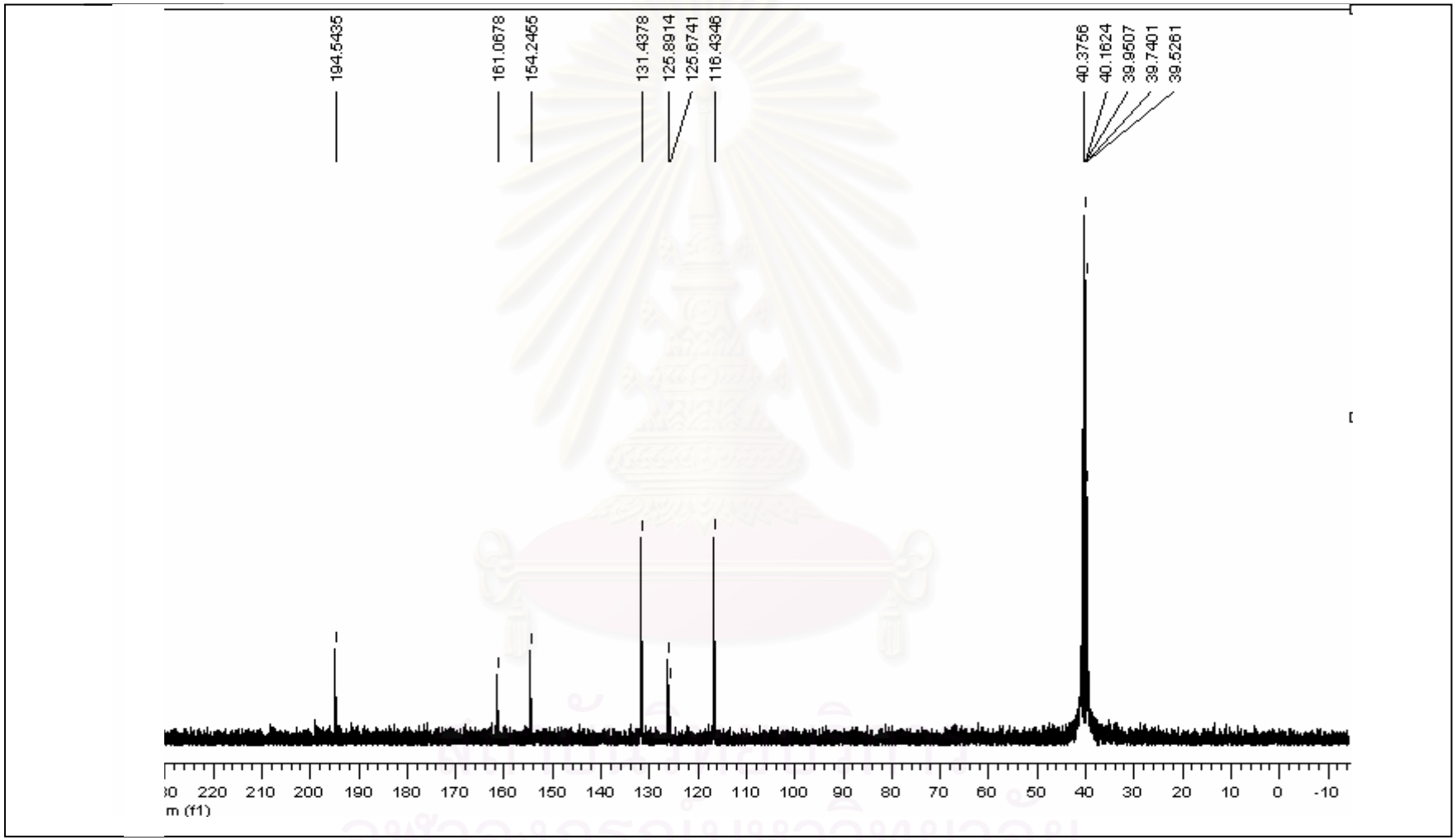

Figure A39 The ^{13}C-NMR spectrum of compound **10**

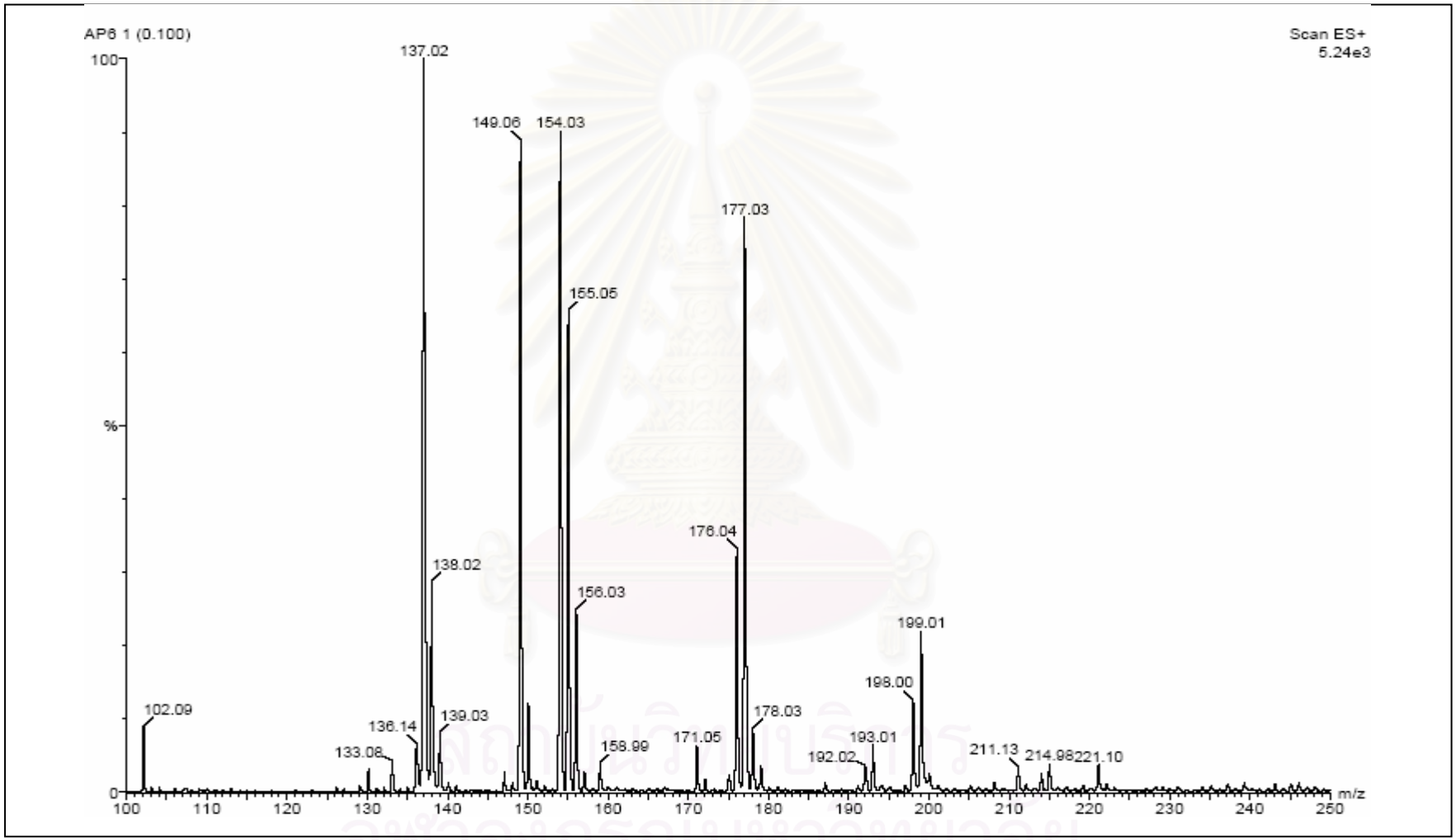

Figure A40 The mass spectrum of compound **10**

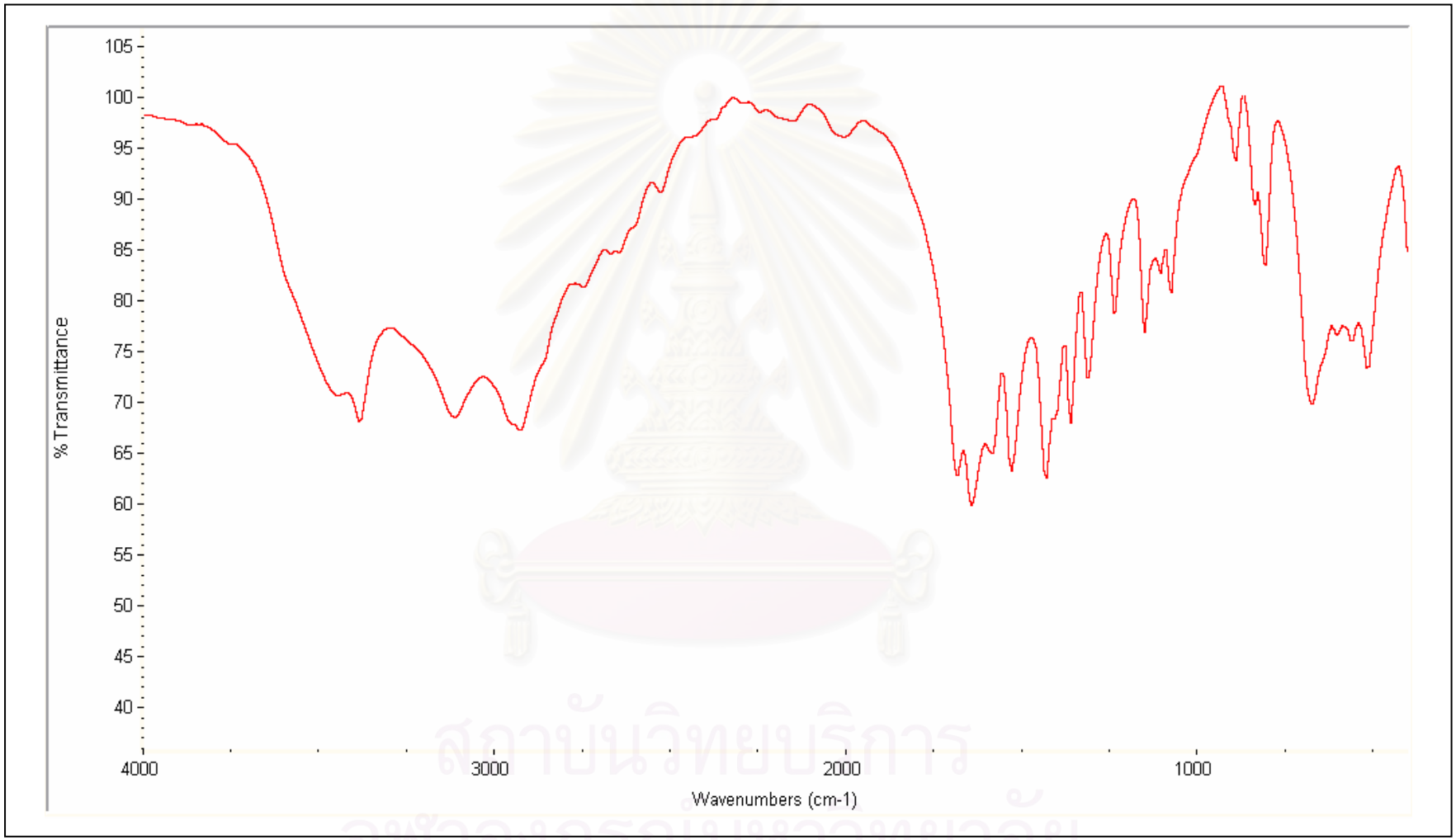

Figure A41 The IR spectrum of compound **11**

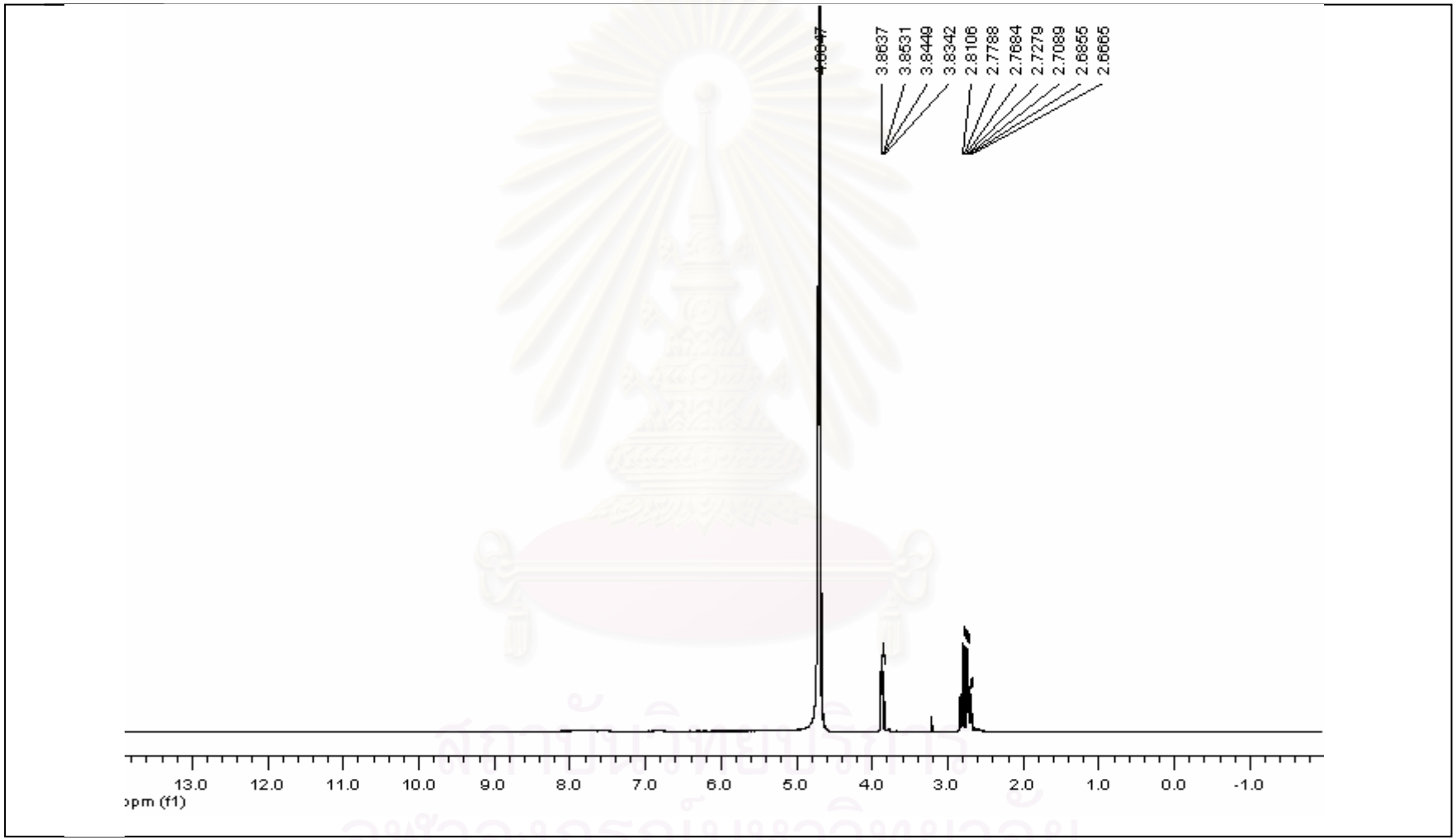

Figure A42 The ^{1}H-NMR spectrum of compound **11**

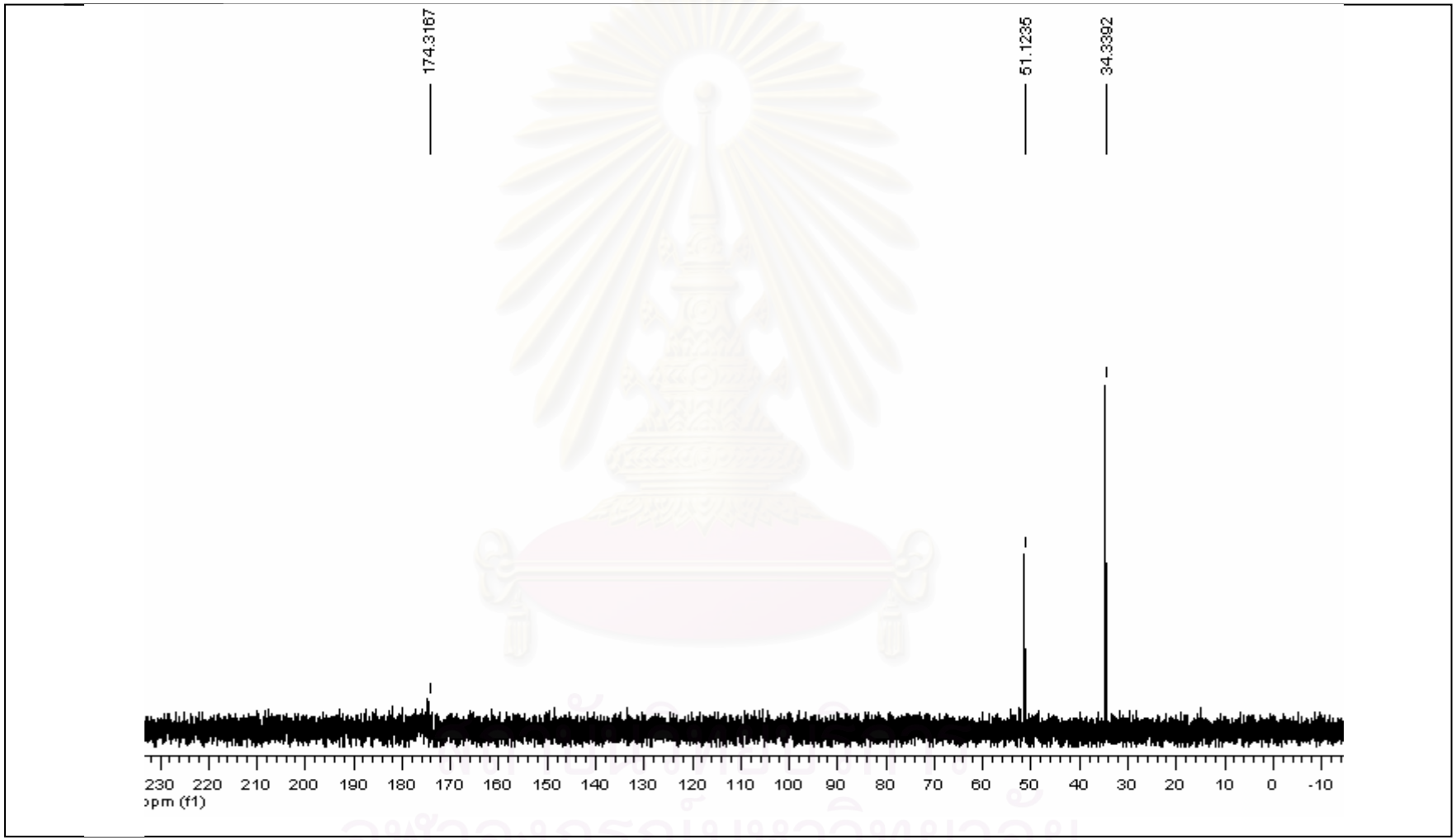

Figure A43 The ^{13}C-NMR spectrum of compound **11**

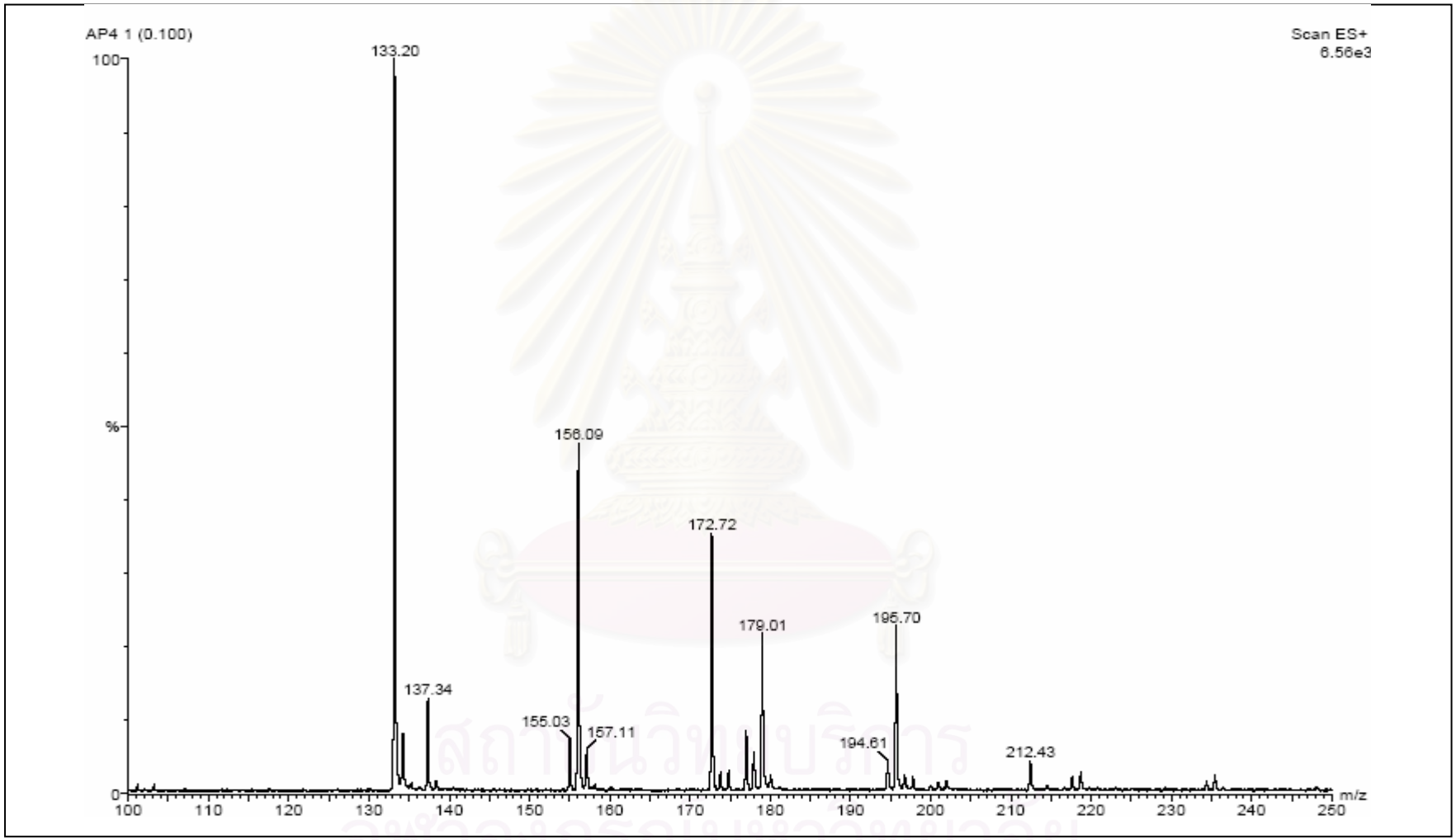

Figure A44 The mass spectrum of compound **11**

Figure A45 The IR spectrum of compound **12**

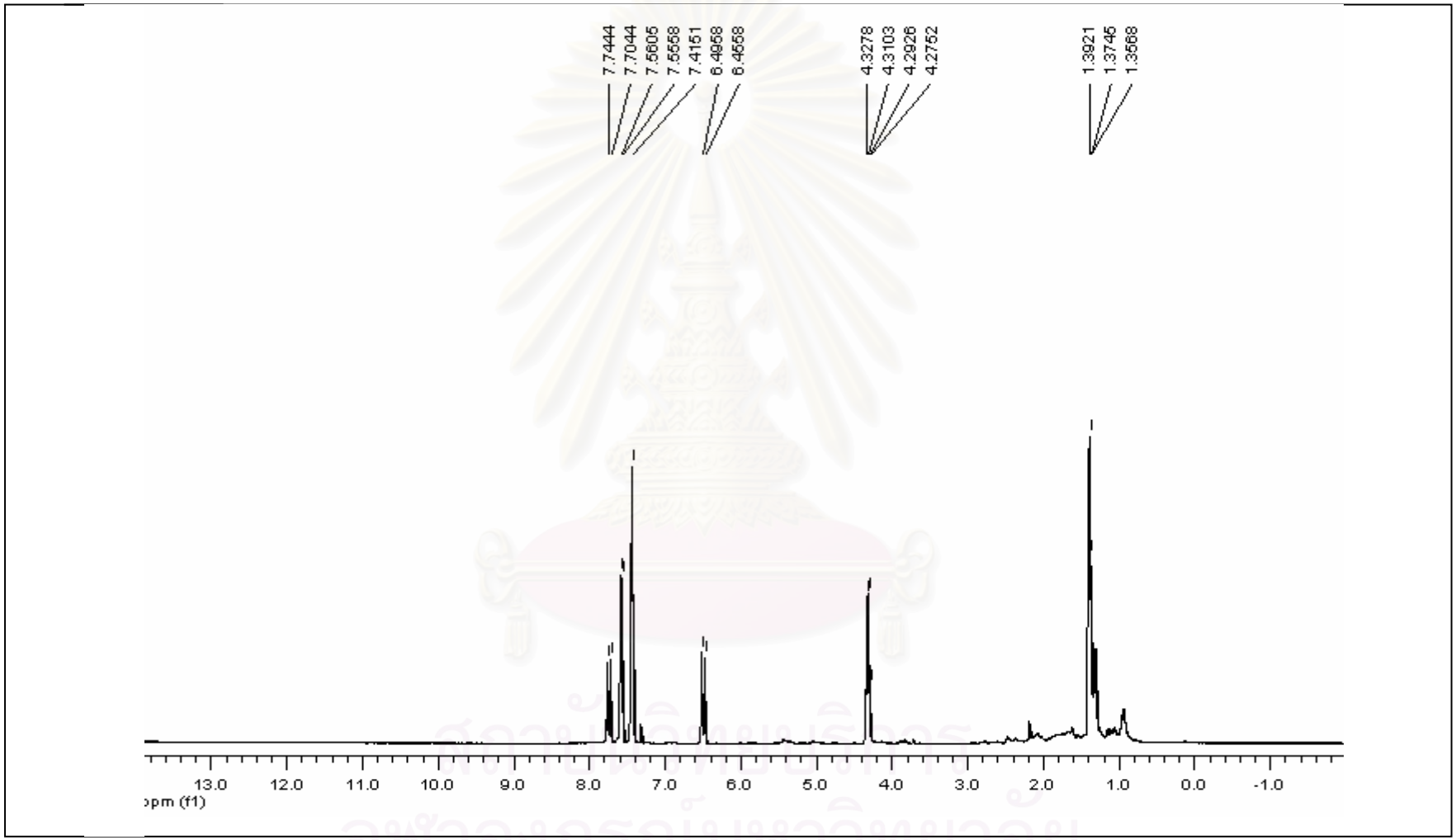

Figure A46 The ^{1}H-NMR spectrum of compound 12

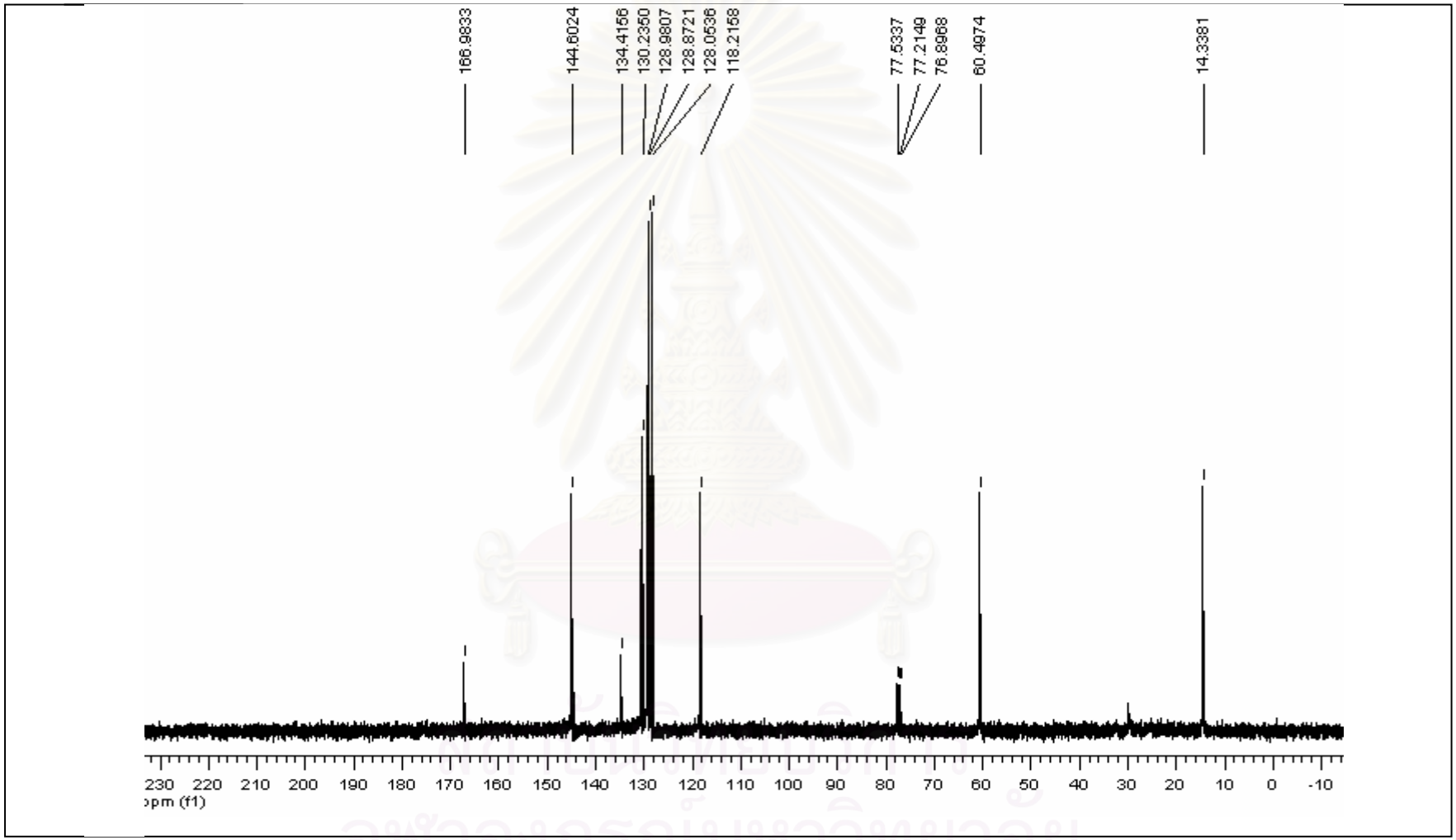

Figure A47 The ^{13}C-NMR spectrum of compound 12

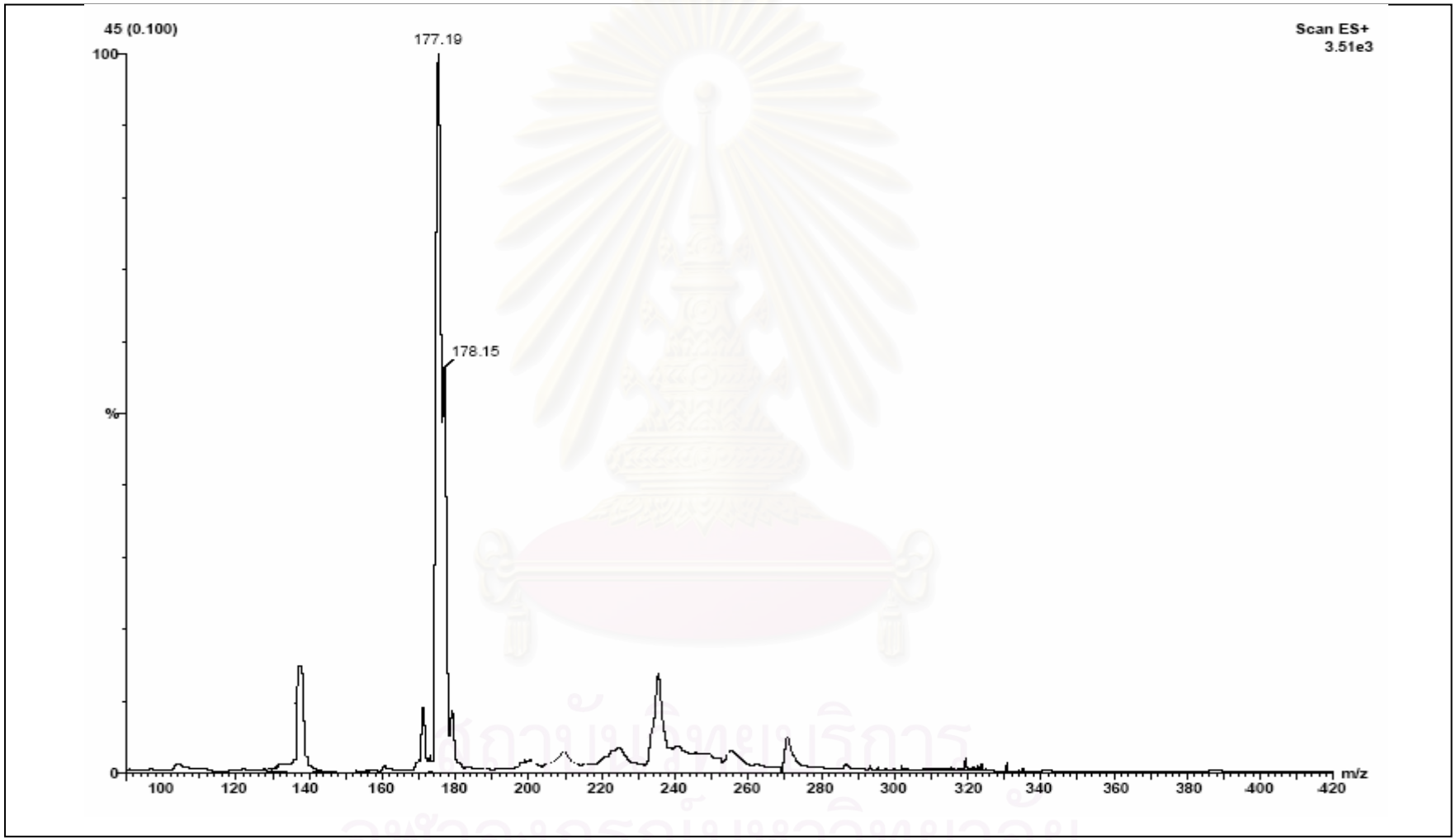

Figure A48 The mass spectrum of compound 12

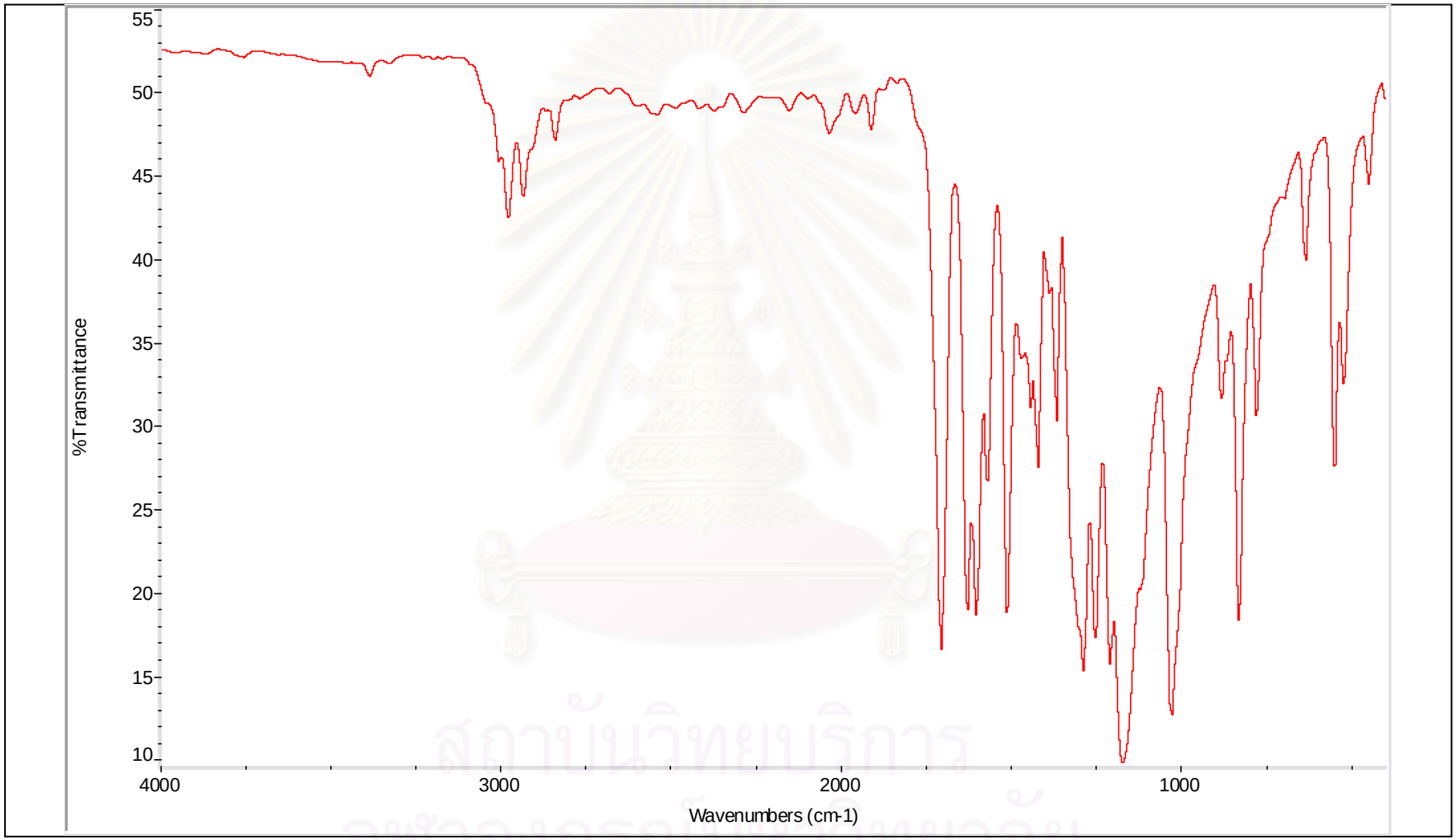

Figure A49 The IR spectrum of compound **13**

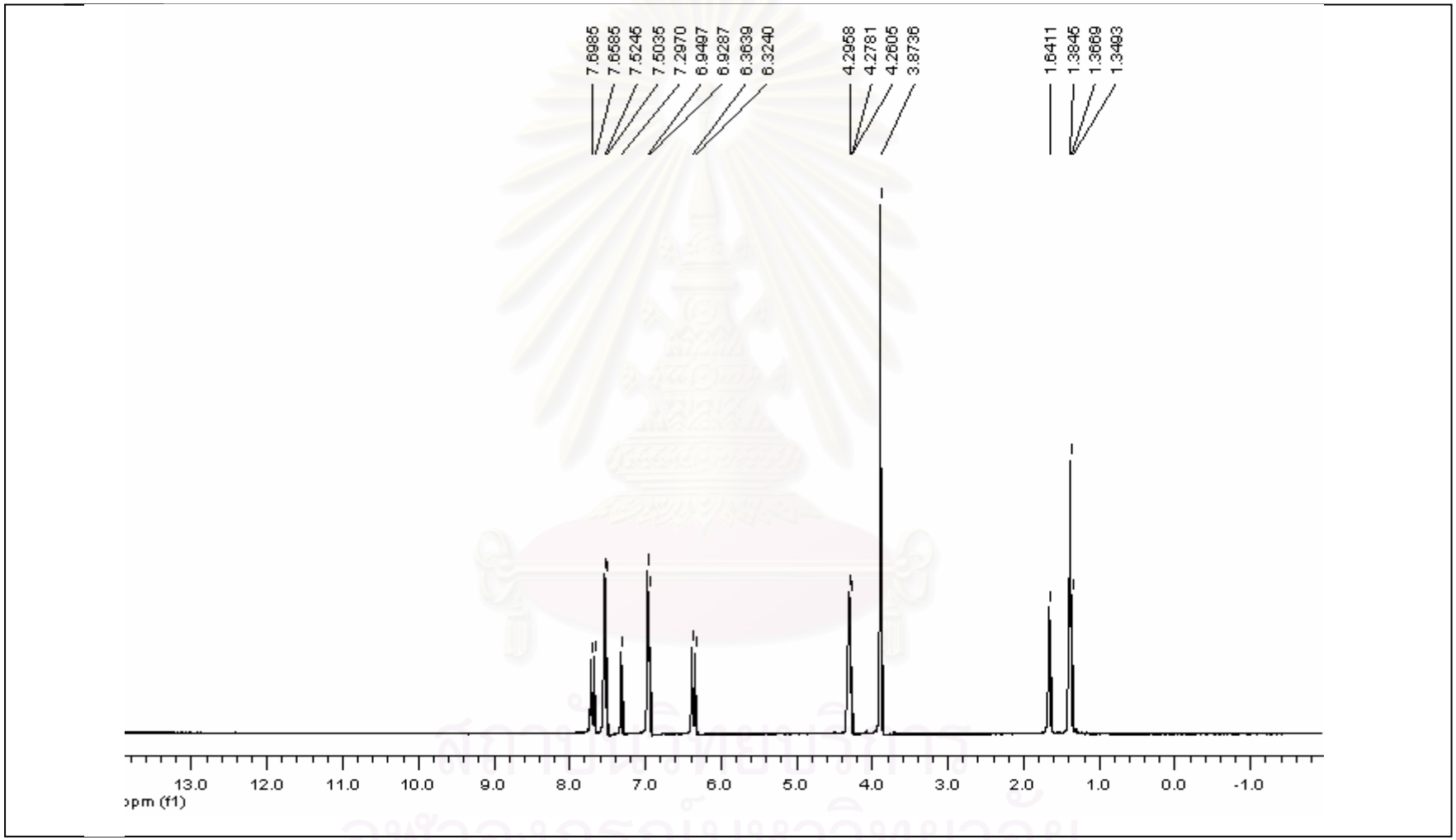

Figure A50 The ^{1}H-NMR spectrum of compound 13

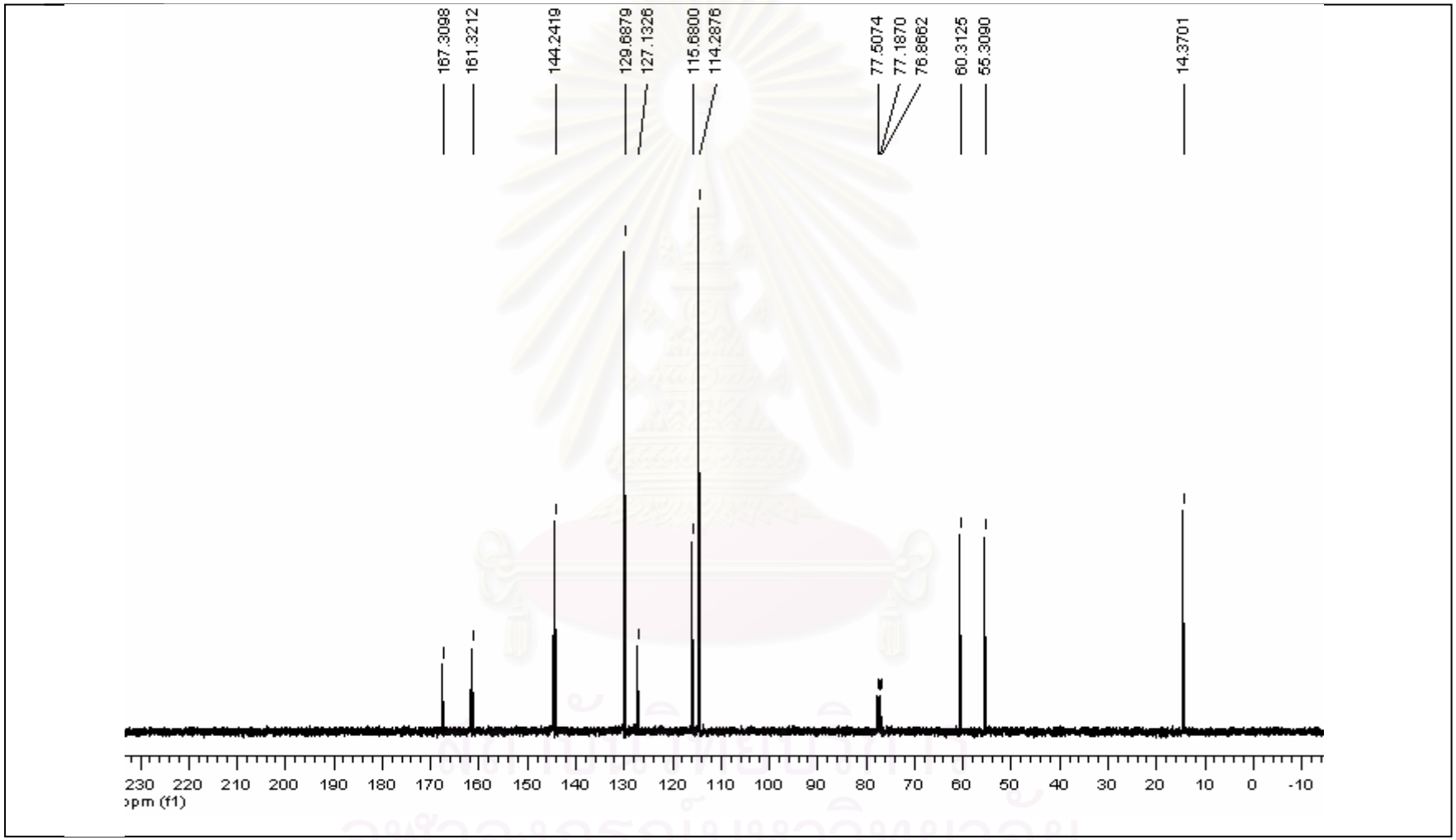

Figure A51 The ^{13}C-NMR spectrum of compound **13**

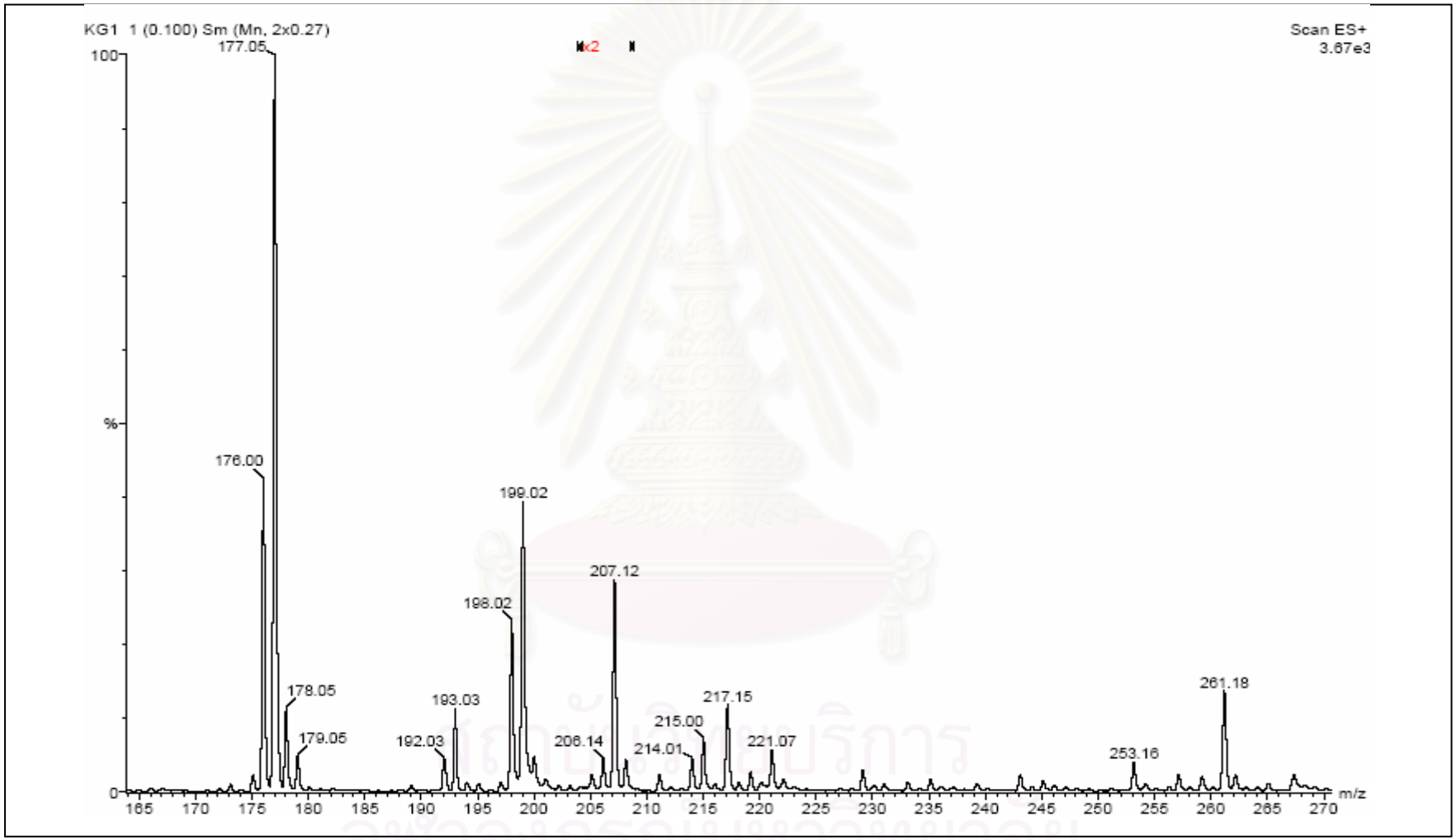

Figure A52 The mass spectrum of compound **13**

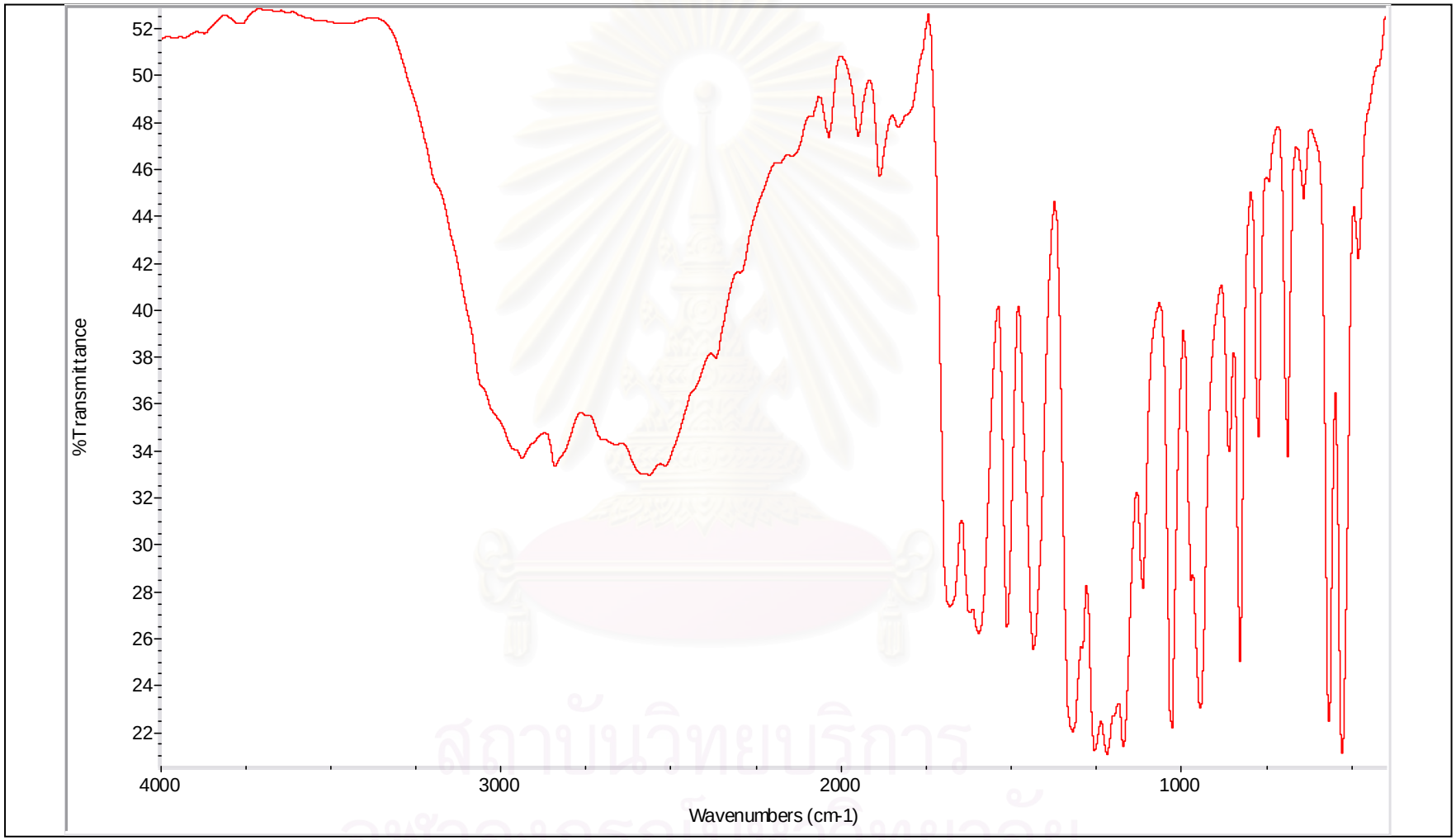

Figure A53 The IR spectrum of compound **14**

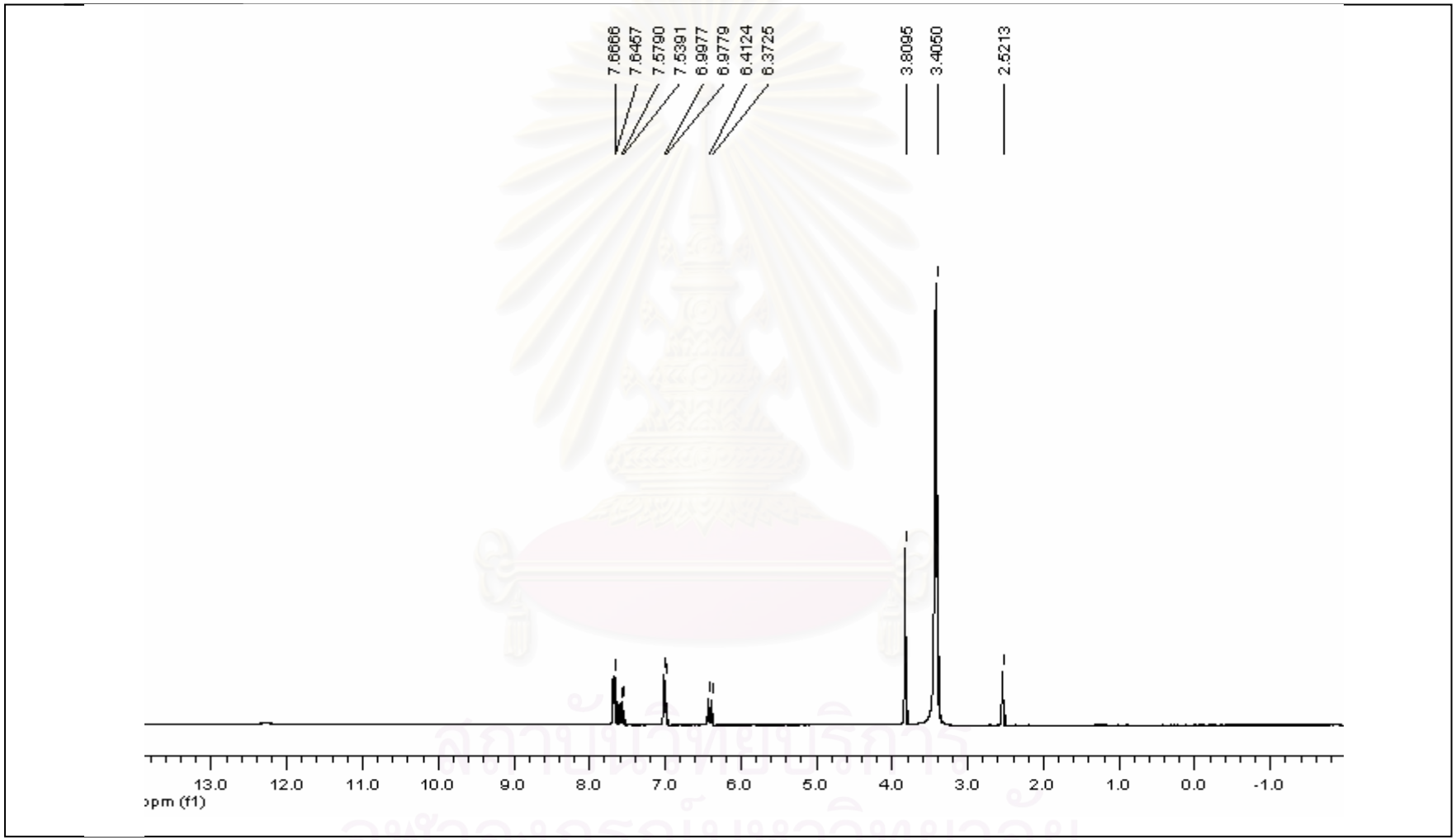

Figure A54 The ^{1}H-NMR spectrum of compound **14**

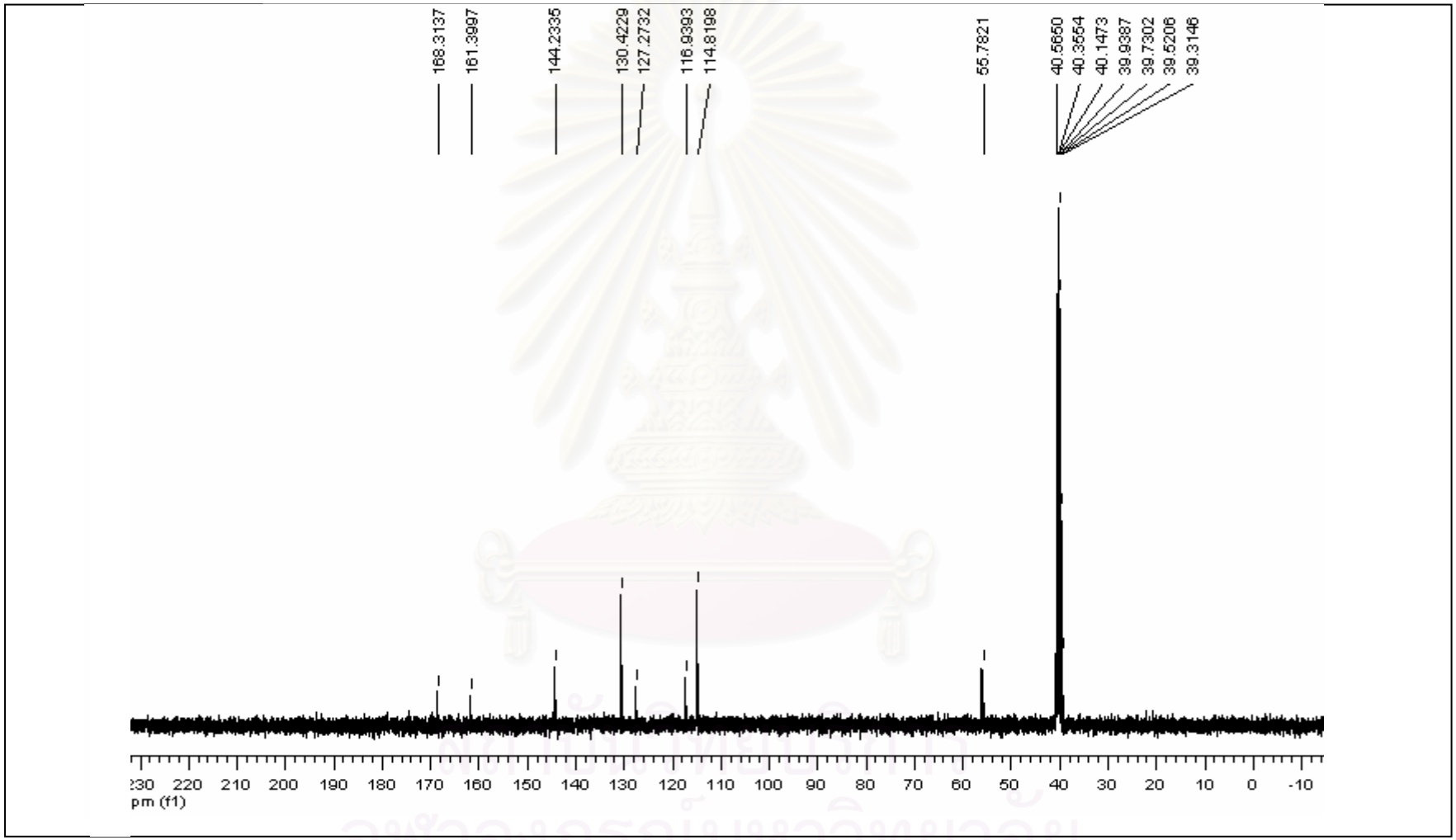

Figure A55 The ^{13}C-NMR spectrum of compound **14**

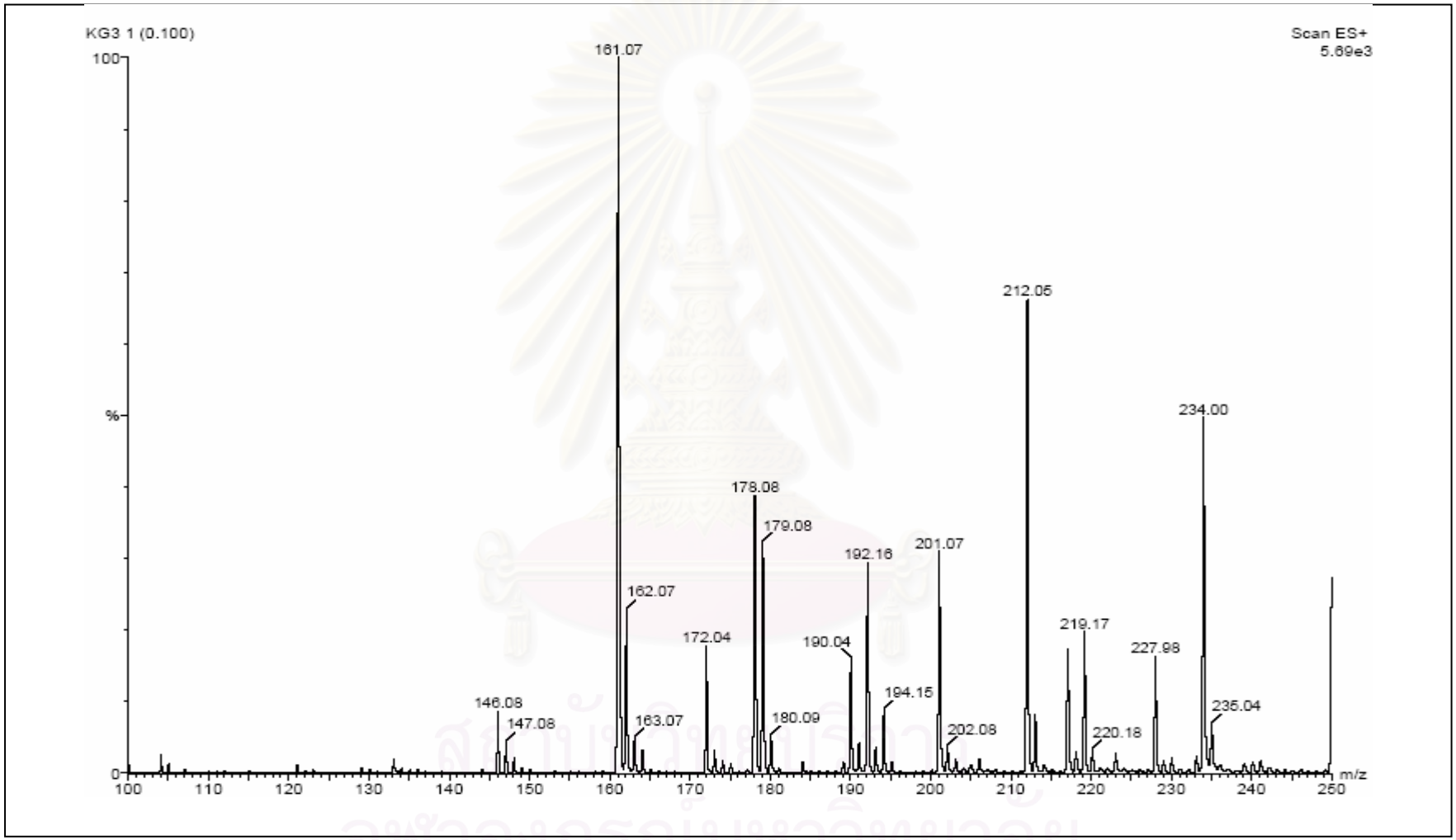

Figure A56 The mass spectrum of compound 14

VITA

Mr. Kasem Sookkongwaree was born on November 18, 1977 at Chonburi province. He graduated with a Bachelor Degree of Science in April 1998, Master Degree of Science, in organic chemistry in April 2000 from Department of Chemistry, Faculty of Science, Chulalongkorn University. Then he continued his Ph. D. Degree in organic chemistry and got the scholarship from The Royal Golden Jubilee Program (RGJ Ph. D.), The Thailand Research Fund and The Swedish Foundation for International Cooperation in Research and Higher Education (STINT) to carry out research at Uppsala University in Sweden for one year.